[1] Politecnico di Milano (Italy)
[2] University of Science and Technology of China, Hefei (China)
[3] National Synchrotron Radiation Laboratory, Hefei (China)
[4] Technical University of Denmark (Denmark)

POLITECNICO DI MILANO

A. Cuoci[1], A. Frassoldati[1], T. Faravelli[1], H. Jin[2], Y. Wang[2], K. Zhang[3], P. Glarborg[4], F. Qi[2,3]

Experimental and detailed kinetic modeling study of PAH formation in laminar coflow methane flames

34th International Symposium on Combustion
Warsaw, July 29-August 3, 2012

Motivations (I)

Methane is still today the most important gaseous fuel for practical applications

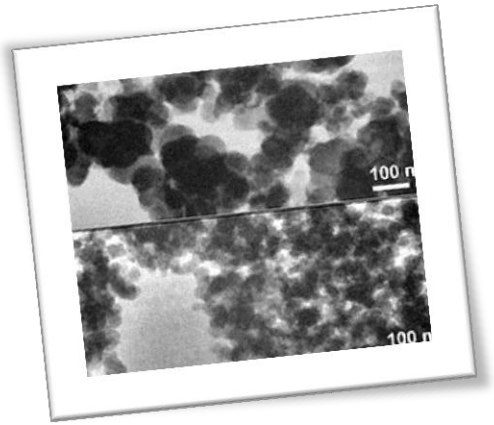

Investigations of PAH formation in methane flames played a **minor role** because of the **smaller propensity** to form aromatics and soot and because of experimental difficulties

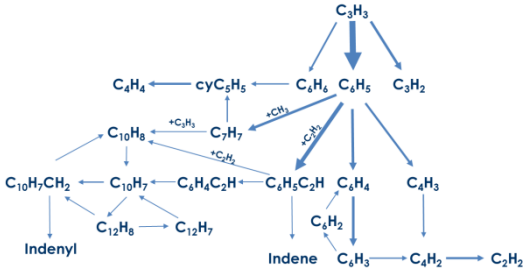

PAH formation pathways in methane flames are **different** from those of large hydrocarbons, especially because the large concentrations of CH_3 radical

McEnally et al., Prog. Energy Combust. Sci., 32 (2006), pp. 247-294
D'Anna, et al., Combustion and Flame, 132 (2003), pp. 715-722
McEnally et al., Comb. Flame, 117 (1999), pp. 362-372
Anderson, et al., Proc. Comb. Inst., 28 (2000), pp. 2577-2583

Motivations (II)

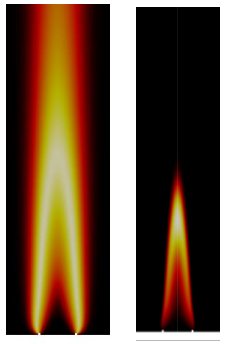

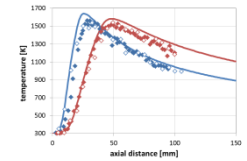

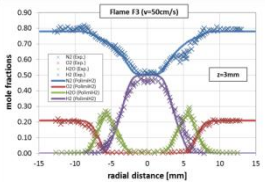

Synchrotron VUV photoionization mass spectrometry (PIMS)

Multi-dimensional **numerical simulations** with detailed kinetic mechanisms

- ✓ Study the **formation of PAHs** in **methane coflow diffusion flames** that resemble more closely the conditions of practical flames
- ✓ Using the numerical simulations to **better interpret** the experimental observations

Outline

- ✓ **Experimental methods**
- ✓ Numerical simulations
  - ✓ Mathematical model
  - ✓ Numerical methodology
- ✓ Comparison between experimental data and numerical results
- ✓ Kinetic analysis of PAHs formation
  - ✓ Reaction paths to PAHs
  - ✓ Formation of naphthalene
- ✓ Conclusions

Experimental methods (I)

Experiments were carried out at the U14C vacuum ultraviolet (VUV) beamline of the National Synchroton Radiation Laboratory (NSRL) in Hefei, China

The syncrothron VUV photoionization mass spectrometry was applied to study the detailed chemistry of a set of coflow diffusion flames fed with methane

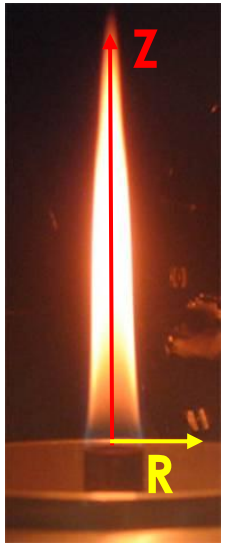

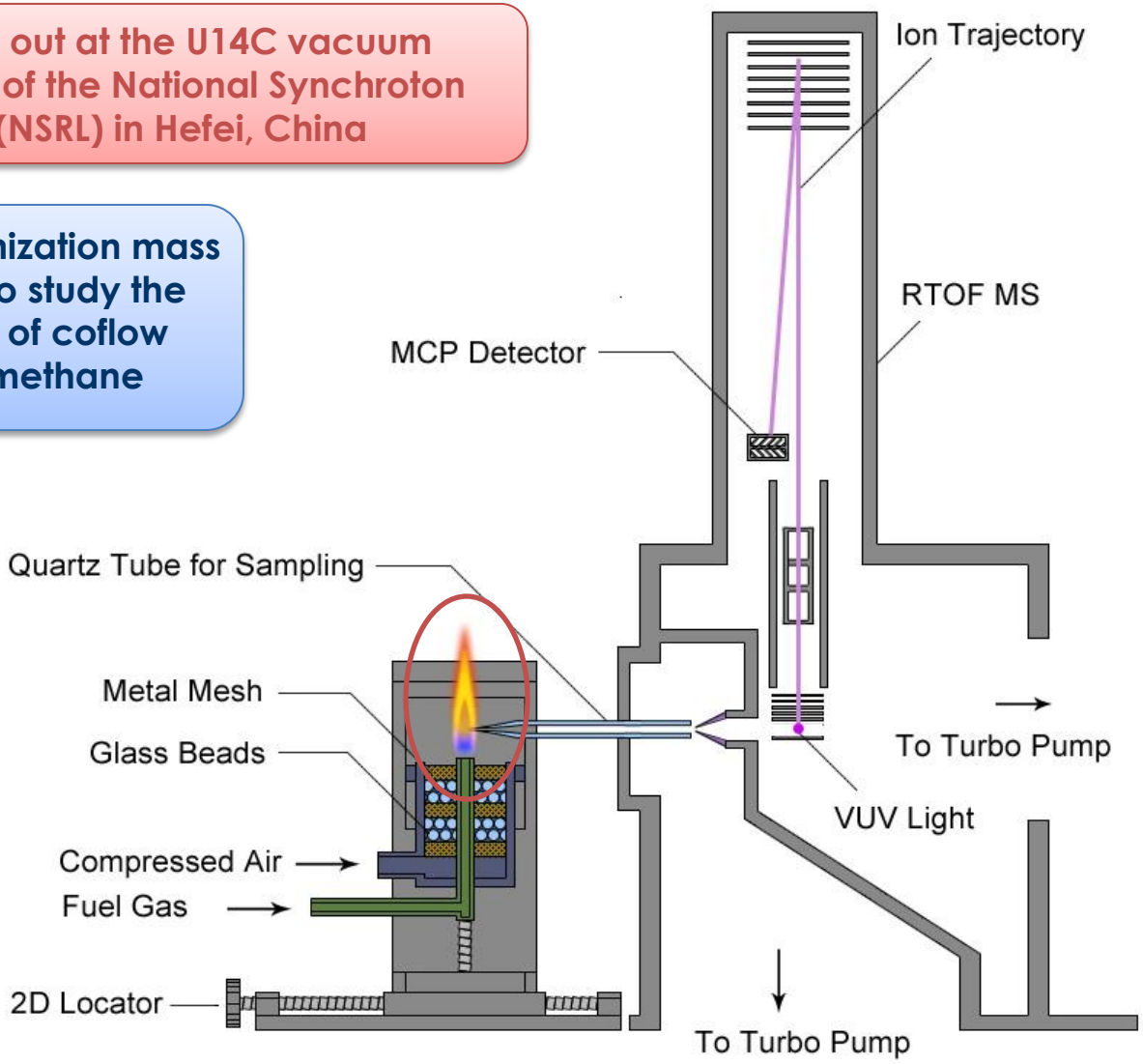

Experimental methods (II)

Quartz-probe (150 micron) was used for sampling

Flame species are measured along the centerline of the flame

The temperature profiles were measured by Pt-6%Rh/Pt-30%Rh thermocouples (diameter of 0.1 mm)

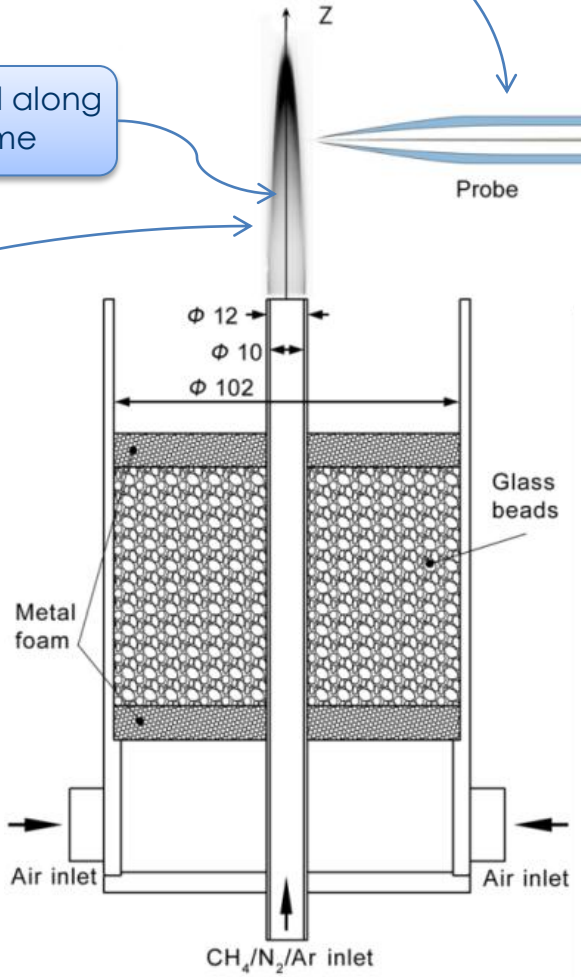

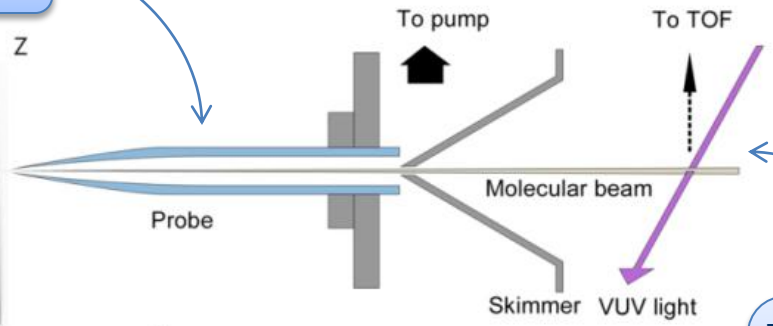

The sample species were ionized by synchrotron VUV light and detected by RTOF-MS

Qi et al., Rev. Sci. Instrum., 77 (2006)
Li et al., Comb. Flame, 152 (2008), pp. 336-359

Investigated flames

Flame	Flow rate(SCCM)				Mole fractions (%)		
	air	N_2	CH_4	Ar	N_2	CH_4	Ar
F1	160,000	314	308	5.87	**50**	49.066	0.934
F2	160,000	345	277	5.87	**55**	44.066	0.934
F3	160,000	377	245	5.87	**60**	39.066	0.934
F4	160,000	408	214	5.87	**65**	34.066	0.934

Increasing dilution

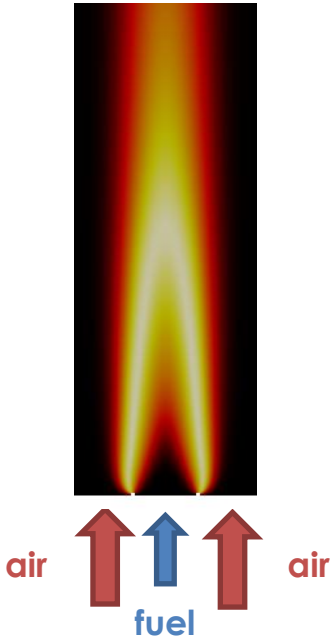

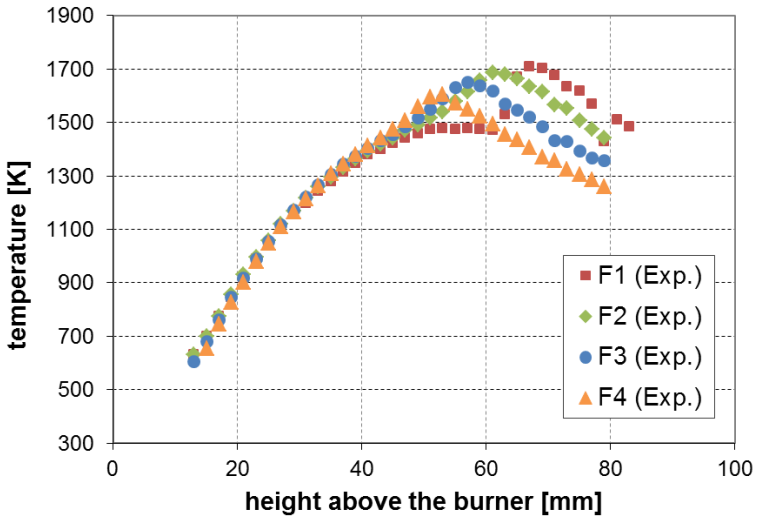

- The mole fraction of Ar was kept at 0.934% in the inlet gas flow
- The mole fraction of N_2 in the inlet gas flow was changed from 50% to 65% in steps of 5%
- The total inlet gas flow rate was kept constant

Detected species

- **Main C1/C2 species**
- **Unsaturated C3 species** (C_3H_2, C_3H_3, aC_3H_4, pC_3H_4)
- **Unsaturated C4 species** (C_4H_2, C_4H_4, C_4H_6)
- **Unsaturated C6 species** (C_6H_2)
- **First aromatics** (C_6H_6, C_7H_8, $C_{10}H_8$, $C_{12}H_8$)

List of flame species and uncertainties

MW	Species	Uncertainties
40	Ar	<20%
32	O_2	<20%
18	H_2O	<20%
2	H_2	<20%
28	N_2	<50%
44	CO_2	<20%
28	CO	<20%
16	CH_4	<20%

MW	Species	Uncertainties
30	CH_2O	<50%
26	C_2H_2	<50%
28	C_2H_4	<50%
42	CH_2CO	factor of 2
38	C_3H_2	factor of 2
39	C_3H_3	<50%
40	aC_3H_4	<50%
40	pC_3H_4	<50%
50	C_4H_2	<50%

MW	Species	Uncertainties
52	C_4H_4	<50%
54	C_4H_6	<50%
66	C_5H_6	factor of 2
74	C_6H_2	factor of 2
78	C_6H_6	<50%
92	C_7H_8	<50%
128	$C_{10}H_8$	<50%
152	$C_{12}H_8$	<50%

List of C5+ species

	Name	Structure
C5H6	1,3-cyclopentadiene	
C6H2	1,3,5-hexatriyne	
C6H6	benzene	
C7H8	toluene	
C6H5C2H	phenylacetylene	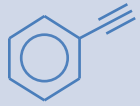
C10H8	naphthalene	
C12H8	acenaphthylene	

Outline

- ✓ Experimental methods
- ✓ **Numerical simulations**
  - ✓ Mathematical model
  - ✓ Numerical methodology
- ✓ Comparison between experimental data and numerical results
- ✓ Kinetic analysis of PAHs formation
  - ✓ Reaction paths to PAHs
  - ✓ Formation of naphthalene
- ✓ Conclusions

Mathematical model

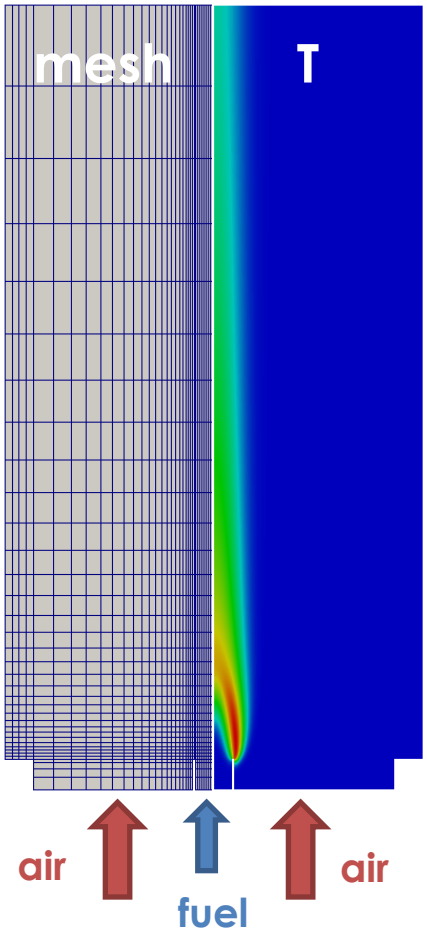

Governing Equations

Mass $$\frac{\partial \rho}{\partial t} + \nabla(\rho \mathbf{v}) = 0$$

Momentum $$\frac{\partial}{\partial t}(\rho \mathbf{v}) + \nabla(\rho \mathbf{v}\mathbf{v} + p\mathbf{I}) = \nabla \boldsymbol{\tau} + \rho \mathbf{g}$$

Energy $$\rho C_P \frac{\partial T}{\partial t} + \rho C_P \mathbf{v} \nabla T = -\nabla \mathbf{q} - \rho \sum_{k=1}^{NC} C_{P,k} \omega_k \mathbf{V}_k - \sum_{k=1}^{NC} h_k \dot{\Omega}_k$$

Species $$\frac{\partial}{\partial t}(\rho \omega_k) + \nabla(\rho \omega_k \mathbf{v}) = -\nabla(\rho \omega_k \mathbf{V}_k) + \dot{\Omega}_k \qquad k = 1,\ldots,NC$$

- ✓ Laminar conditions
- ✓ Ideal gas
- ✓ Fick and thermal diffusion
- ✓ Optically-thin radiation model

Hall, et al., J. Quant. Spectrosc. Radiat. Transfer 49 (1993), pp. 517-523
Kee et al., Sandia Report SAND89-8009 (1989)

Smooke et al., Combustion Science and Technology 67, 1986 pp. 85-122

Numerical methodology

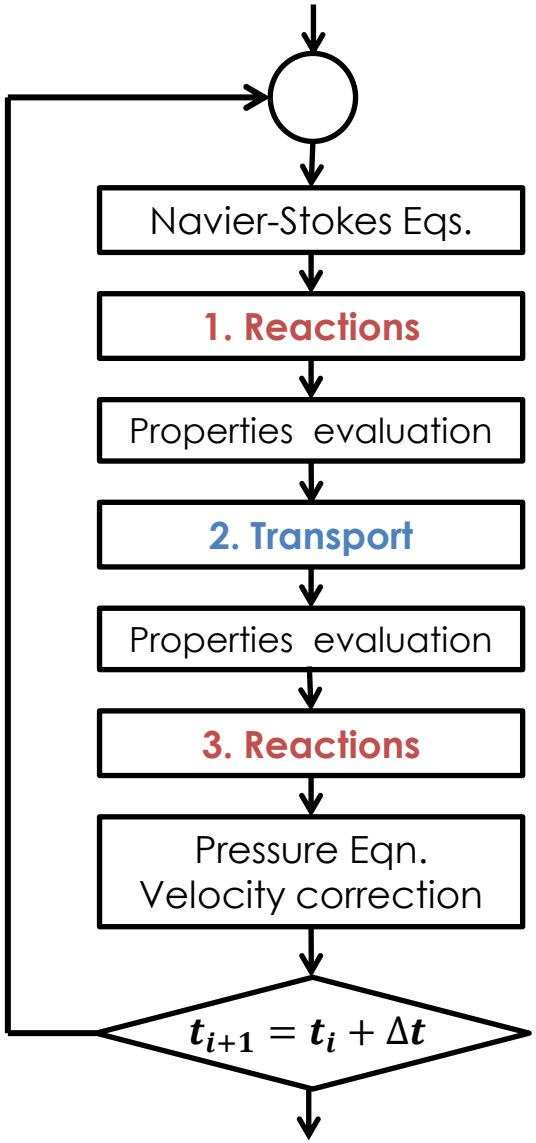

Uncoupled, stiff ODE systems

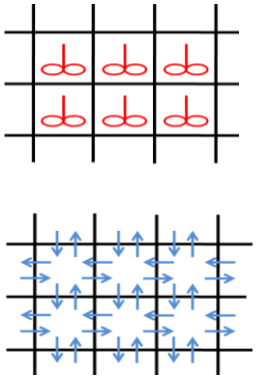

$$\frac{d\boldsymbol{\Psi}}{dt} = \mathbf{S}(\boldsymbol{\Psi}) + \mathbf{M}(\boldsymbol{\Psi}, t)$$

$\boldsymbol{\Psi}$: dependent variables (ω_i and T)
$\mathbf{S}(\boldsymbol{\Psi})$: is the rate of change of $\boldsymbol{\Psi}$ due to reactions
$\mathbf{M}(\boldsymbol{\Psi},t)$: the rate of change of $\boldsymbol{\Psi}$ due to transport

Sub-step 1. The reaction terms are integrated over $\Delta t/2$ through the solution of an ODE system:

$$\frac{d\boldsymbol{\Psi}^a}{dt} = \mathbf{S}(\boldsymbol{\Psi}^a)$$

Sub-step 2. The transport terms (convection and diffusion) are integrated over Δt by solving:

$$\frac{d\boldsymbol{\Psi}^b}{dt} = \mathbf{M}(\boldsymbol{\Psi}^b, t)$$

Sub-step 3. identical to Sub-step 1

Strang, G., *"On the construction and comparison of difference schemes"*, SIAM Journal of Numerical Analysis, 5 (1968), p. 506-517

Ren, Z. and S.B. Pope, *"Second-order splitting schemes for a class of reactive systems"*, Journal of Computational Physics, 227 (2008), p. 8165-8176

laminarSMOKE solver

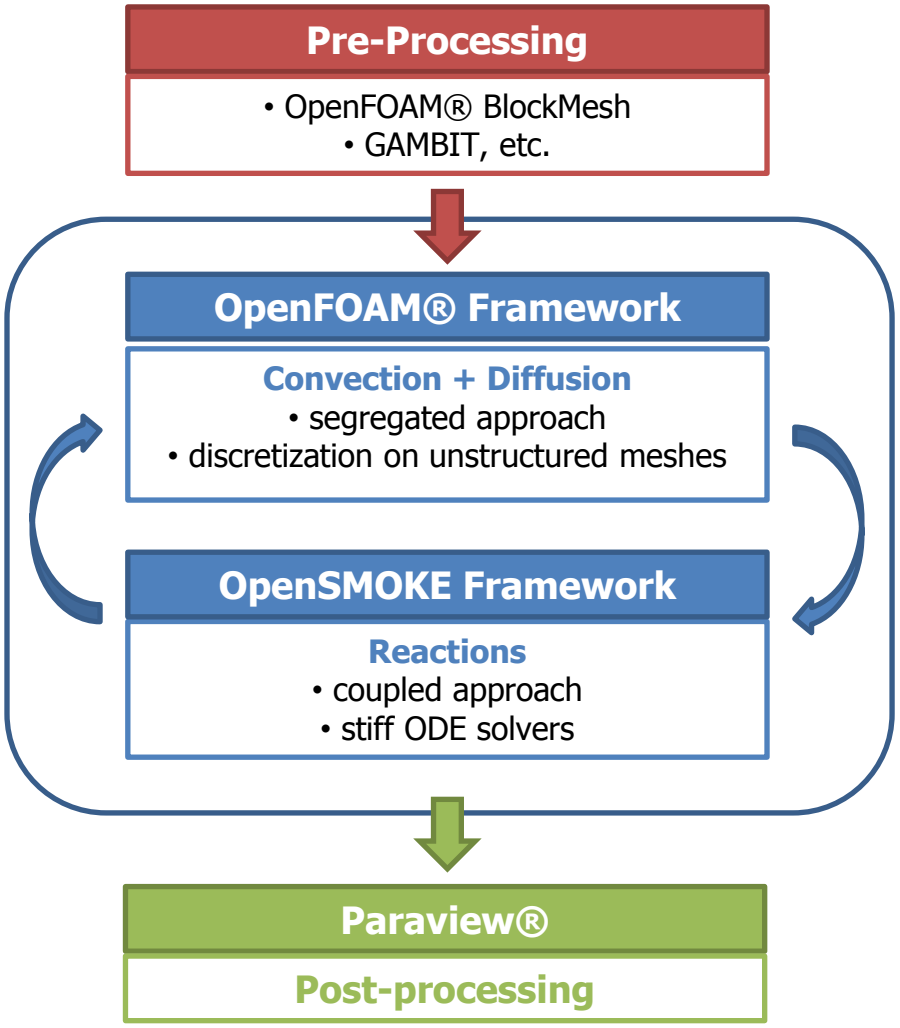

- ✓ Multidimensional, finite-volume code
- ✓ Structured and unstructured meshes
- ✓ Unsteady solutions
- ✓ Kinetics in CHEMKIN format
- ✓ Several ODE solvers (BzzMath, CVODE, DVODE, RADAU, LIMEX)
- ✓ Freely available (open-source)

The code will be released in the next months

www.opensmoke.polimi.it

Cuoci A. et al., Submitted to Combustion and Flame (2012)

Kinetic mechanism (I)

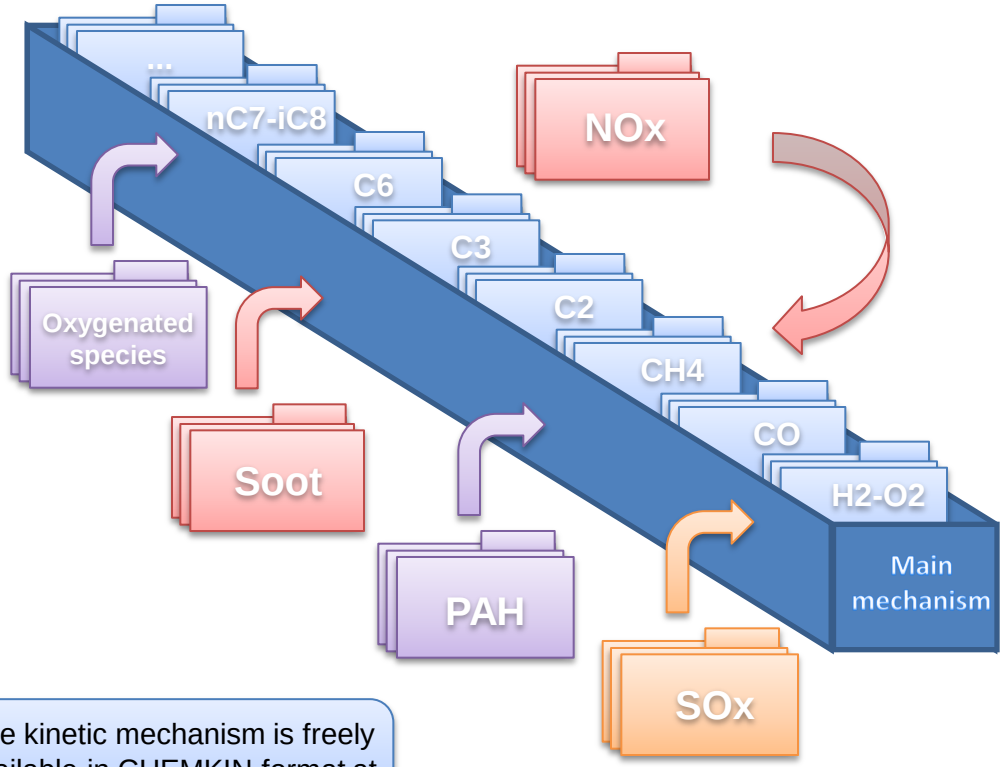

The kinetic mechanism is freely available in CHEMKIN format at this web address:

http://creckmodeling.chem.polimi.it

Kinetic mechanism includes hydrocarbons up to Diesel and jet fuels as well as several pollutants

Hierarchy

Modularity

Generality

~ 450 chemical species

~ 14,000 reactions

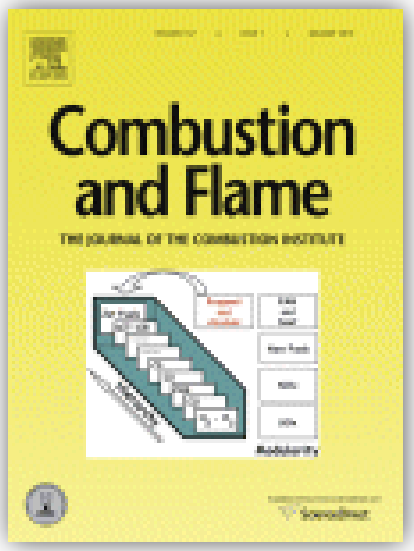

Frassoldati, A. et al., Combustion and Flame 157(2010), pp. 2-16

Ranzi, E. at al., Progress in Energy and Combustion Science 38 (2012), pp. 468-501

Kinetic mechanism (II)

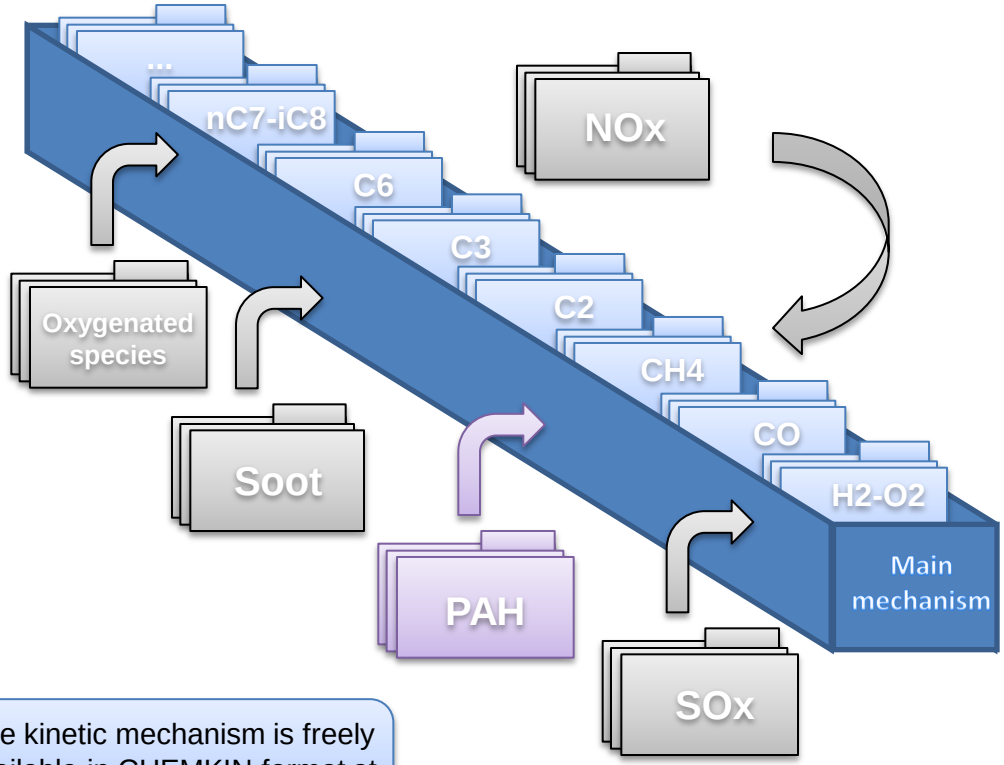

The kinetic mechanism is freely available in CHEMKIN format at this web address:

http://creckmodeling.chem.polimi.it

Frassoldati, A. et al., Combustion and Flame 157(2010), pp. 2-16

Ranzi, E. at al., Progress in Energy and Combustion Science 38 (2012), pp. 468-501

Kinetic mechanism includes hydrocarbons up to Diesel and jet fuels as well as soot pollutants

Hierarchy

Modularity

Generality

PolimiC1C16HT

~ 180 chemical species

~ 6,000 reactions

The mechanism includes the routes leading to the formation of PAH and soot precursors and has been validated in previous studies:

Goldaniga, et al., Comb. Flame 122 (2000), pp. 350-358

Ranzi, et al., Exp. Thermal Fluid Science 21(2000), pp. 71-78

Granata, et al., Comb. Flame 131 (2002), pp. 273-284

Frassoldati, et al., Comb. Flame 158 (2011), pp. 1264-1276

Details about simulations

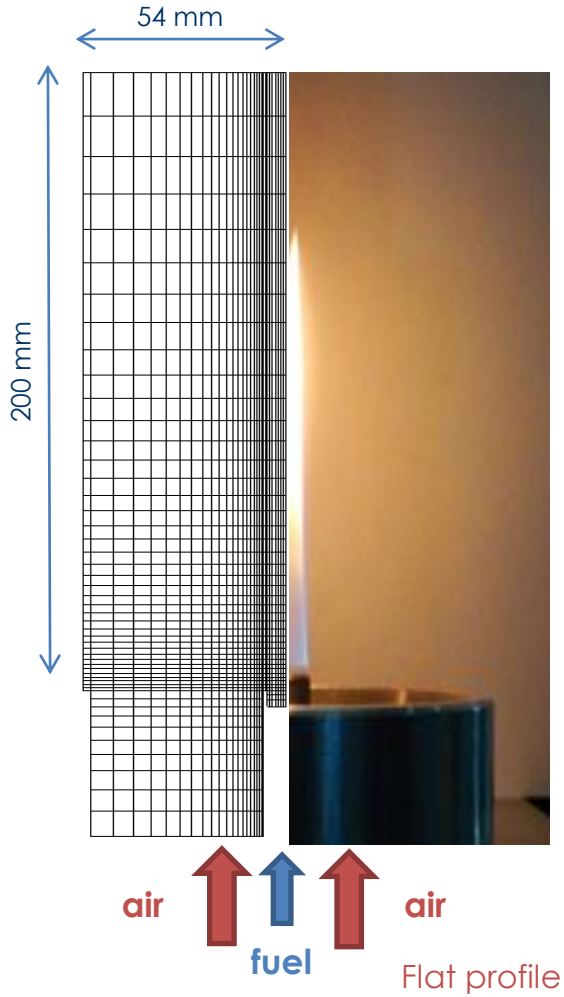

Parabolic profile
V_{mean}=13 cm/s
Re=~160
T=300K

Flat profile
V=33 cm/s
T=300K

The numerical calculations were performed on a **2D structured mesh** with ~10,000 cells (200 mm x 54 mm)

centered, 2nd order discretization schemes
max Courant number: 0.10

Calculations were performed on 12 CPUs and ~5-7 days are needed for each flame

The steady-state solution was reached by using different kinetic schemes, with different levels of details, to minimize the computational cost

Polimi Skeletal (25 species)
↓ First guess
Polimi C1C3HT (89 species)
↓ First guess
Polimi C1C16HT (187 species)

Outline

- ✓ Experimental methods
- ✓ Numerical simulations
  - ✓ Mathematical model
  - ✓ Numerical methodology
- ✓ **Comparison between experimental data and numerical results**
- ✓ Kinetic analysis of PAHs formation
  - ✓ Reaction paths to PAHs
  - ✓ Formation of naphthalene
- ✓ Conclusions

Flame F1: temperature and major species

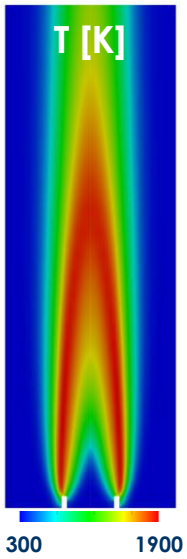

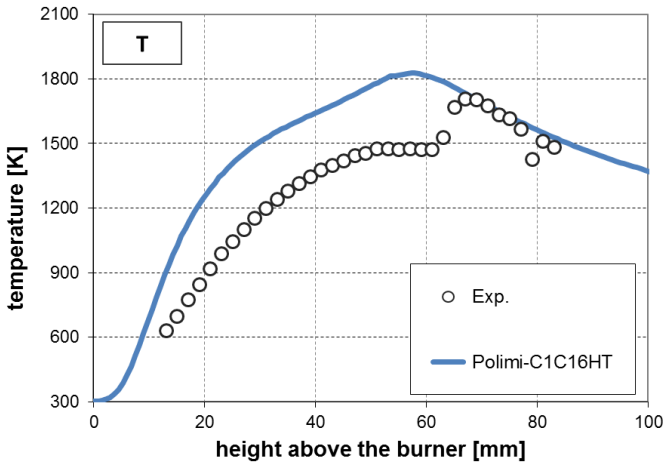

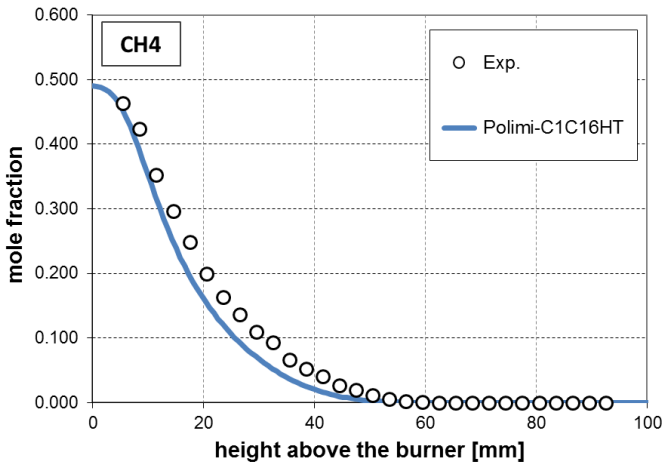

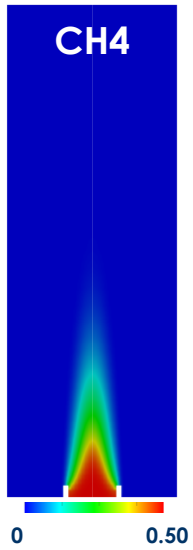

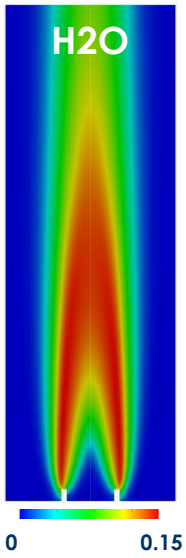

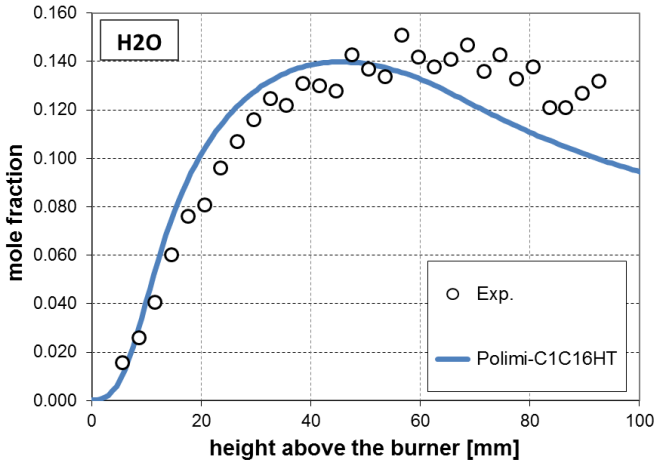

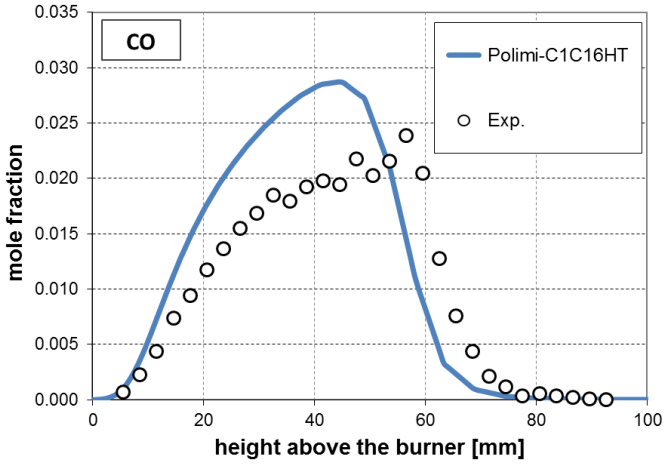

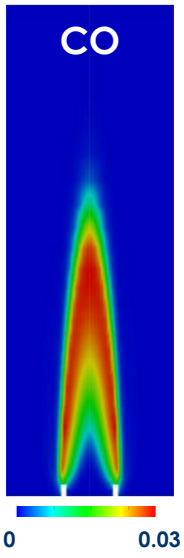

Flame F1: temperature and major species

Significant deviations for the temperature profile
The peak temperature is overestimated by 100K

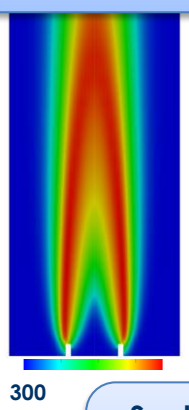

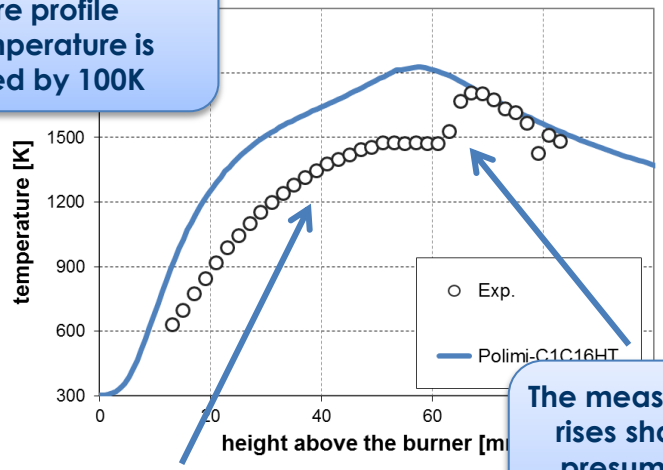

The measured temperature rises sharply at ~60 mm presumably due to the oxidation of soot on the thermocouples

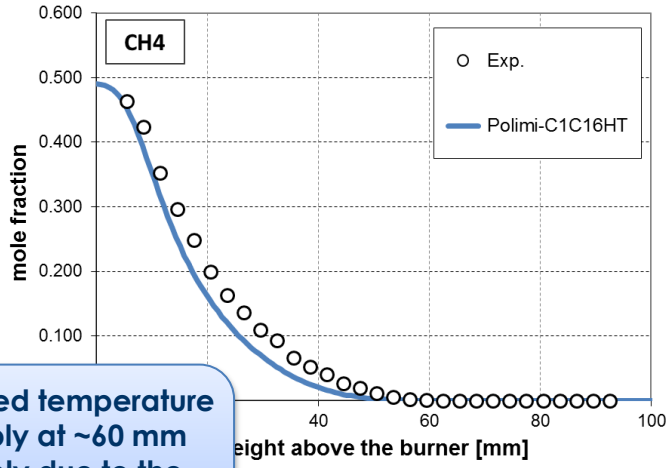

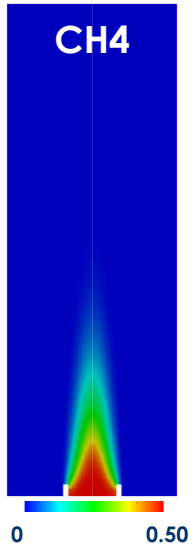

Soot deposited over the thermocouples could affect the measured temperatures

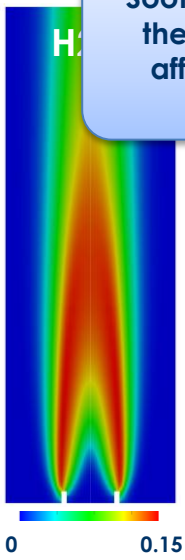

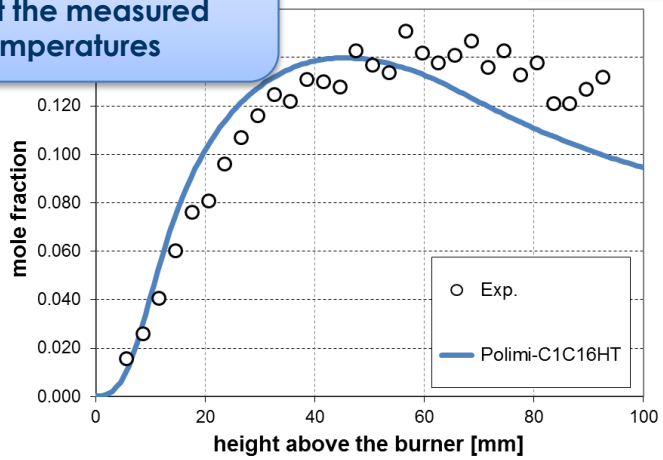

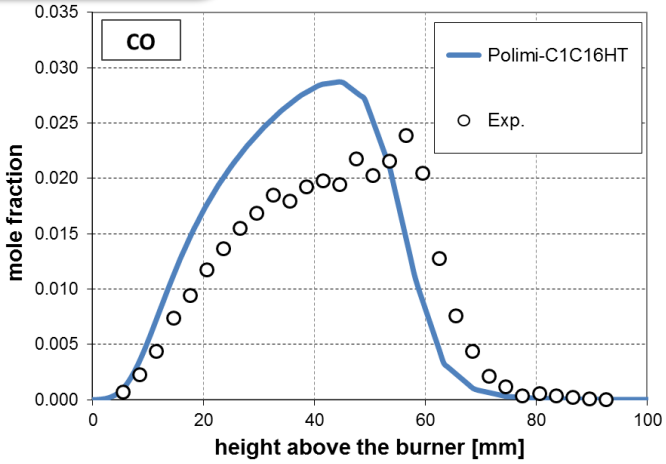

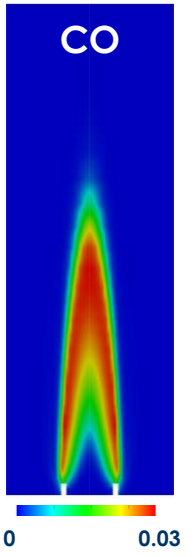

Flame F1: temperature and major species

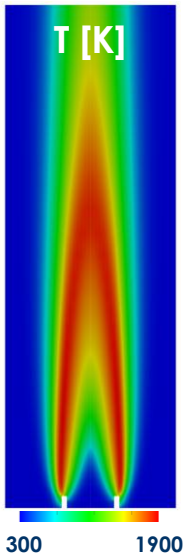

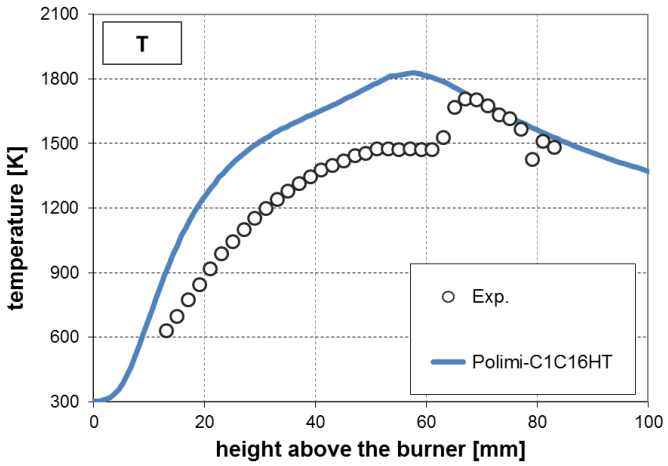

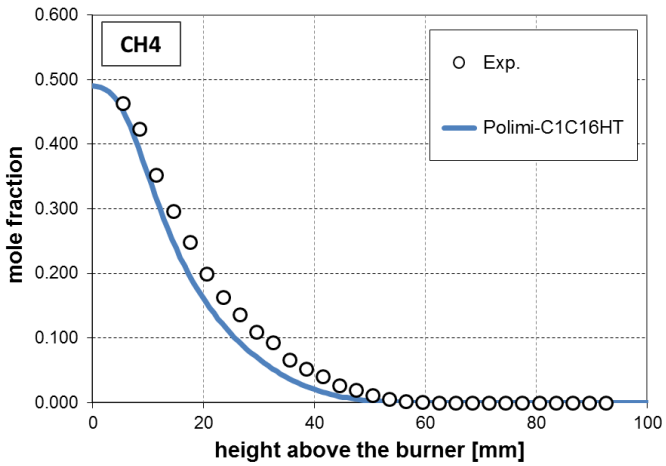

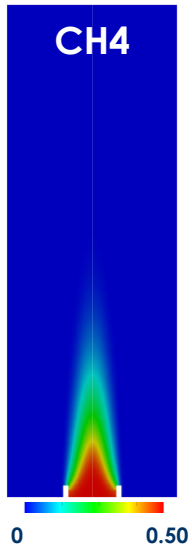

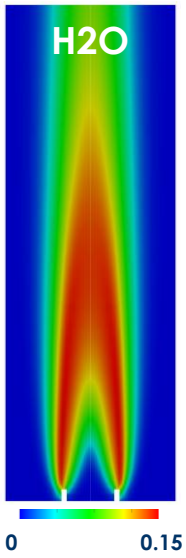

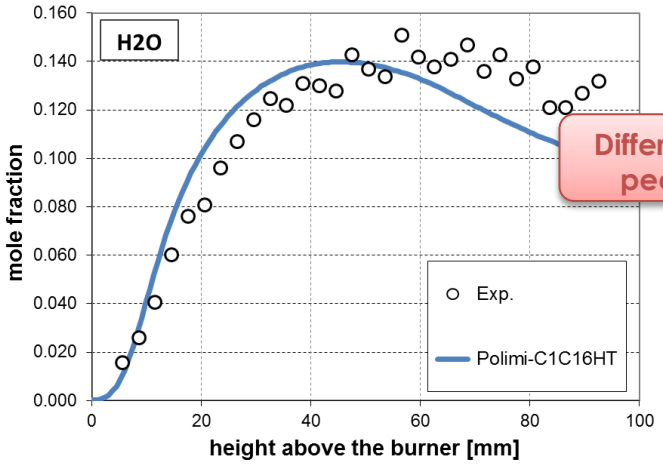

Differences in the peak position

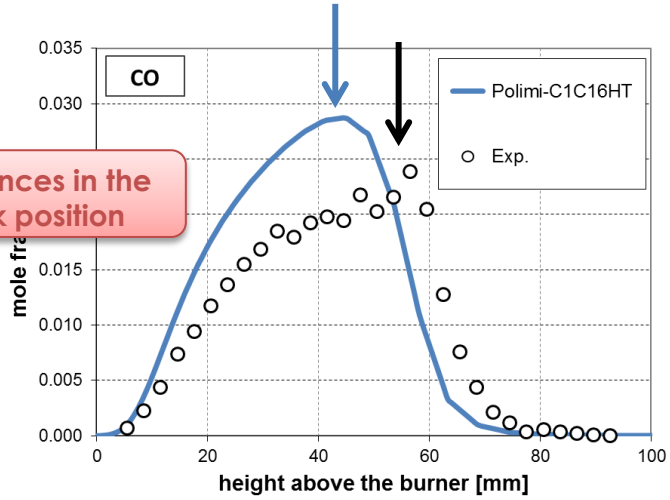

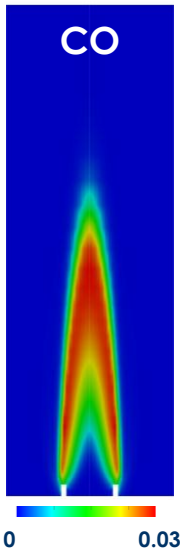

Flame F1: inaccuracies in the flow rates

- deviations can be attributed to **inaccuracies** in the fuel stream flow rate
- additional simulations were performed by varying the **fuel stream velocity**
- the gas flow rate mainly affects the flame length and the peak positions, but only marginally their absolute values
- Flat or parabolic velocity profiles resulted in marginal differences

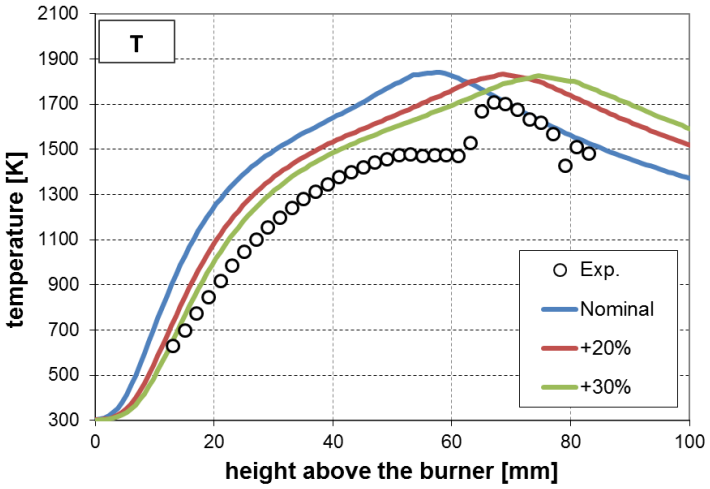

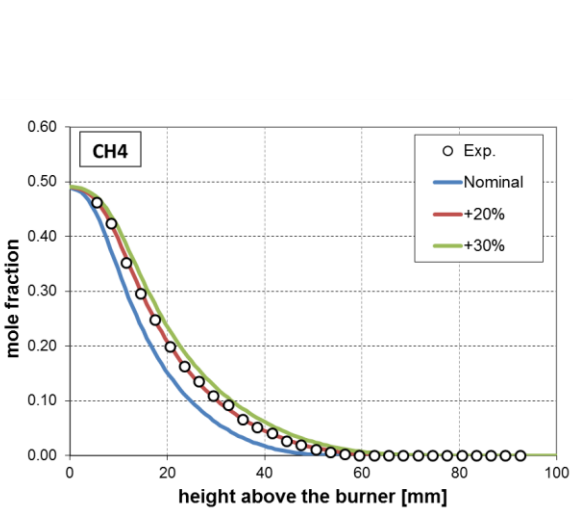

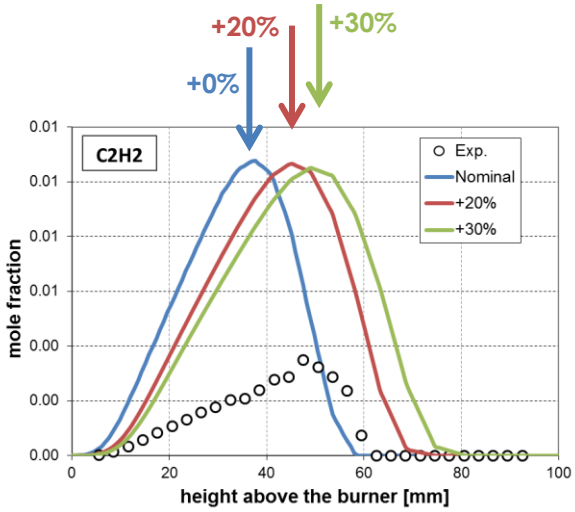

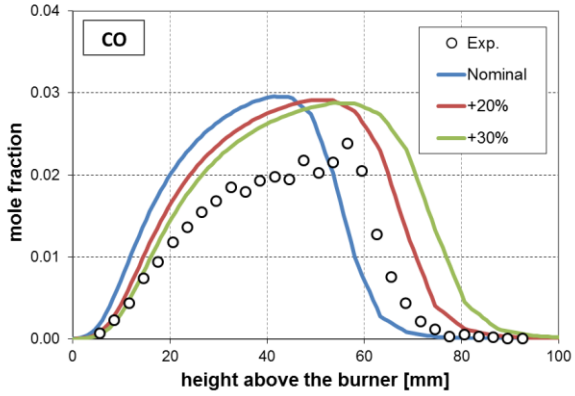

Flame F1: major species

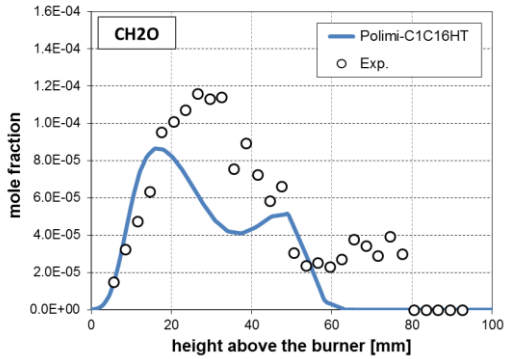

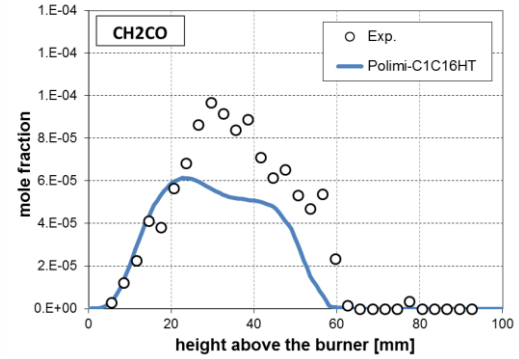

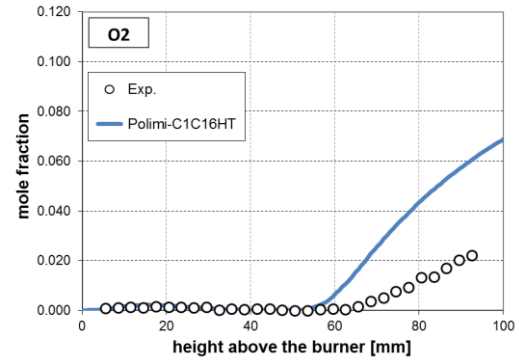

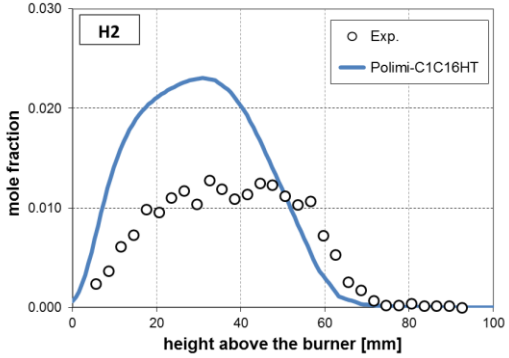

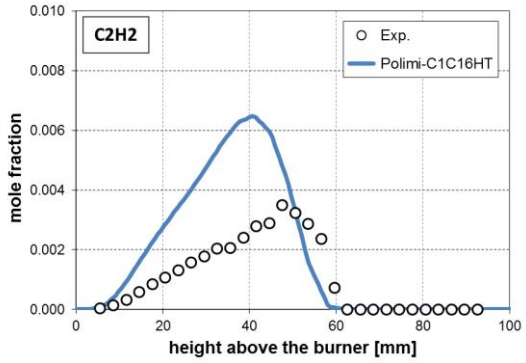

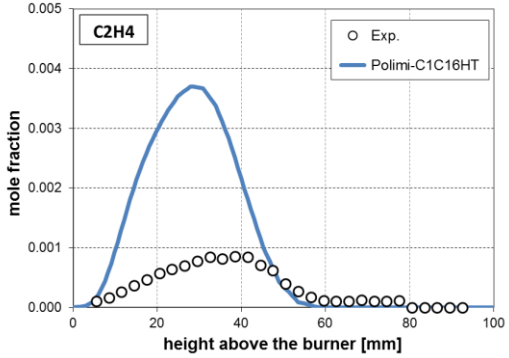

- ✓ The model tends to over-estimate the levels of H_2 and C2 hydrocarbons
- ✓ CH_2O (including the characteristic double peak) and CH_2CO are predicted in a satisfactory way
- ✓ Similar comparisons for flame F2, F3 and F4

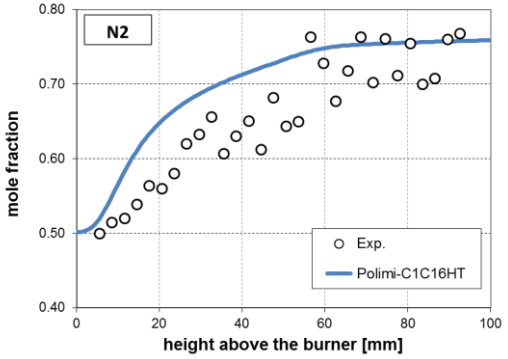

F1 Flame: key PAH precursors and aromatics

Propyne (pC_3H_4)
Allene (aC_3H_4)

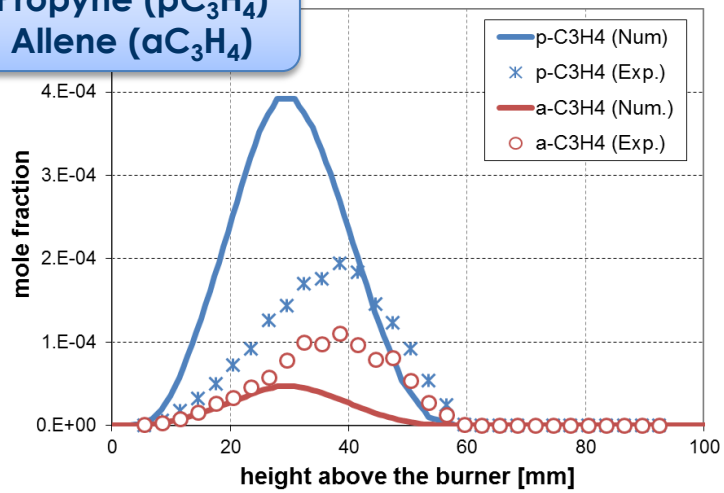

- ✓ **C_3H_4 isomers** are overestimated by a factor of ~2 and this could be attributed to the **overstimation of C_2H_2**
- ✓ **C_6H_6 is overestimated** by a factor ~3
- ✓ The overall agreement is satisfactory, considering the issues related to the flow entrainment and the complexity of the flame

Acetylene (C_2H_2)
Benzene (C_6H_6)

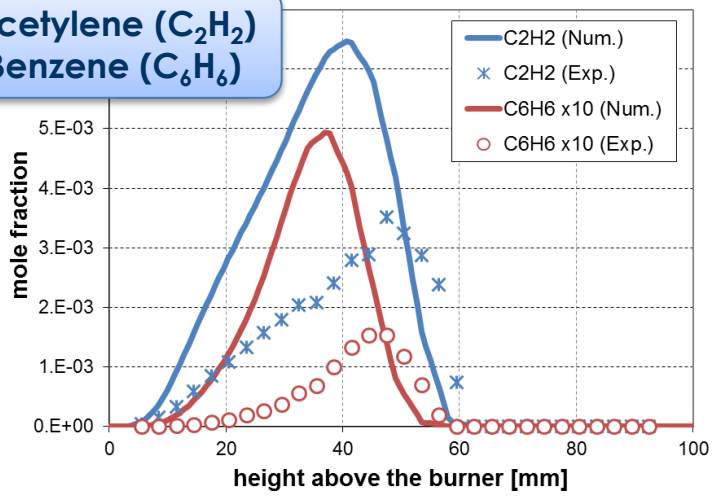

Naphthalene ($C_{10}H_8$)
Acenaphthylene ($C_{12}H_8$)

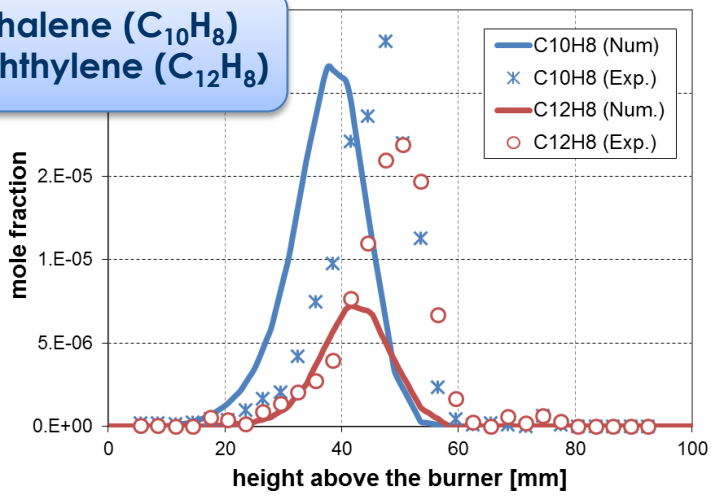

F1 Flame: effect of dilution

The **peak value** of mole fraction profiles along the centerline is reported vs the **content of N_2** in the fuel stream

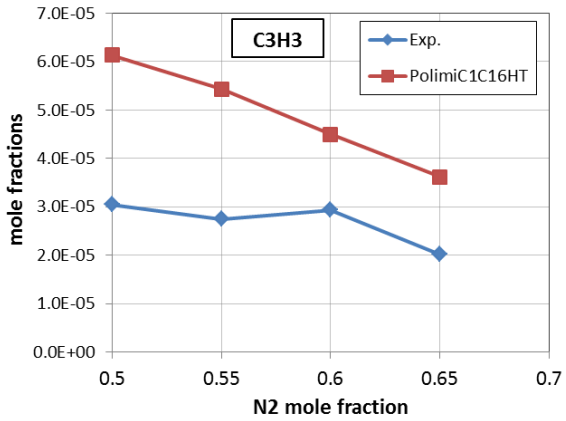

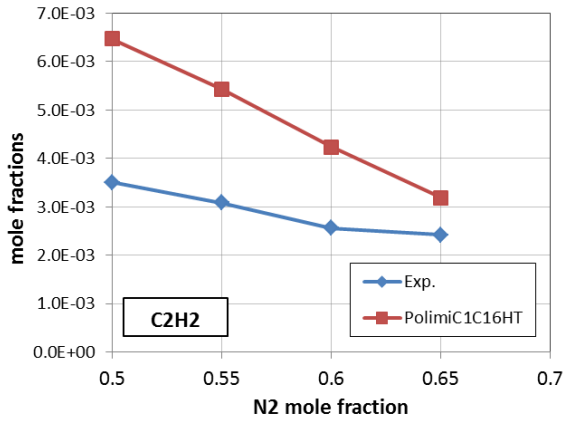

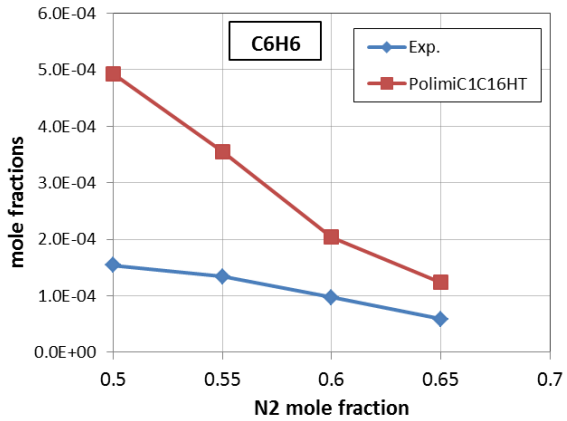

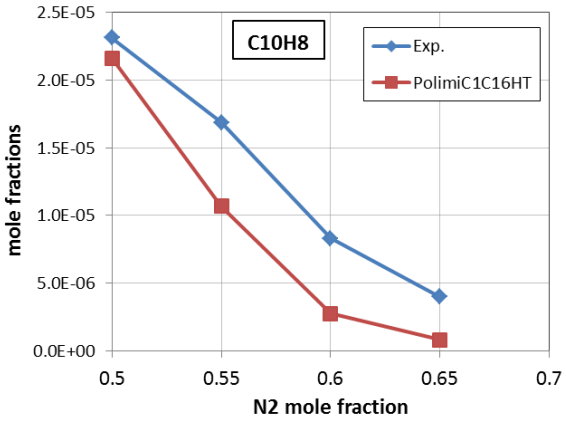

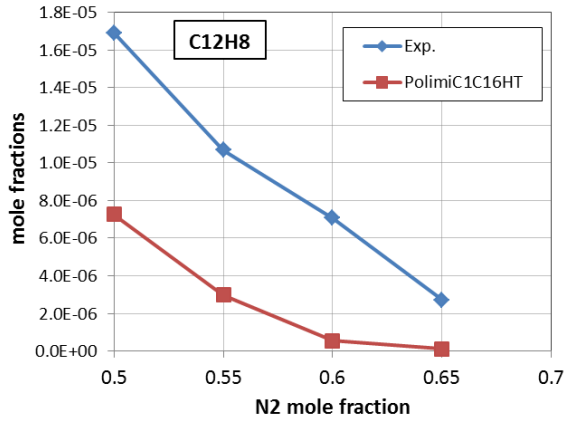

- The effect of dilution on $C_{10}H_8$ and $C_{12}H_8$ is quite strong, leading to a reduction of such species
- The imapct of dilution on C_2H_2 and C_6H_6 is over-predicted by the model

Outline

- ✓ Experimental methods
- ✓ Numerical simulations
  - ✓ Mathematical model
  - ✓ Numerical methodology
- ✓ Comparison between experimental data and numerical results
- ✓ **Kinetic analysis of PAHs formation**
  - ✓ Reaction paths to PAHs
  - ✓ Formation of naphthalene
- ✓ Conclusions

Major reaction paths (Flame F1)

pC_3H_4 is formed in significant amount via the (reverse) reaction[a]:

$pC_3H_4+H=CH_3+C_2H_2$

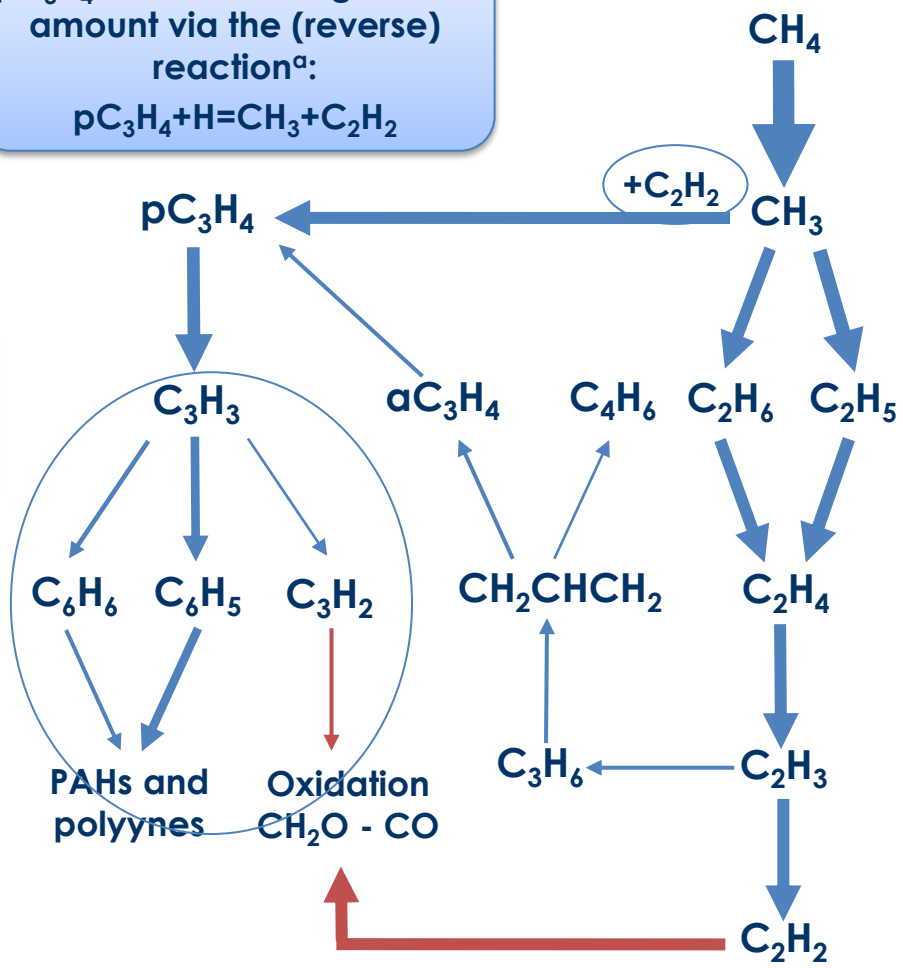

C_3H_3 is the main responsible of formation of aromatic species

Important role of CH_3 radicals, leading to formation of ethylene and acetylene

[a] **Hikada et al.,** International Journal of Physical Chemistry, 21 (1989), pp. 643-666

McEnally et al., Comb. Flame, 117 (1999), pp. 362-372

D'Anna, et al., Combustion and Flame, 132 (2003), pp. 715-722

Minor reaction paths to PAHs (Flame F1)

$C_{10}H_8$ is mainly formed by C_7H_7 + C_3H_3 and also by the interaction between $C_{10}H_7CH_2$ with CH_3 (in competition with formation of indenyl radicals)

$C_2H_2+C_6H_5=C_6H_5C_2H+H$ is the main reaction leading to formation of phenyl-acetylene

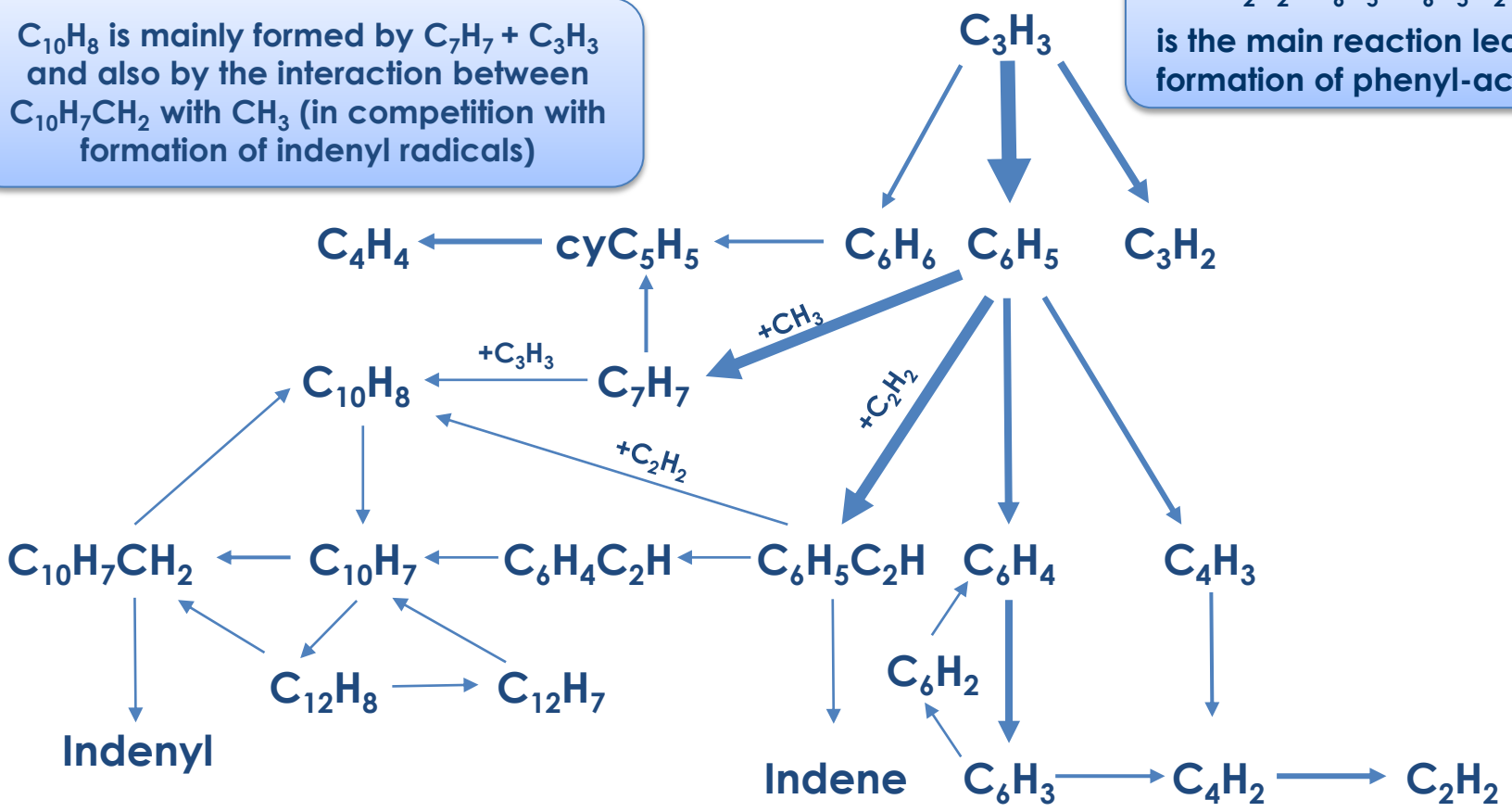

McEnally et al., Progress in Energy and Combustion Science, 32 (2006), pp. 247-294

C_4H_2 and C_6H_2 are formed mainly via C_6H_4

Formation of naphthalene

Naphtlanene ($C_{10}H_8$) was formed by the reaction of benzyl (C_7H_7) with propargyl (C_3H_3)

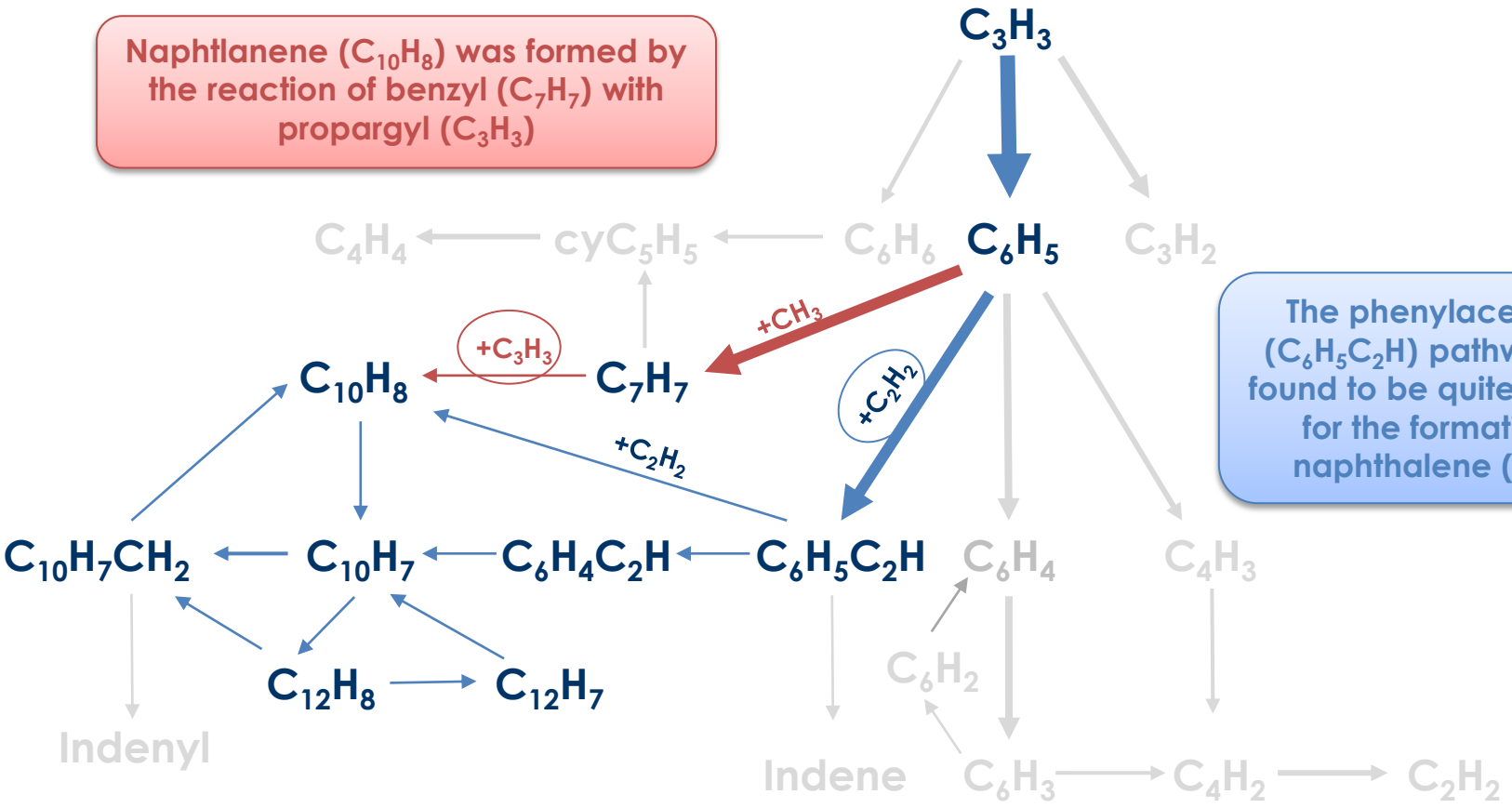

The phenylacetylene ($C_6H_5C_2H$) pathway was found to be quite relevant for the formation of naphthalene ($C_{10}H_8$)

Marinov, et al., Proceedings of the Combustion Institute, 22 (1998), pp. 605-613

D'Anna, et al., Combustion and Flame, 132 (2003), pp. 715-722

Wang, et al., Journal of Physical Chemistry, 98 (1994), pp. 11465-11489

Anderson, et al., Proceedings of the Combustion Institute, 28 (2000), pp. 2577-2583

Sensitivity analysis for naphthalene

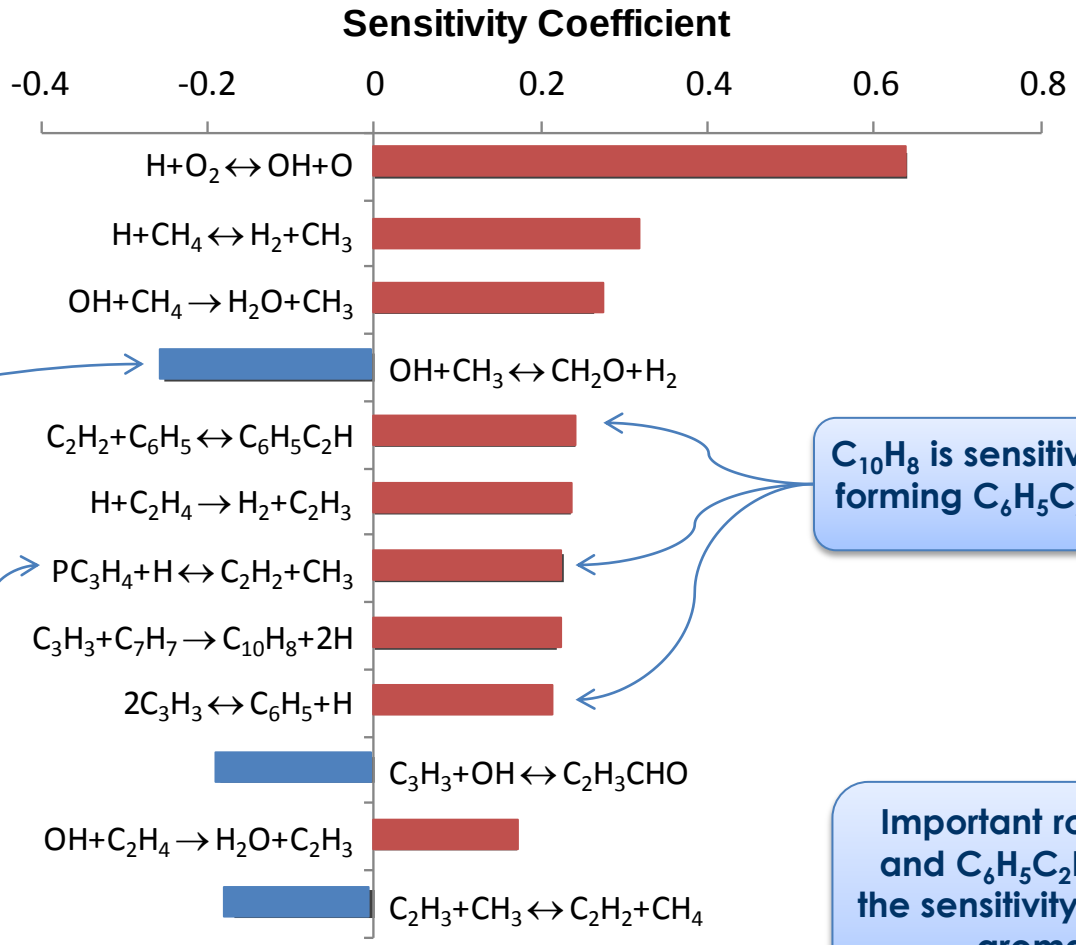

Competition between CH_3 oxidation and the reaction with acetylene forming propyne

$C_{10}H_8$ is sensitive to the reactions forming $C_6H_5C_2H$, C_2H_2 and C_6H_5

Important role of pC_3H_4, C_3H_3 and $C_6H_5C_2H$ is confirmed by the sensitivity analyses for other aromatic species

Outline

- ✓ Experimental methods
- ✓ Numerical simulations
  - ✓ Mathematical model
  - ✓ Numerical methodology
- ✓ Comparison between experimental data and numerical results
- ✓ Kinetic analysis of PAHs formation
  - ✓ Reaction paths to PAHs
  - ✓ Formation of naphthalene
- ✓ **Conclusions**

Conclusions

- ✓ A set of coflow CH_4 diffusion flames was studied using **synchrotron VUV photoionization mass spectrometry** (PIMS) to measure C1/C2 species, unsatured C3-C6 species and first aromatics

- ✓ A **multidimensional code** for reacting, laminar flows with detailed chemistry was developed

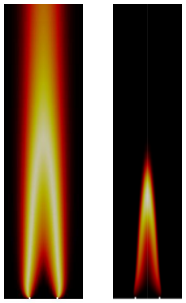

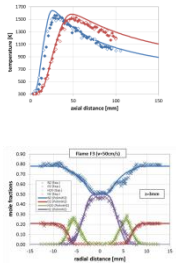

- ✓ The numerical simulations were used to better **interpret the experimental measurements**

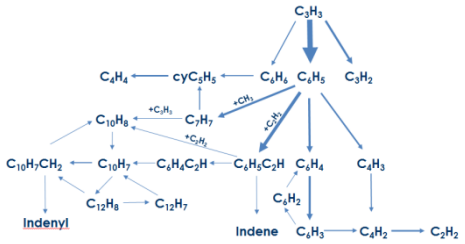

Perspectives

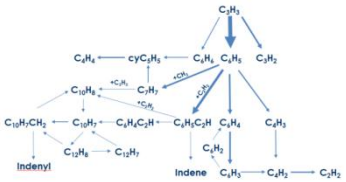

Interpretation of numerical/exp results

Experimental measurements

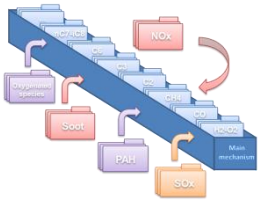

Refinement of the kinetic mechanism

- ✓ Numerical modeling of soot formation in the investigated flames

Acknowledgements

- Financial support for POLIMI activity was provided by the MIUR under the **PRIN 2008 framework**: "Cinetica dettagliata di formazione di idrocarburi poliaromatici e nanoparticelle da processi di combustione"

- Prof. Fei Qi thanks the support of **National Basic Research Program of China** (973 Program, 2012CB719701) and the **Natural Science Foundation of China** (50925623)

- The authors acknowledge **Prof. Eliseo Ranzi** of Politecnico di Milano for his comments and suggestions

Additional slides

CH4 flames (Qi)

- ✓ Comparisons with GRI30
- ✓ CH2O and CH2CO
- ✓ Temperature
- ✓ CH4
- ✓ O2
- ✓ H2O
- ✓ CO2
- ✓ CO
- ✓ H2
- ✓ C2H2
- ✓ C2H4
- ✓ CH2O
- ✓ CH2CO
- ✓ N2
- ✓ C3H3 and C5H6
- ✓ pC3H4 and aC3H4
- ✓ C6H6 and C12H8
- ✓ C7H8 and C10H8
- ✓ C4H4 and C4H6
- ✓ C4H2 and C6H2
- ✓ Grid sensitivity
- ✓ Parabolic vs flat profile
- ✓ Radiative heat transfer

CH4 McEnally Flames

- ✓ Phi = 12
- ✓ Phi = 6
- ✓ Phi = 4
- ✓ Phi = 3
- ✓ Phi = 2

C2H4 McEnally Flames

CH4 Lifted Flame

C2H4/CH4 RoeslerFlames

Flame F1: major species

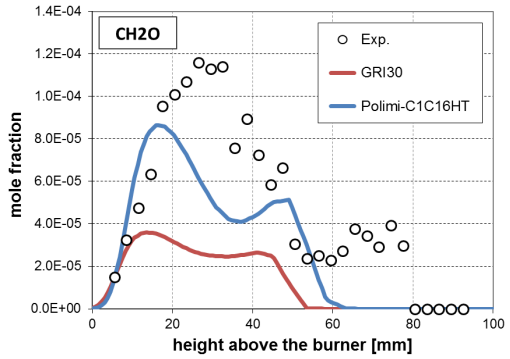

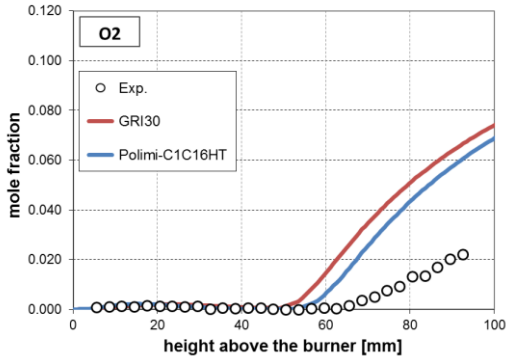

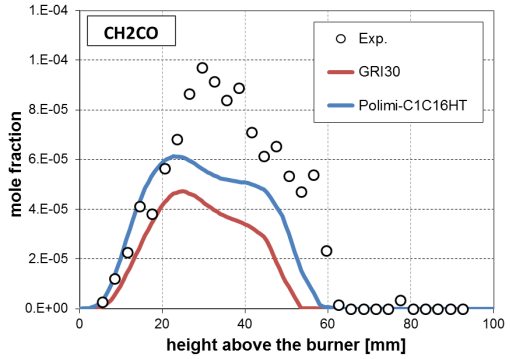

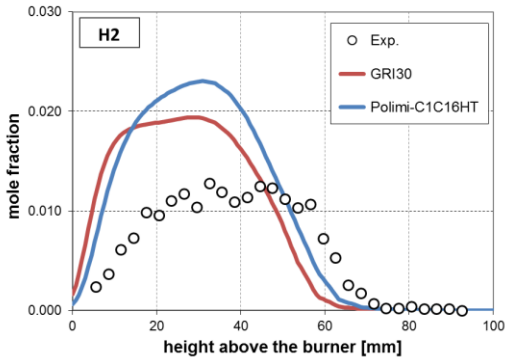

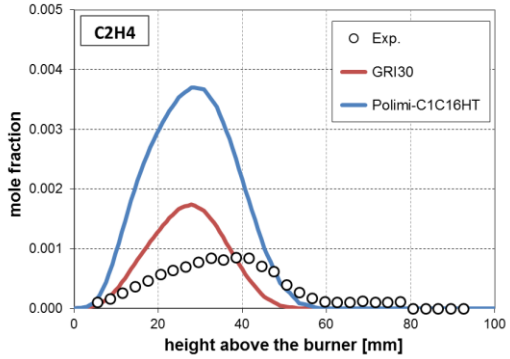

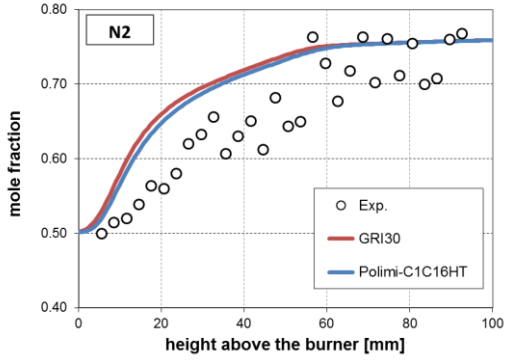

- ✓ The model tends to over-estimate the levels of H_2 and C2 hydrocarbons
- ✓ CH_2O (including the characteristic double peak) and CH_2CO are predicted in a satisfactory way
- ✓ Similar comparisons for flame F2, F3 and F4

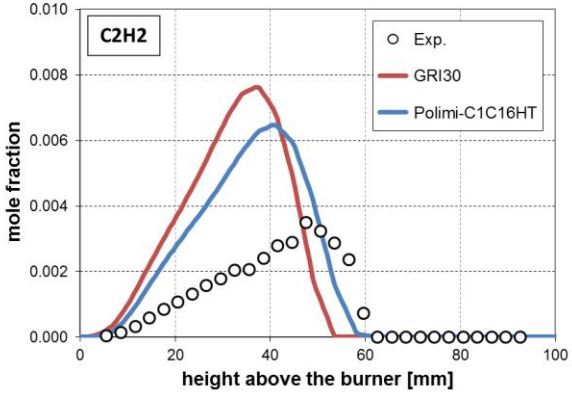

CH_2O and CH_2CO

Formaldehyde (Flame F1)

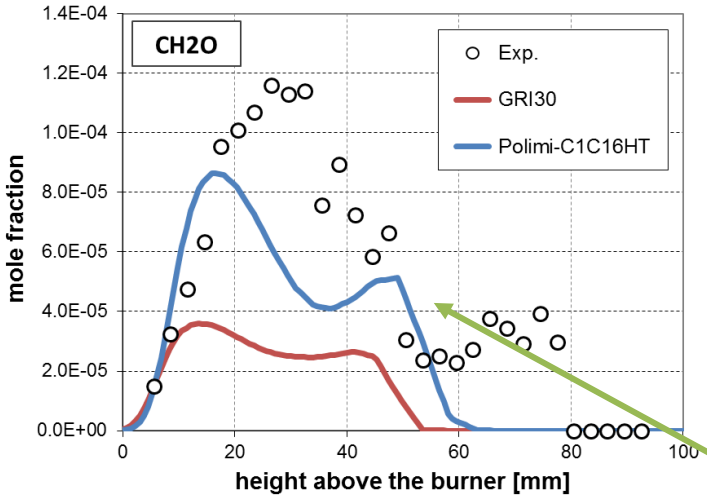

Ketene (Flame F1)

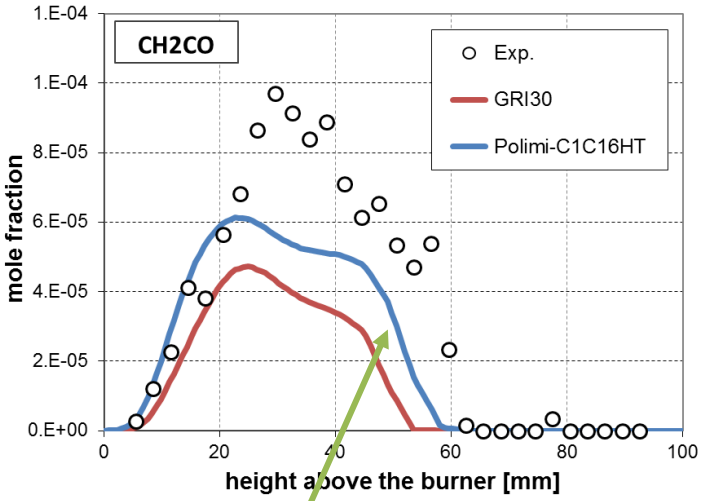

Formaldehyde is mainly formed via ketene and through the reactions:

CH3+OH=CH2O+H2

and

CH3+OH=CH2OH+H

(followed by CH2OH decomposition)

The consumption of ketene is associated to the second peak in the profile of the formaldehyde

Temperature

Flame F1 (50% N_2)

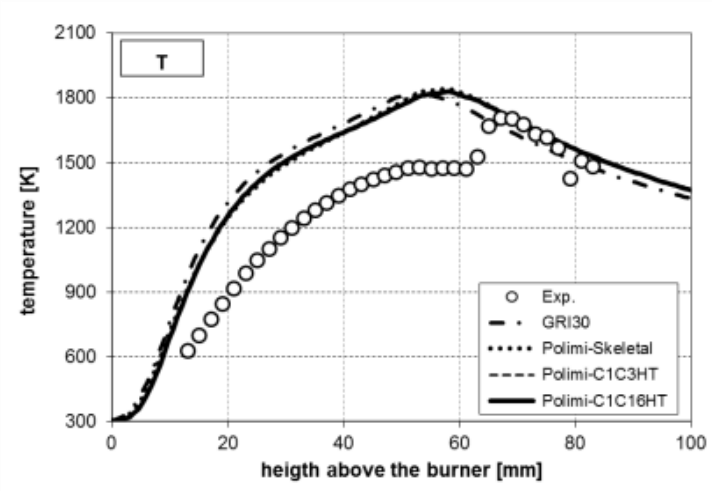

Flame F2 (55% N_2)

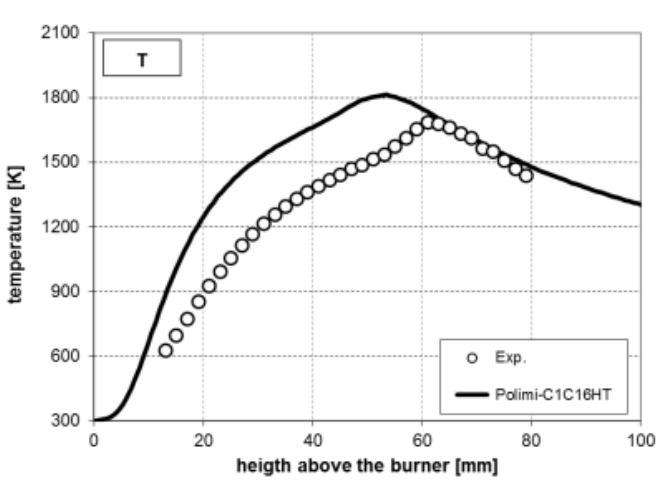

Flame F3 (60% N_2)

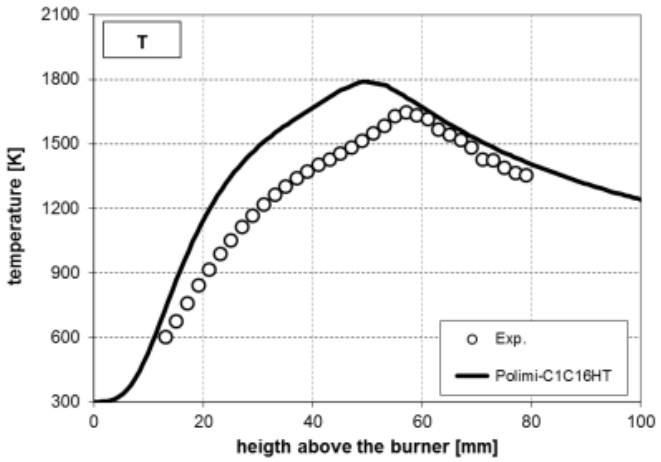

Flame F4 (65% N_2)

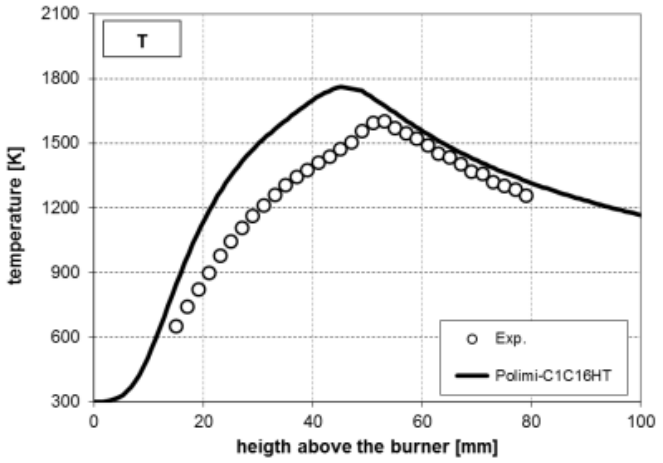

CH4

Flame F1 (50% N_2)

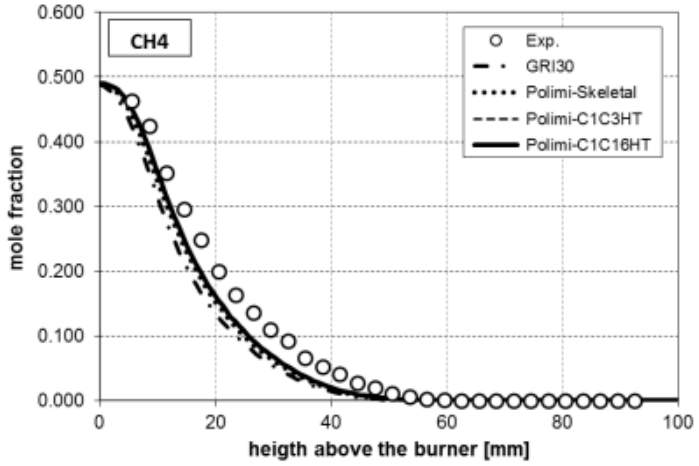

Flame F2 (55% N_2)

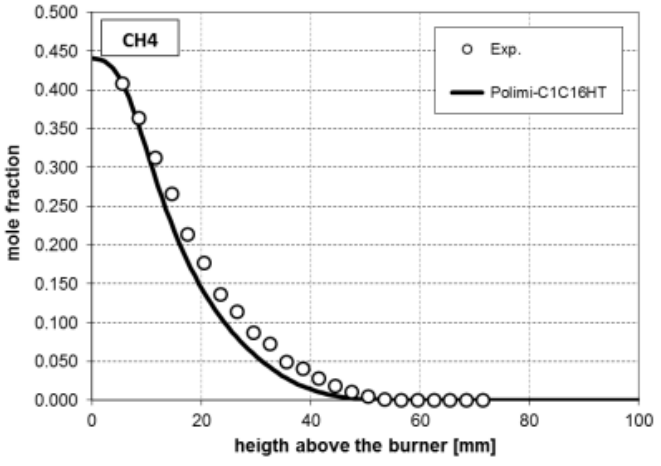

Flame F3 (60% N_2)

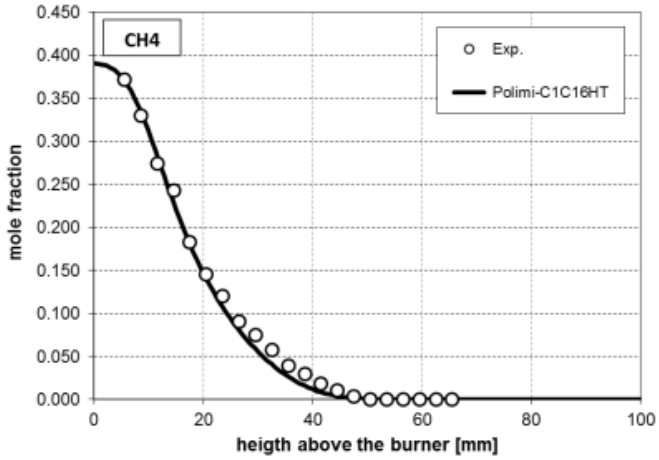

Flame F4 (65% N_2)

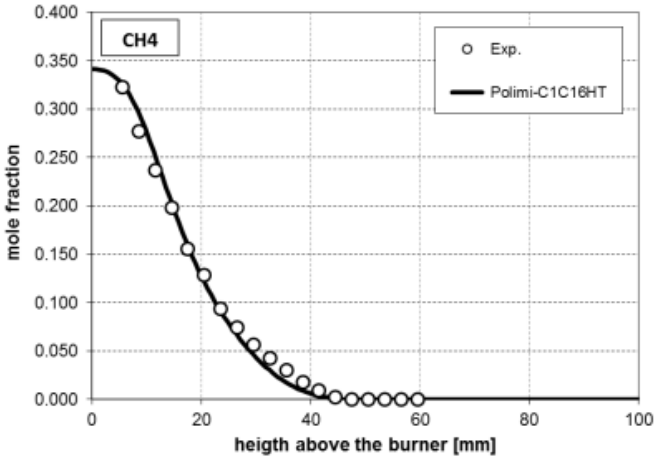

Flame F1 (50% N_2)

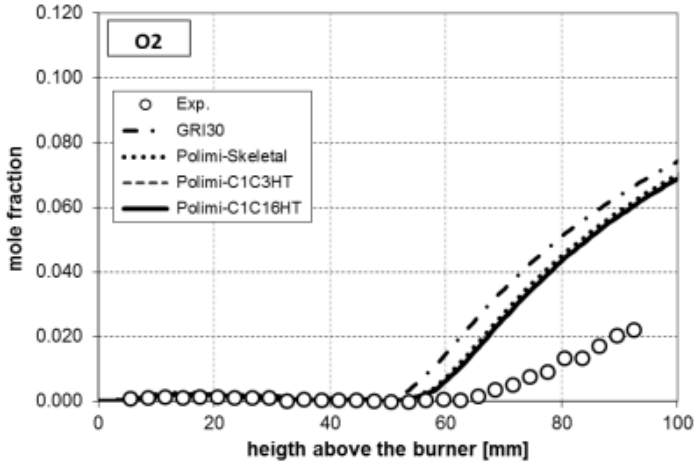

Flame F2 (55% N_2)

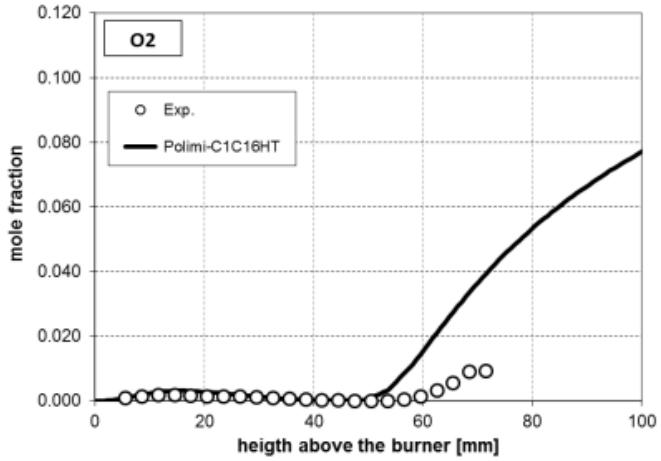

Flame F3 (60% N_2)

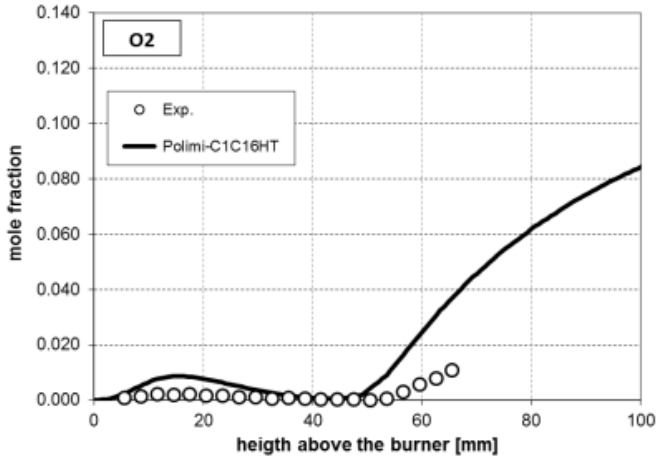

Flame F4 (65% N_2)

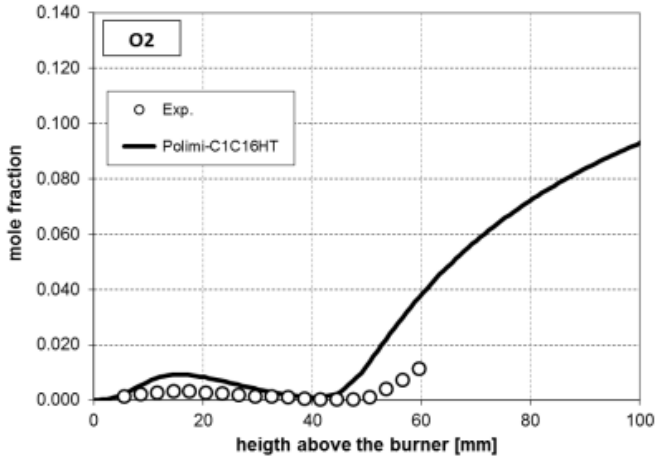

H2O

Flame F1 (50% N_2)

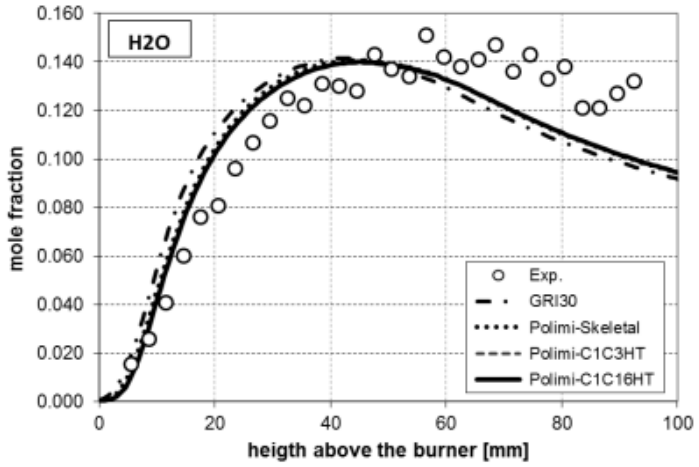

Flame F2 (55% N_2)

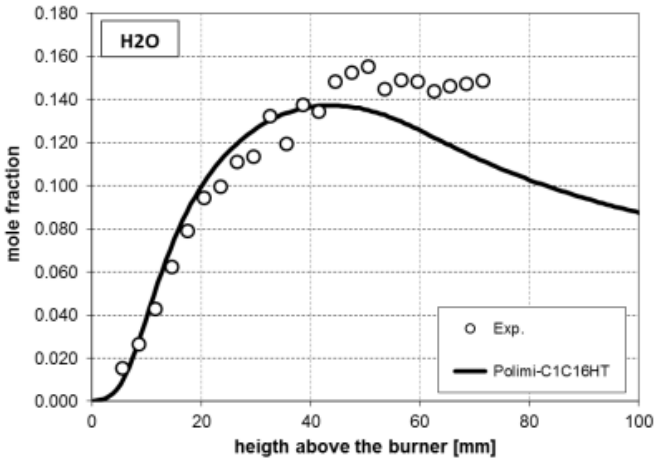

Flame F3 (60% N_2)

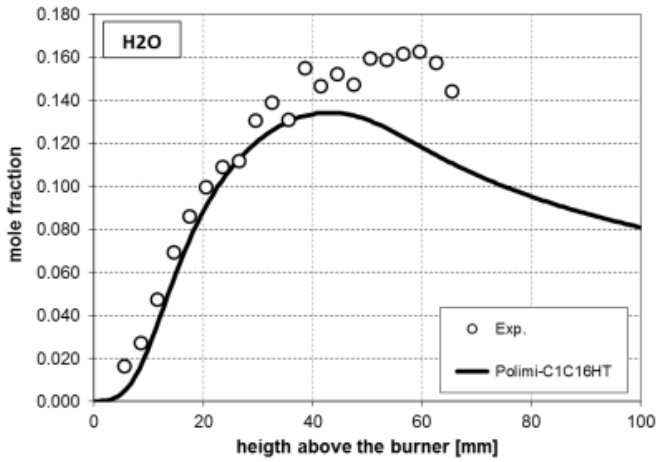

Flame F4 (65% N_2)

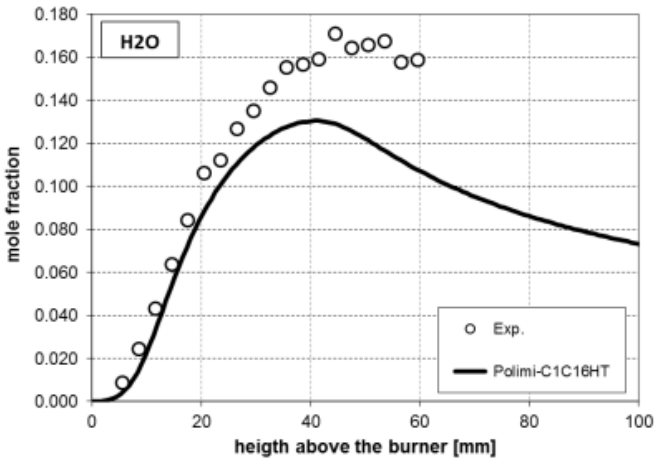

CO2

Flame F1 (50% N_2)

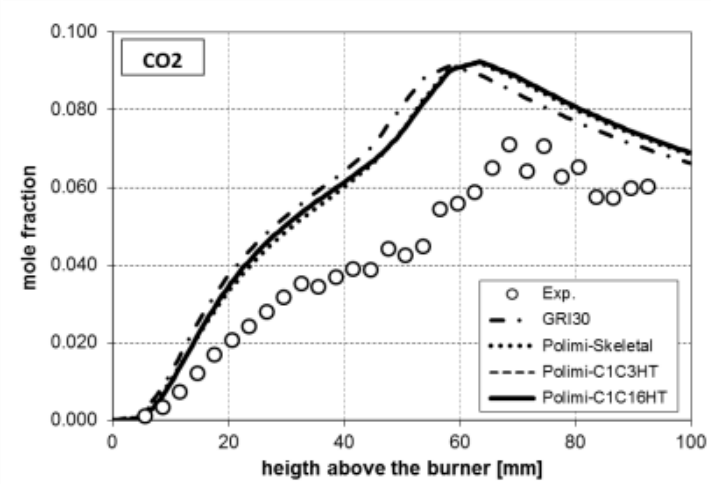

Flame F2 (55% N_2)

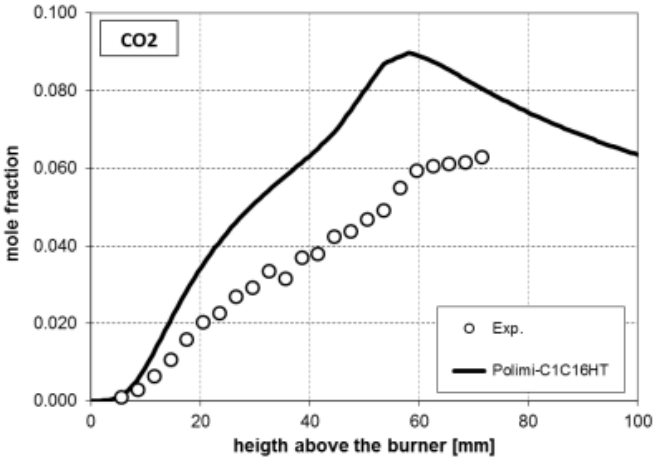

Flame F3 (60% N_2)

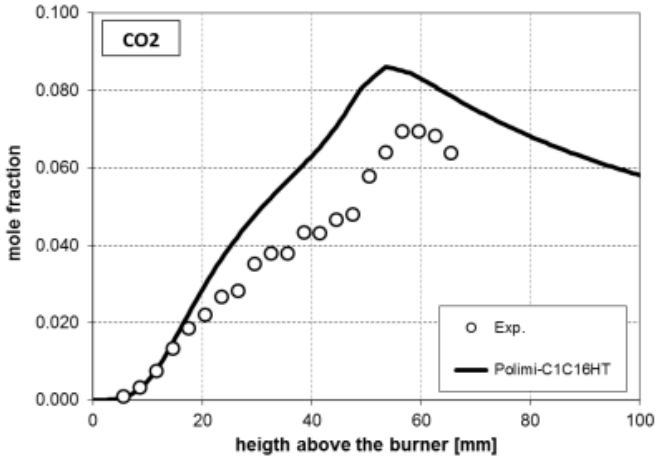

Flame F4 (65% N_2)

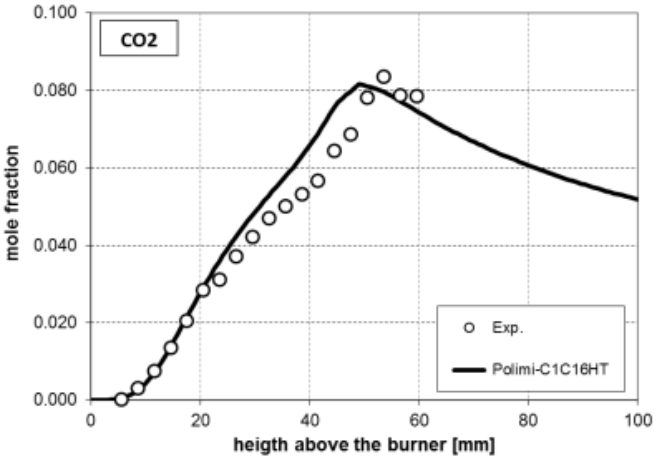

CO

Flame F1 (50% N_2)

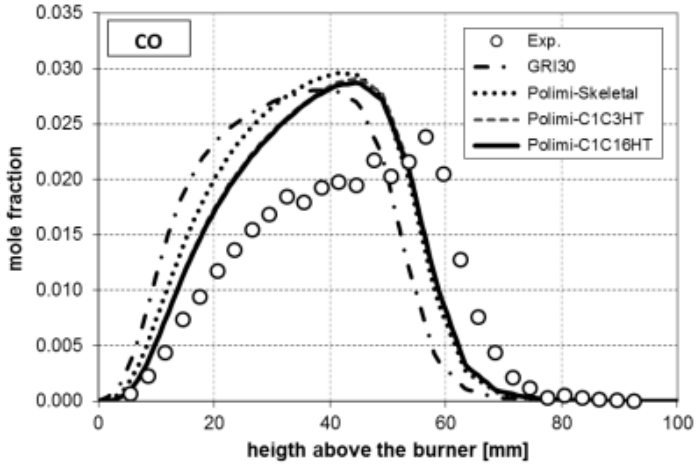

Flame F2 (55% N_2)

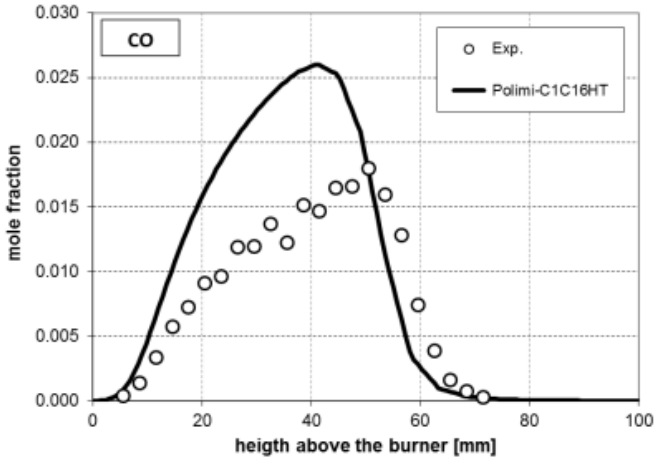

Flame F3 (60% N_2)

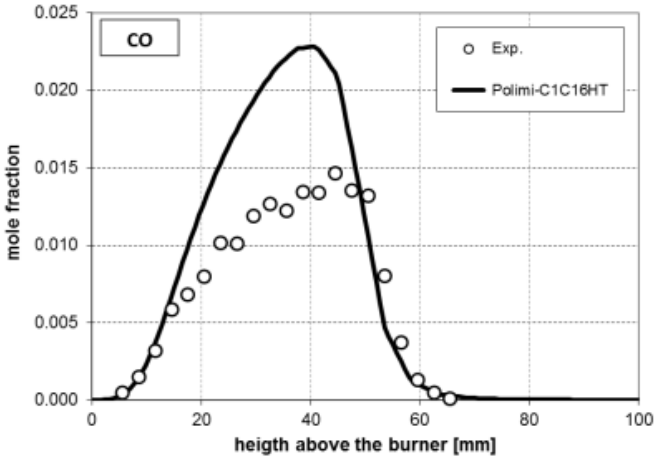

Flame F4 (65% N_2)

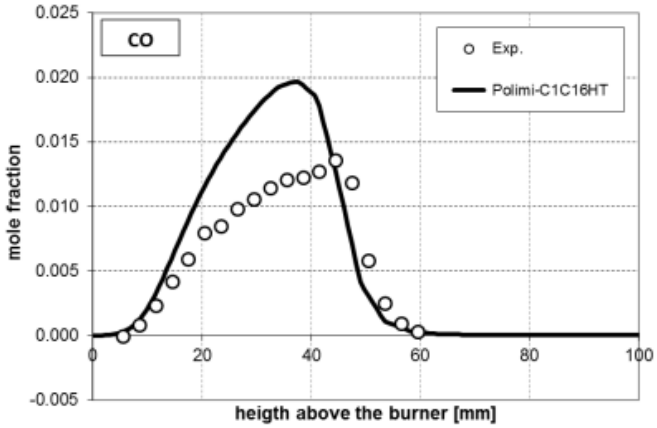

H2

Flame F1 (50% N_2)

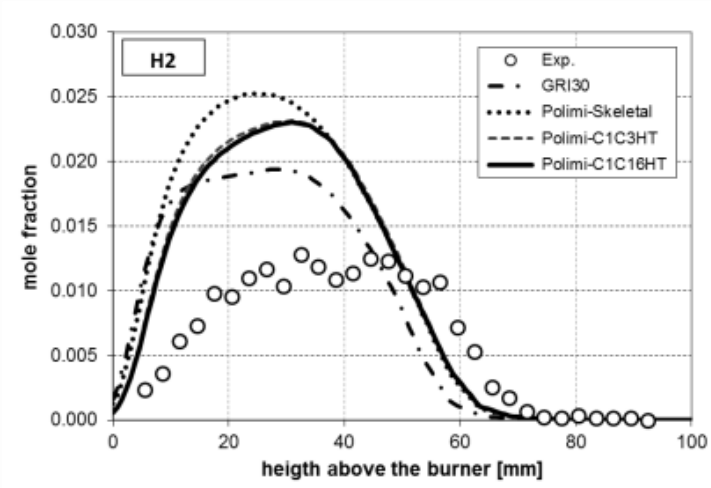

Flame F2 (55% N_2)

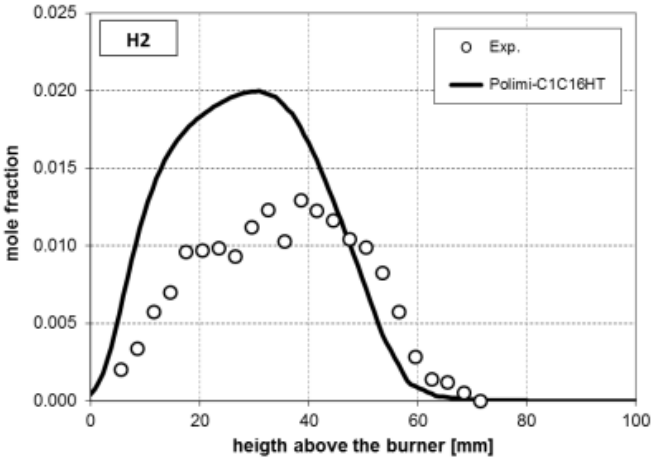

Flame F3 (60% N_2)

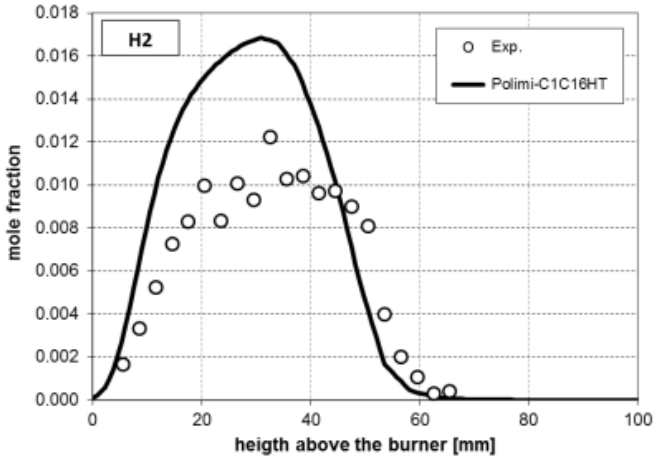

Flame F4 (65% N_2)

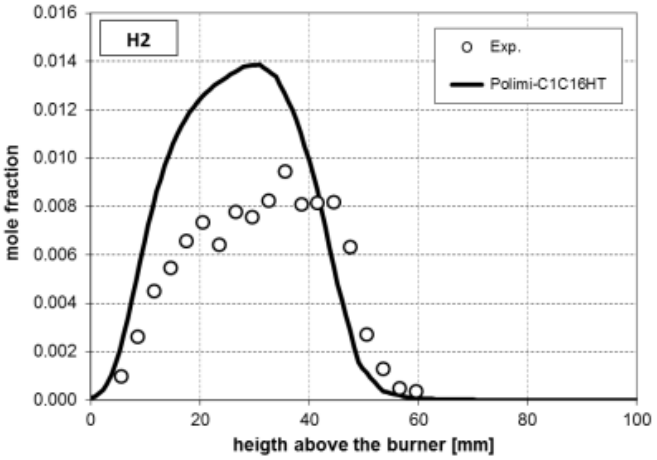

C2H2

Flame F1 (50% N_2)

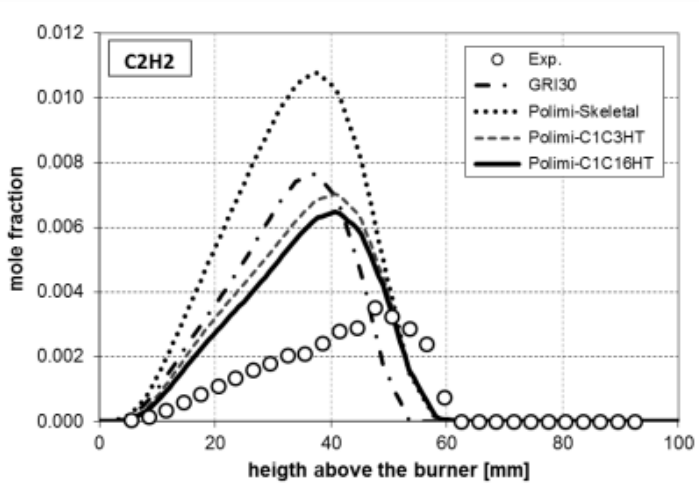

Flame F2 (55% N_2)

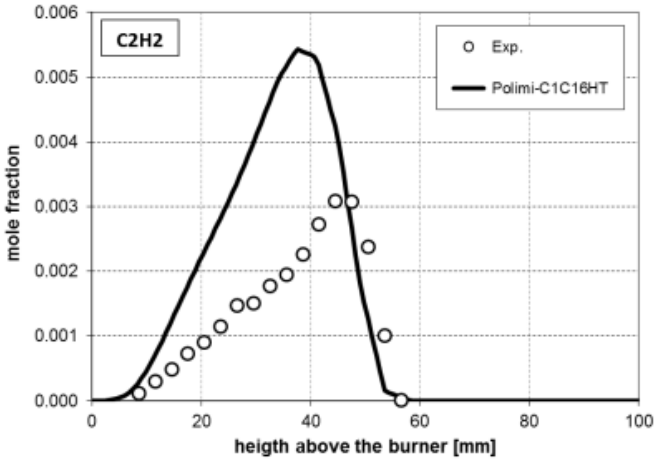

Flame F3 (60% N_2)

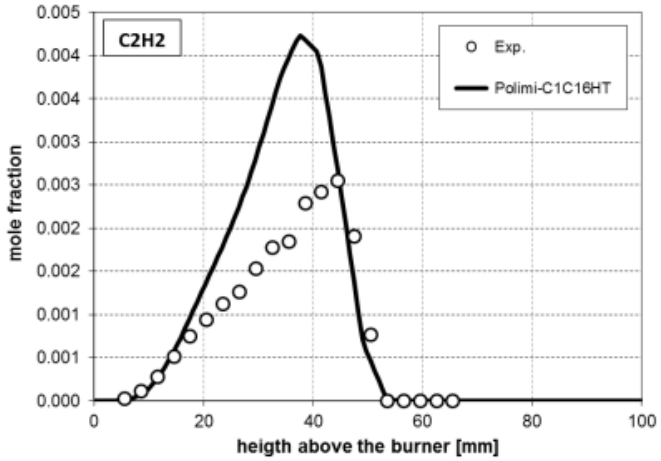

Flame F4 (65% N_2)

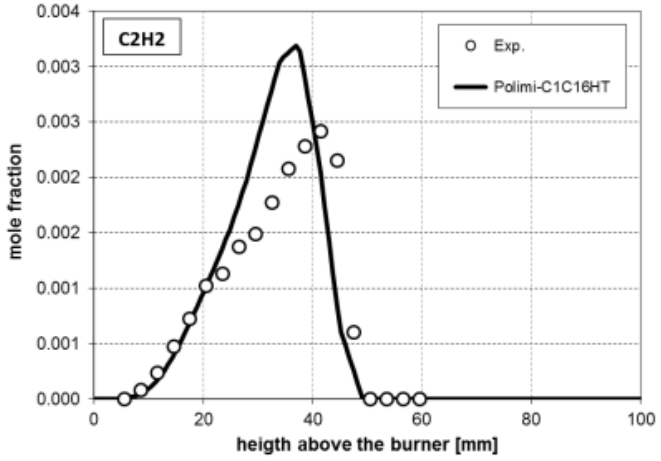

C2H4

Flame F1 (50% N_2)

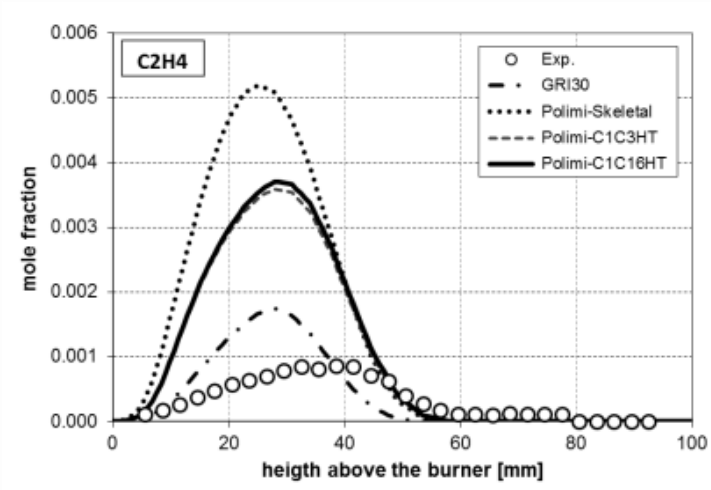

Flame F2 (55% N_2)

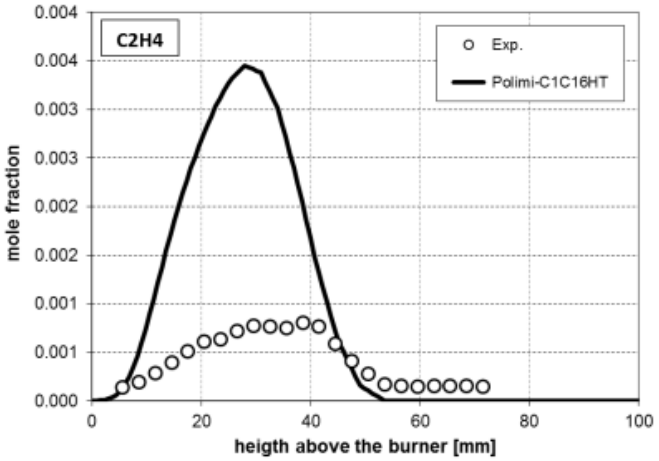

Flame F3 (60% N_2)

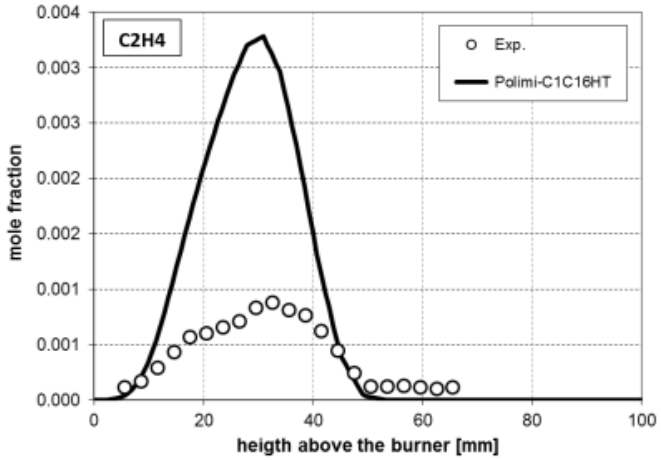

Flame F4 (65% N_2)

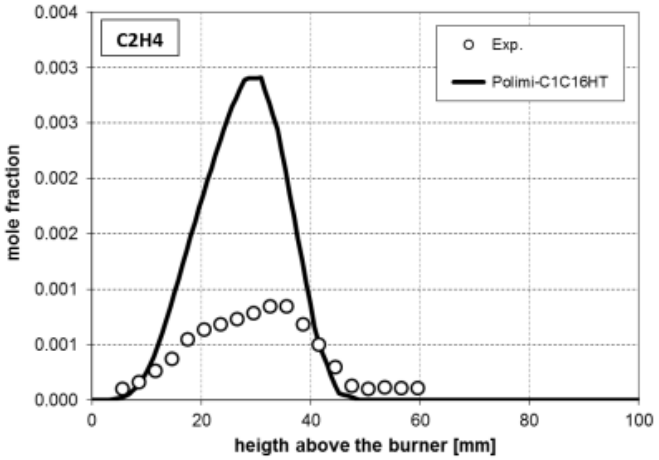

CH2O

Flame F1 (50% N_2)

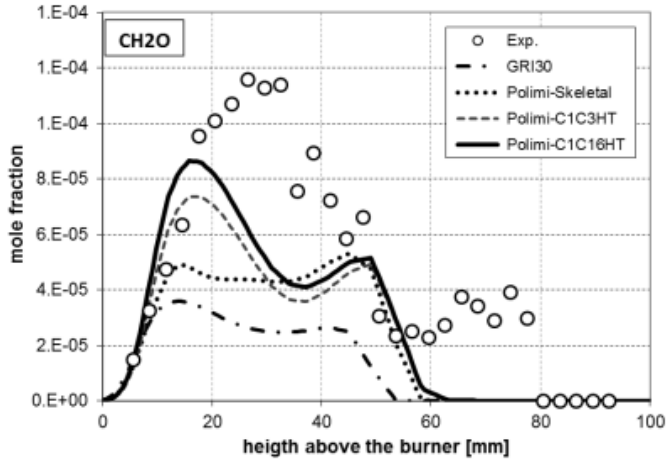

Flame F2 (55% N_2)

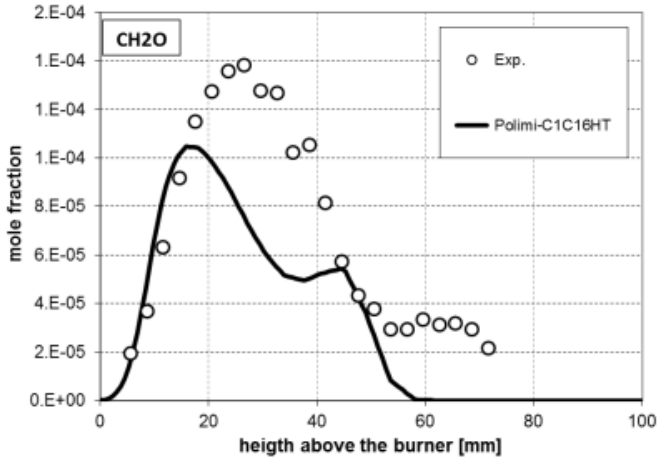

Flame F3 (60% N_2)

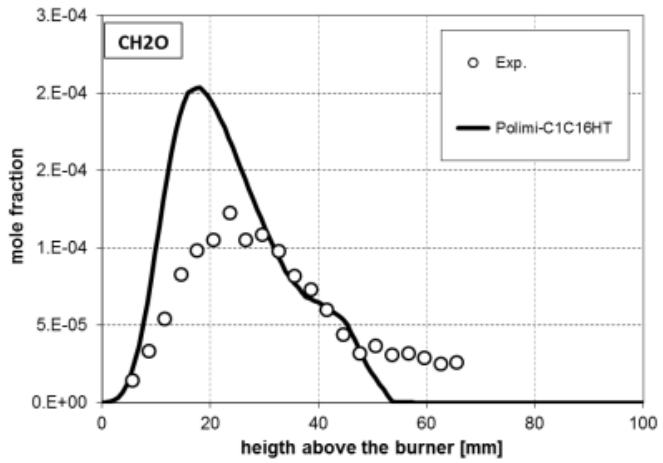

Flame F4 (65% N_2)

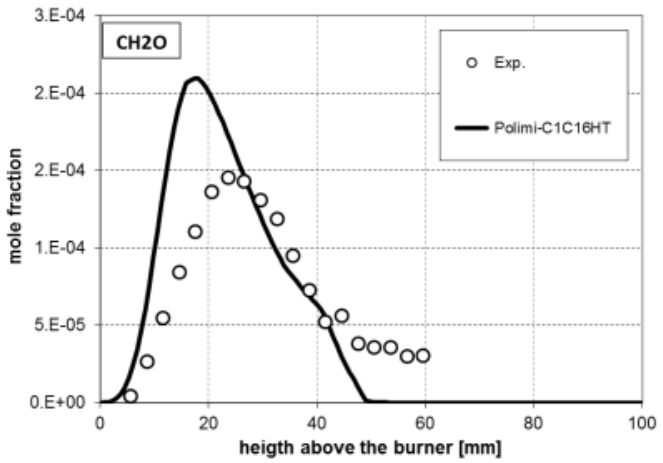

CH2CO

Flame F1 (50% N_2)

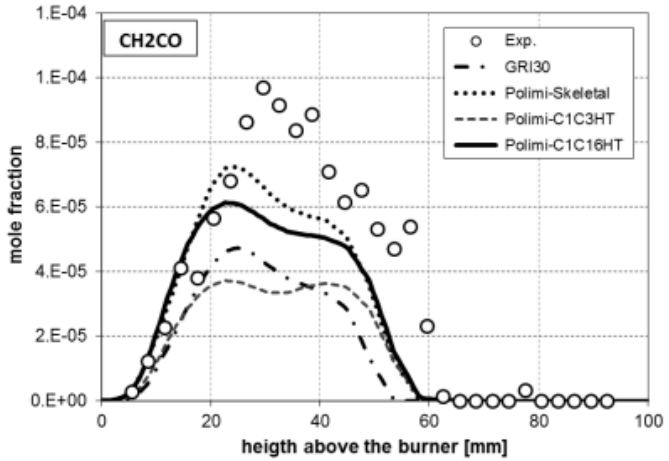

Flame F2 (55% N_2)

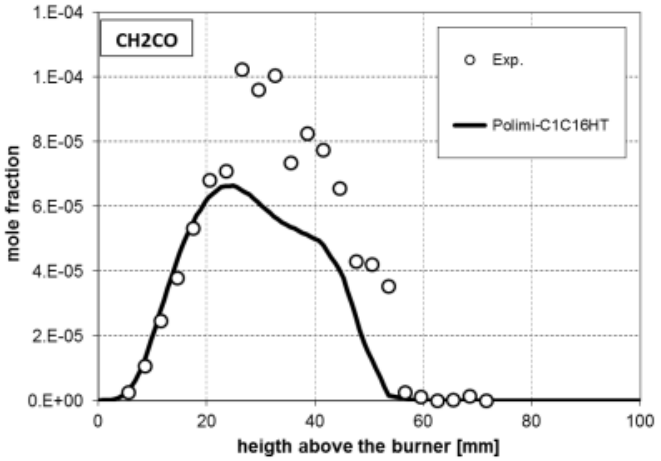

Flame F3 (60% N_2)

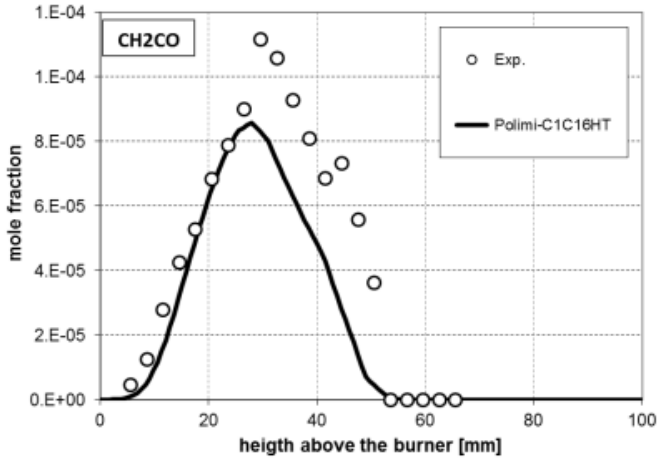

Flame F4 (65% N_2)

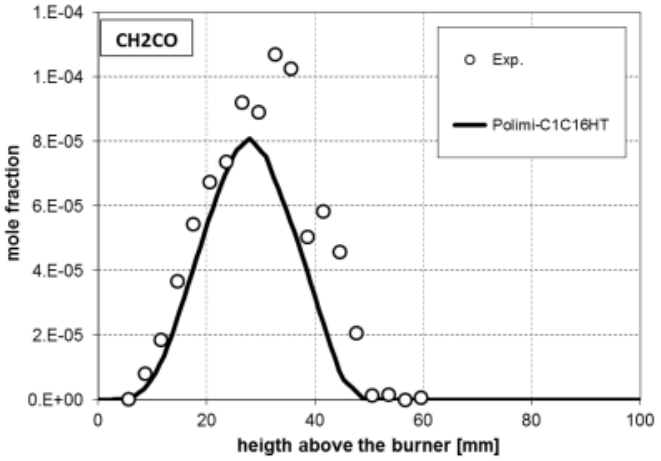

N2

Flame F1 (50% N_2)

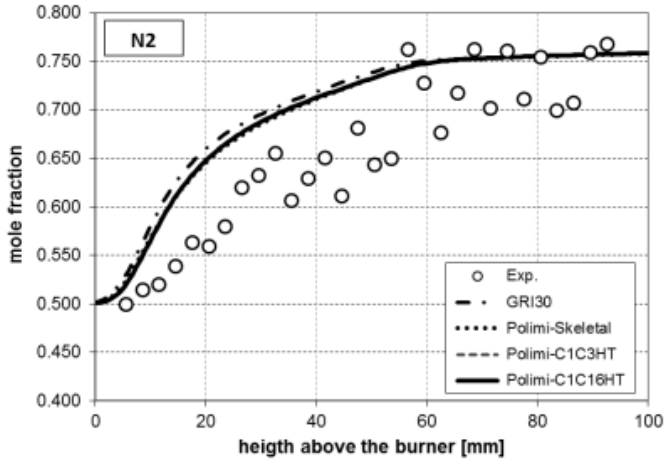

Flame F2 (55% N_2)

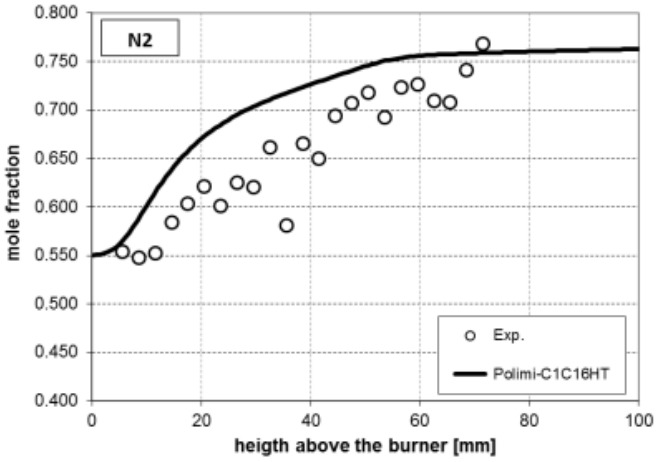

Flame F3 (60% N_2)

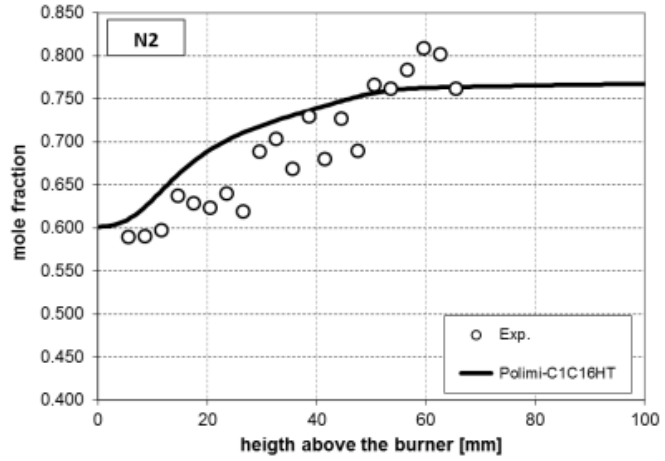

Flame F4 (65% N_2)

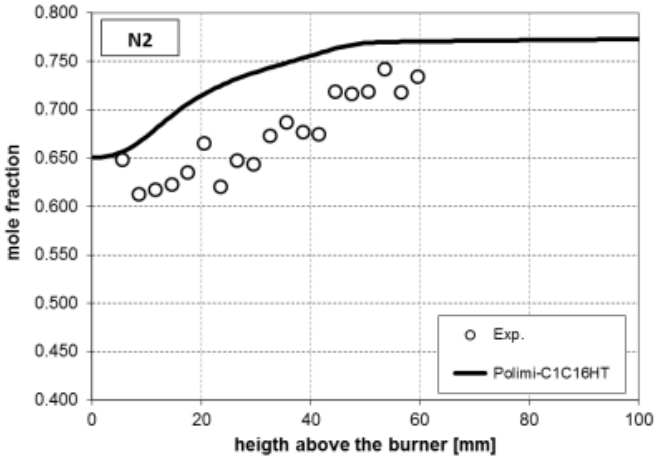

C_3H_3 (propargyl) and C_5H_6 (1,3-cyclopentadiene)

Flame F1 (50% N_2)

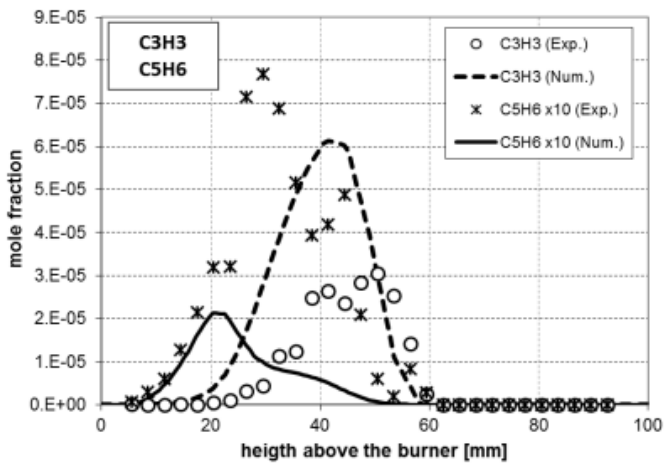

Flame F2 (55% N_2)

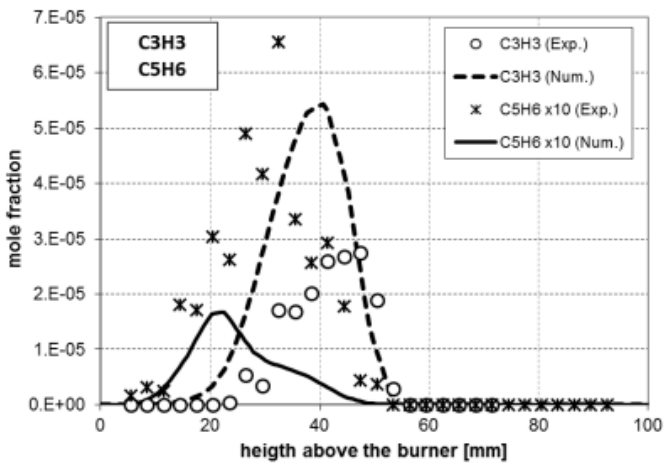

Flame F3 (60% N_2)

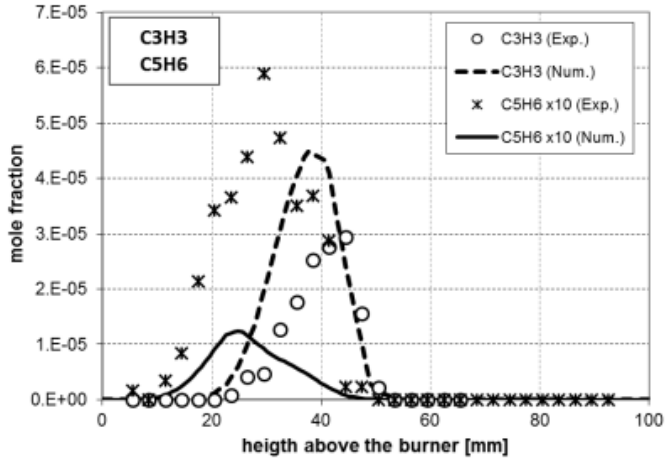

Flame F4 (65% N_2)

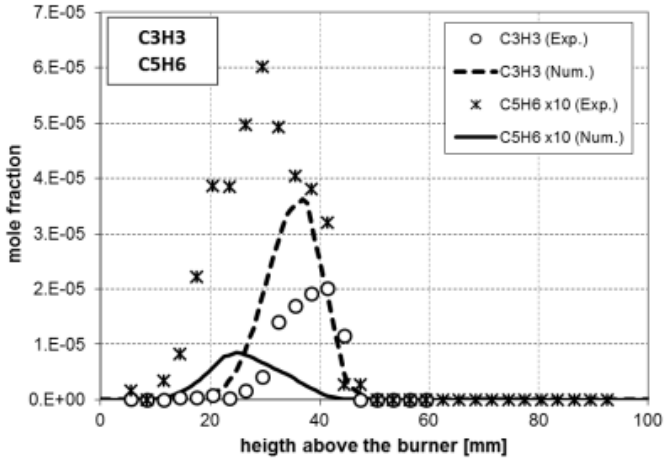

pC_3H_4 (propyne) and aC_3H_4 (allene)

Flame F1 (50% N_2)

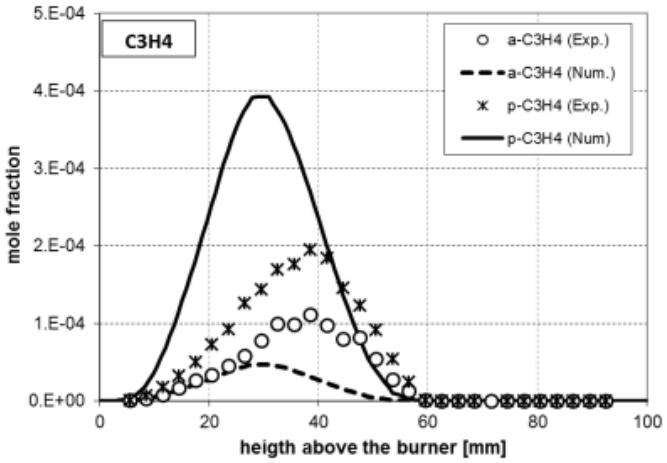

Flame F2 (55% N_2)

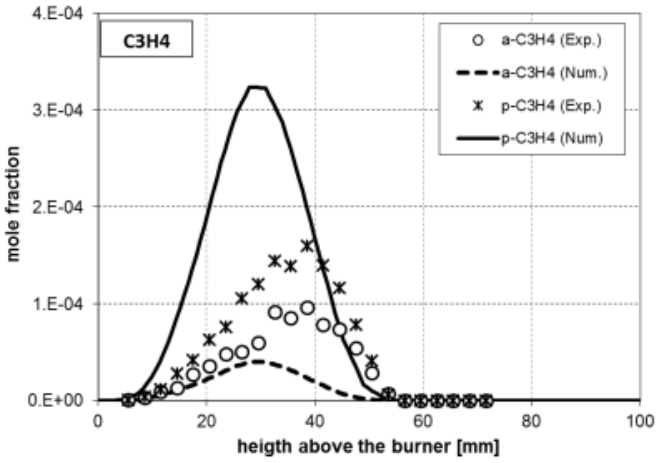

Flame F3 (60% N_2)

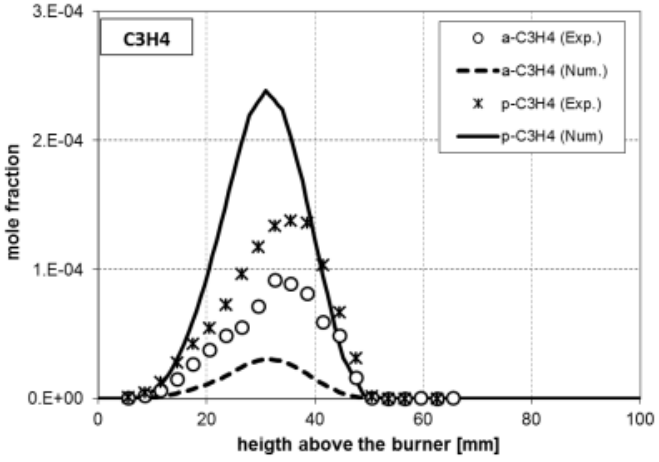

Flame F4 (65% N_2)

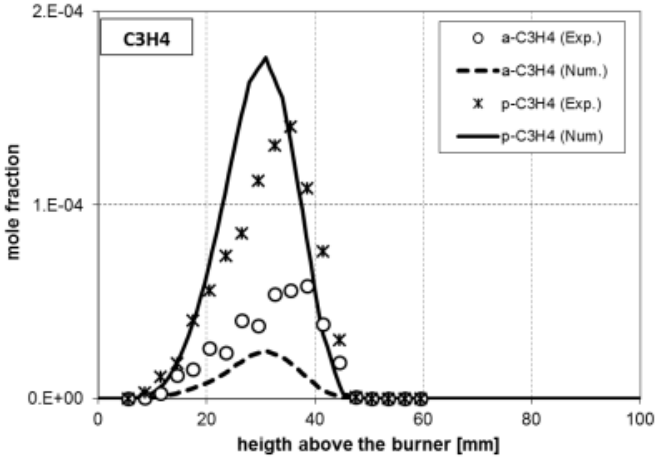

C_6H_6 (benzene) and $C_{12}H_8$ (Acenaphthylene)

Flame F1 (50% N_2)

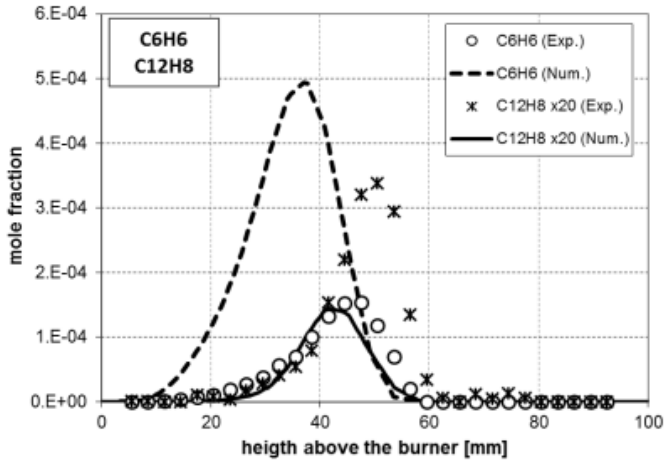

Flame F2 (55% N_2)

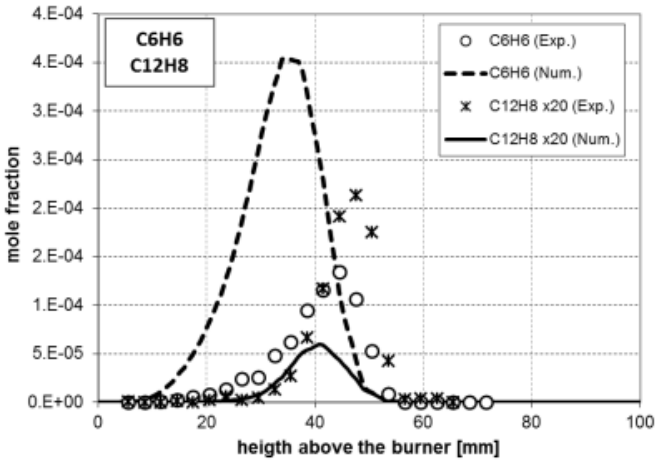

Flame F3 (60% N_2)

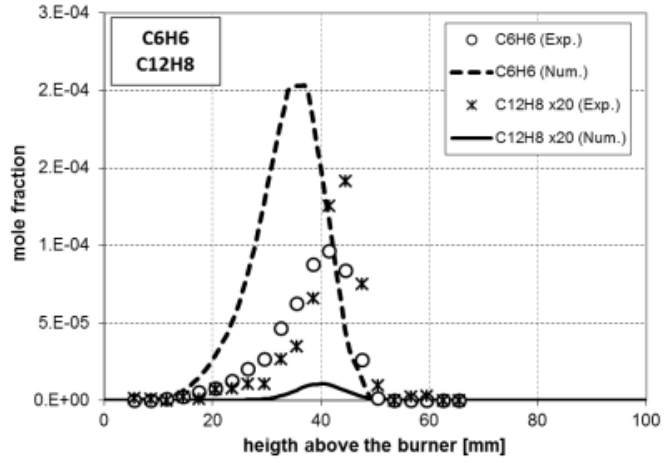

Flame F4 (65% N_2)

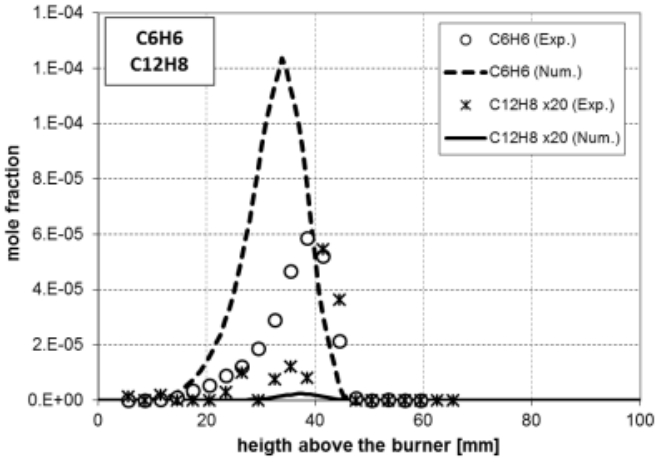

C_7H_8 (toluene) and $C_{10}H_8$ (naphthalene)

Flame F1 (50% N_2)

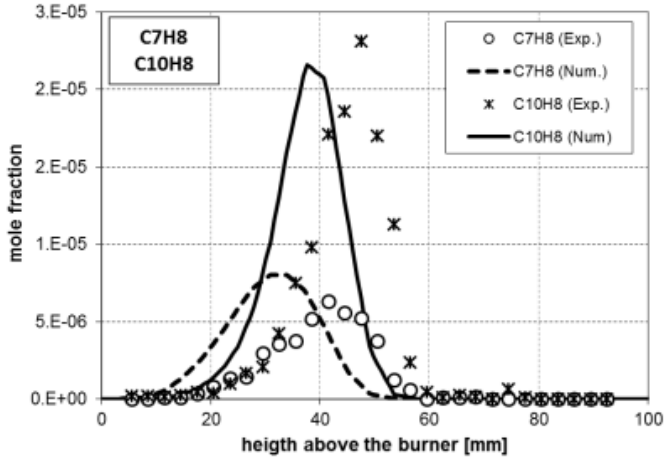

Flame F2 (55% N_2)

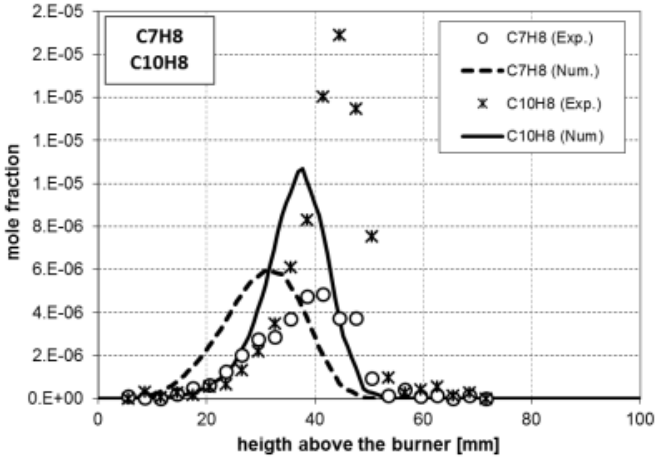

Flame F3 (60% N_2)

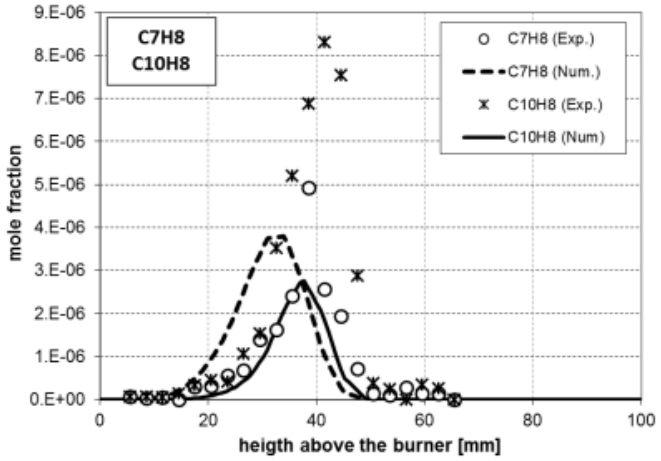

Flame F4 (65% N_2)

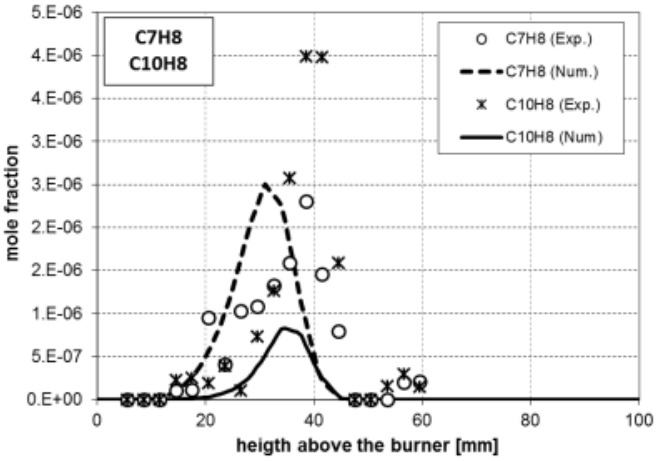

C_4H_4 (vinylacetylene) and C_4H_6 (butadienes+butyne)

Flame F1 (50% N_2)

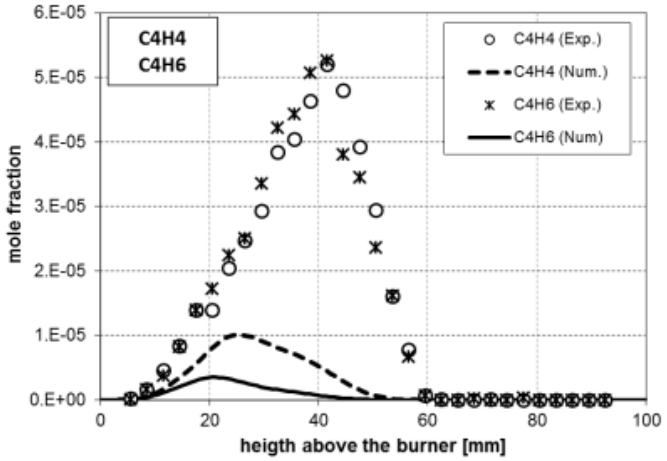

Flame F2 (55% N_2)

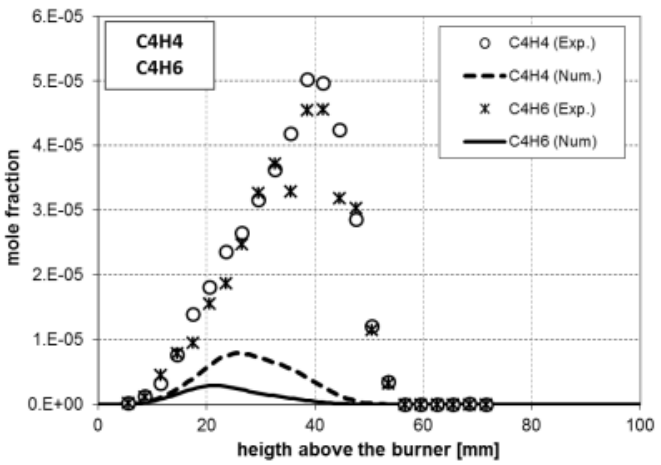

Flame F3 (60% N_2)

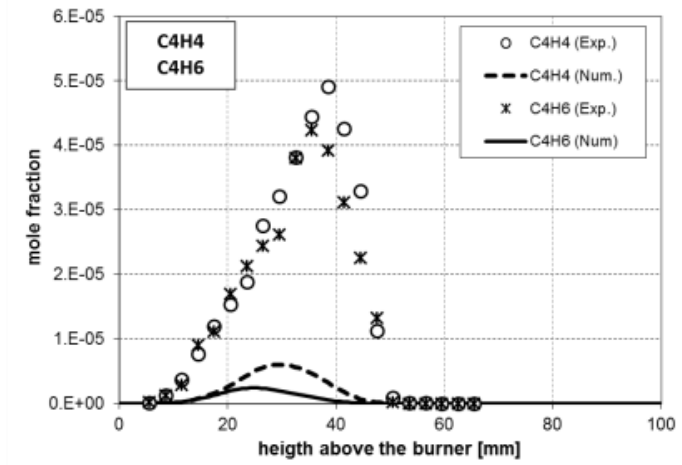

Flame F4 (65% N_2)

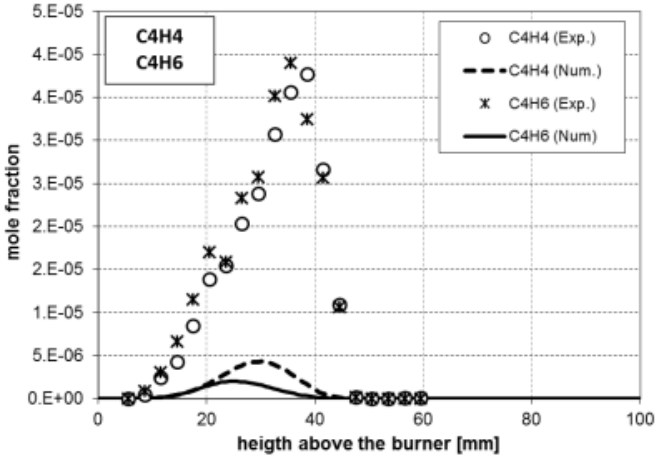

C_4H_2 (diacetylene) and C_6H_2 (triacetylene)

Flame F1 (50% N_2)

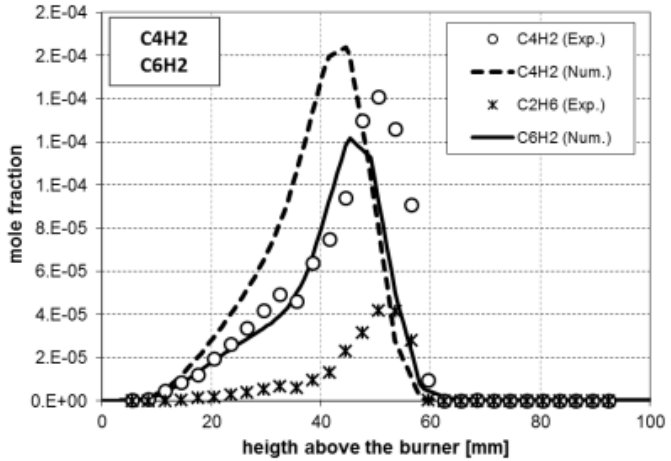

Flame F2 (55% N_2)

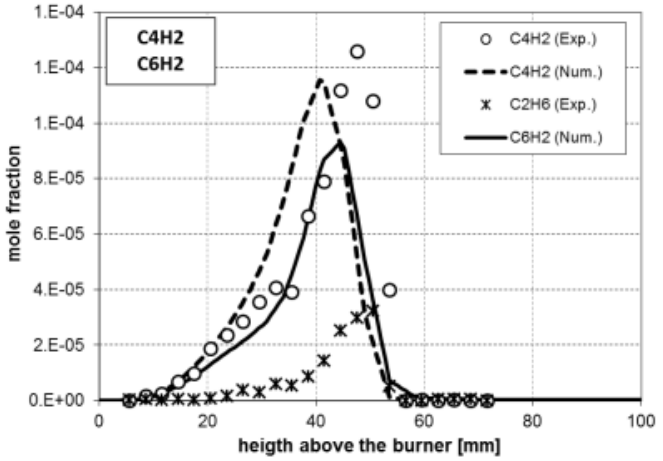

Flame F3 (60% N_2)

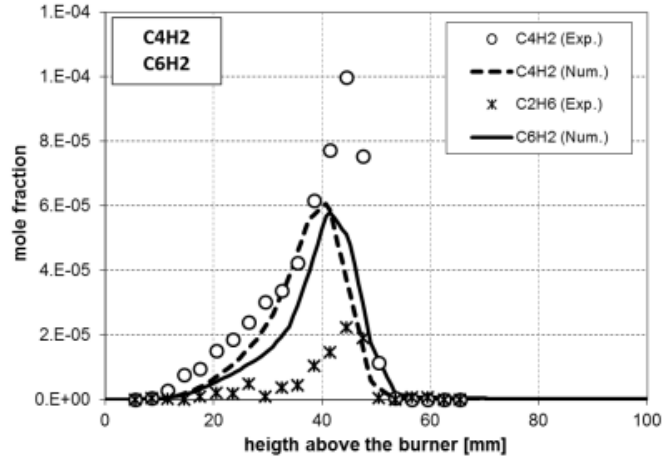

Flame F4 (65% N_2)

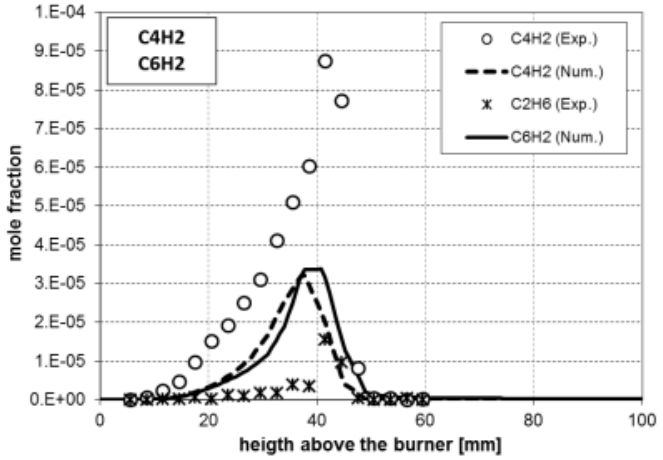

Mixture fraction

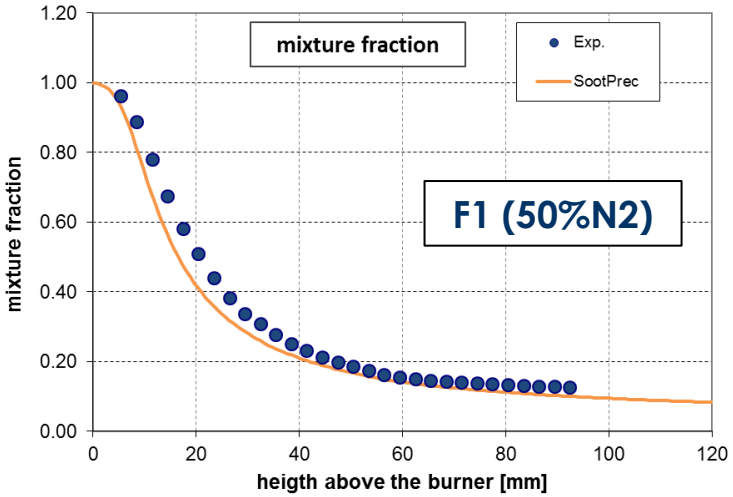

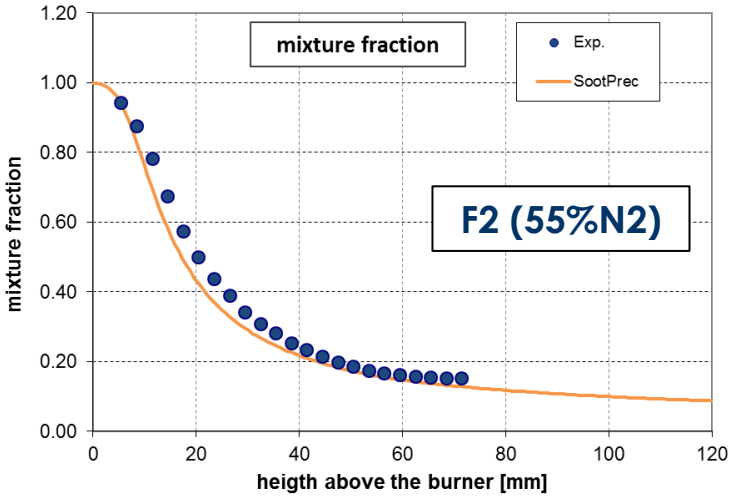

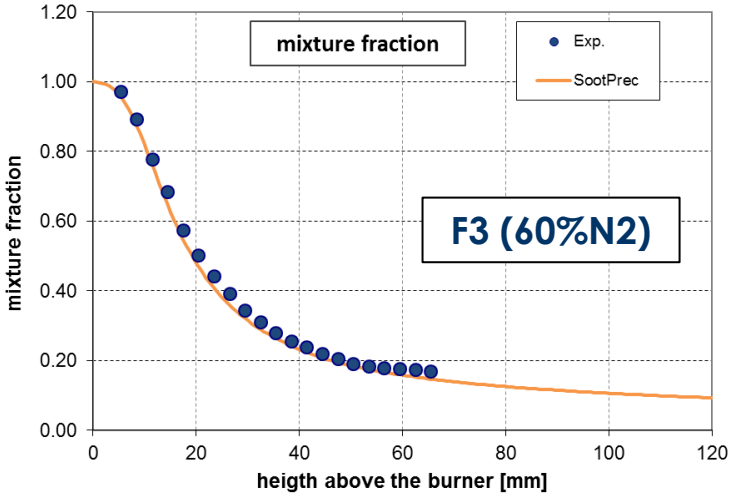

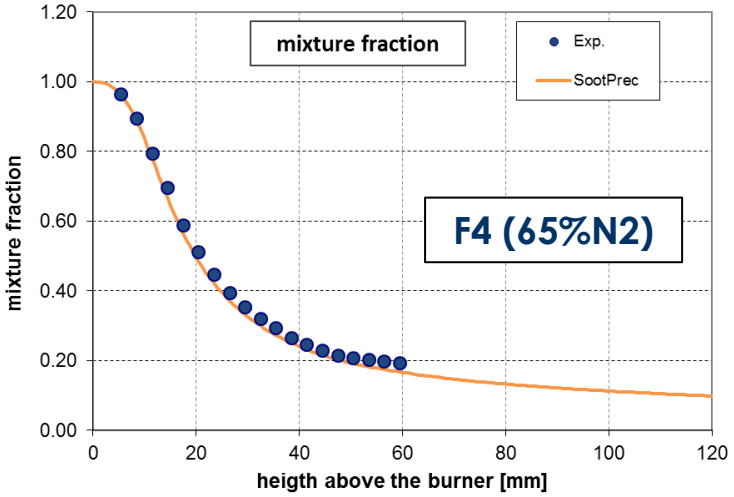

Effect of radiative heat transfer

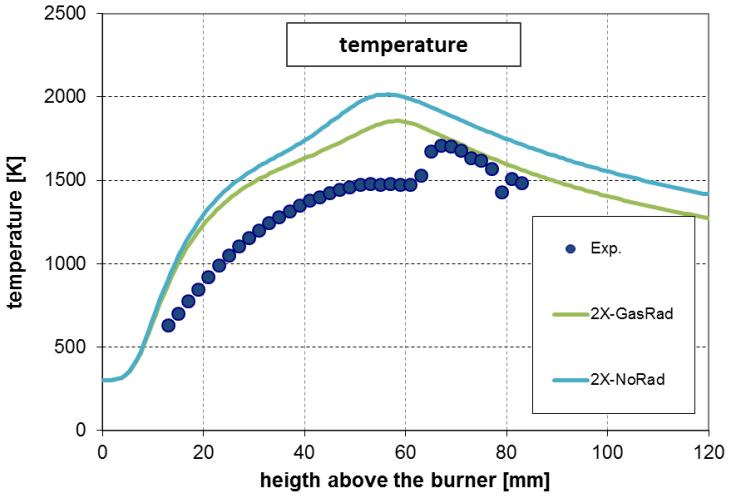

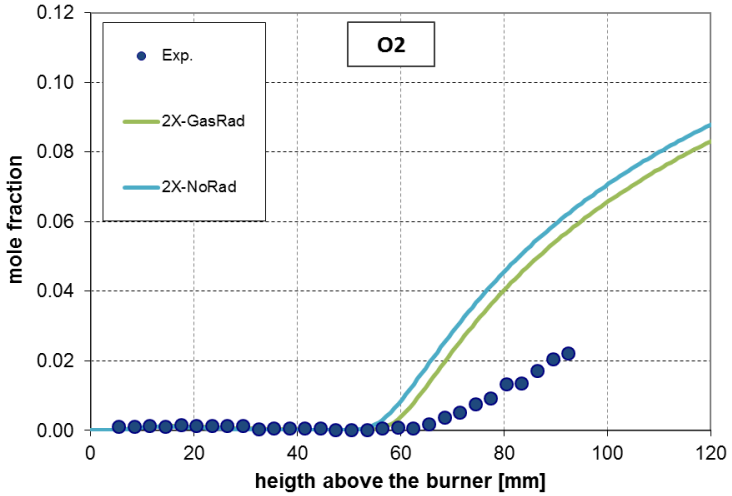

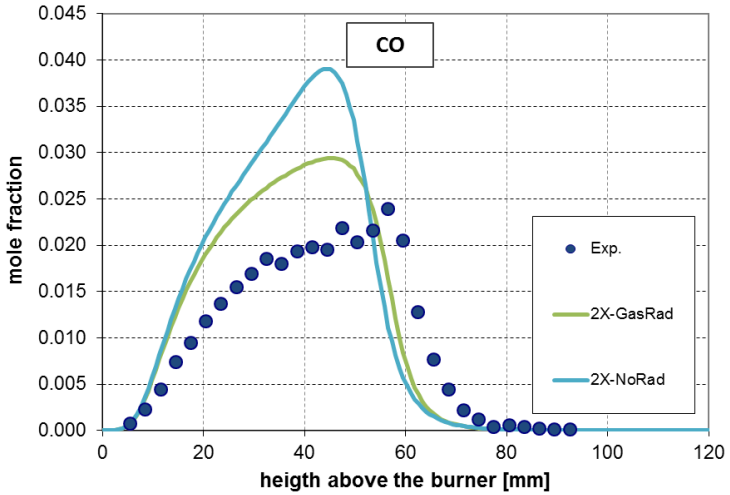

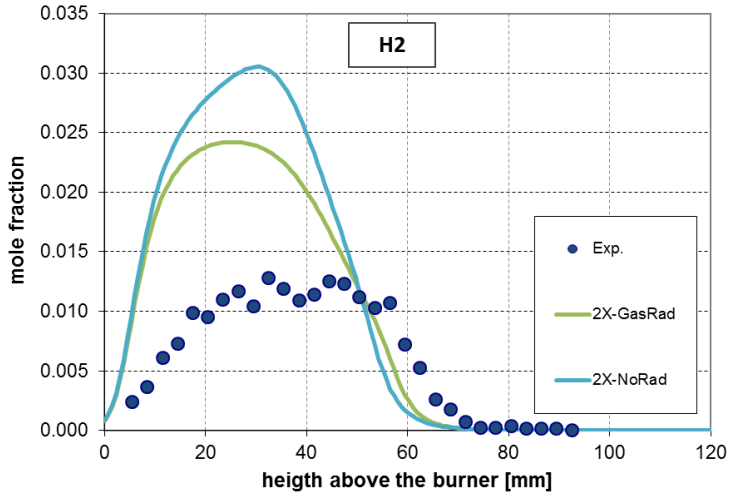

Parabolic vs flat profile

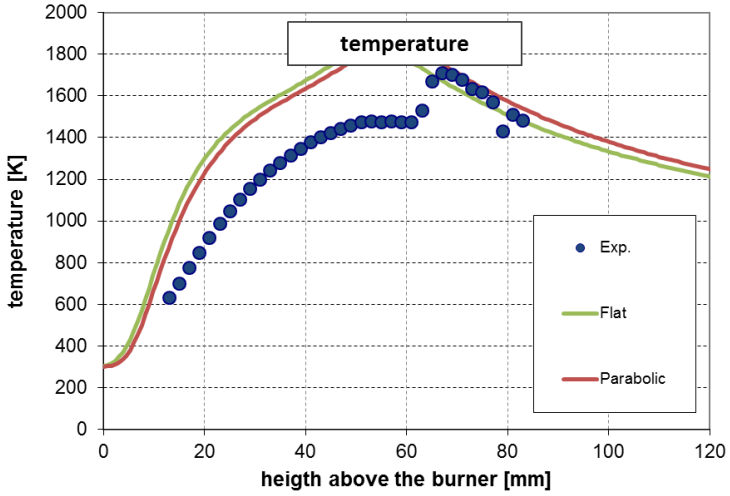

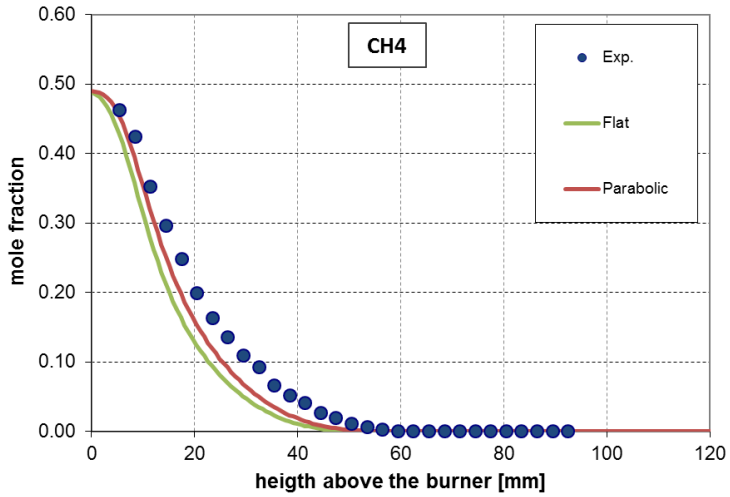

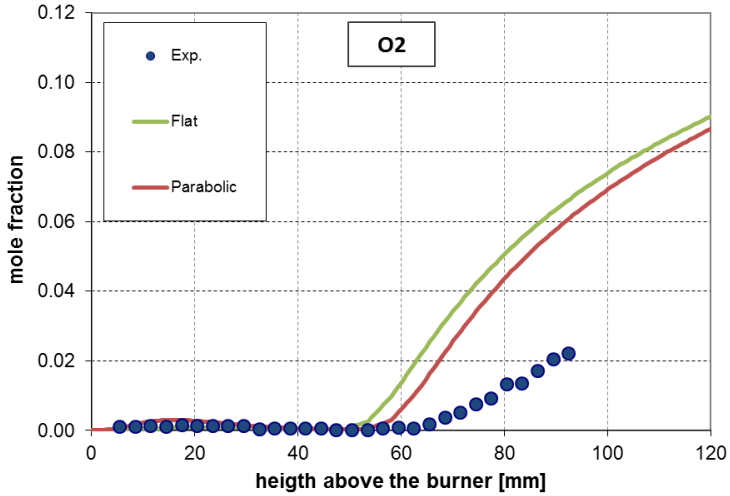

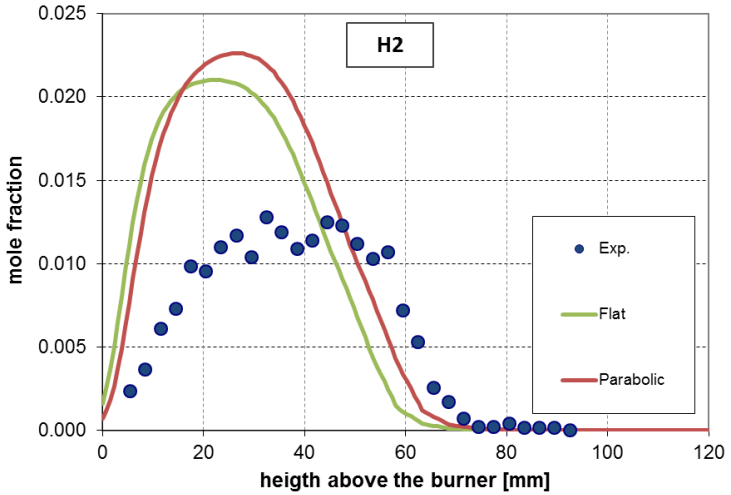

Grid sensitivity (I)

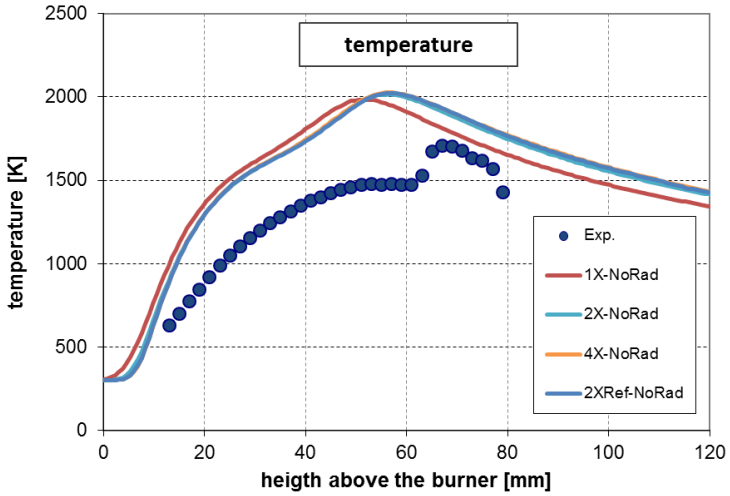

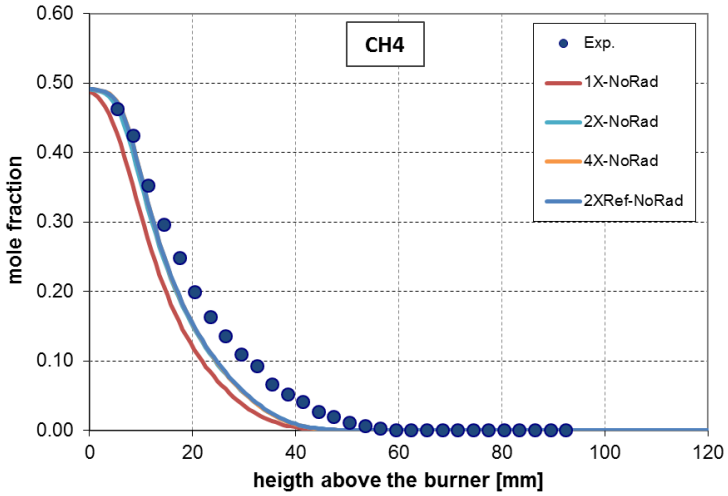

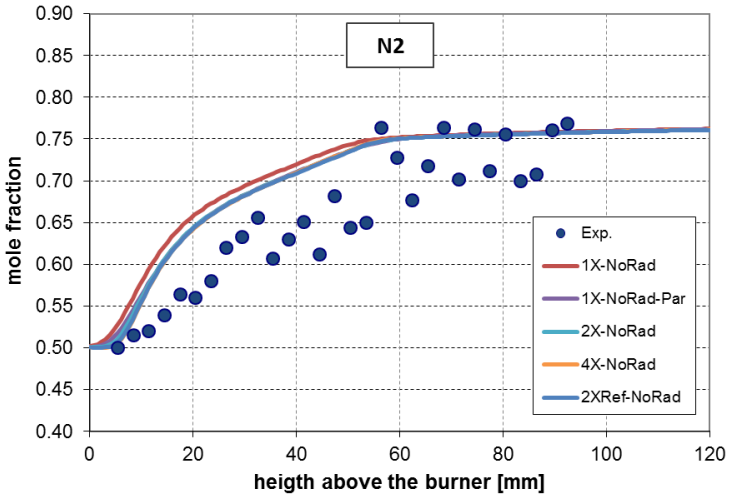

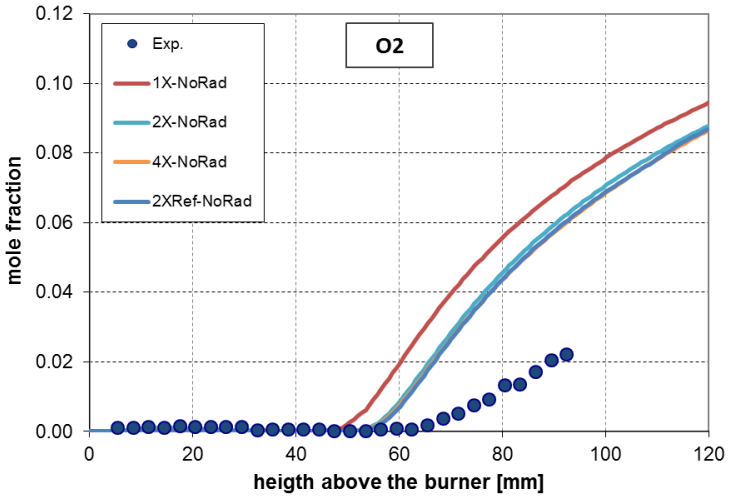

Grid sensitivity (II)

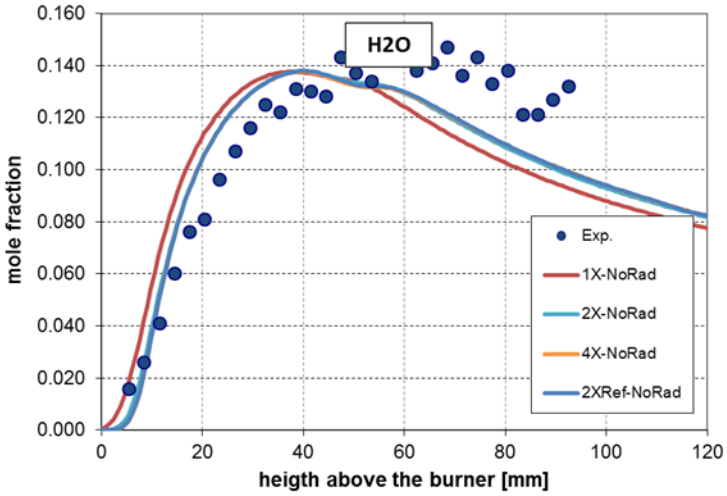

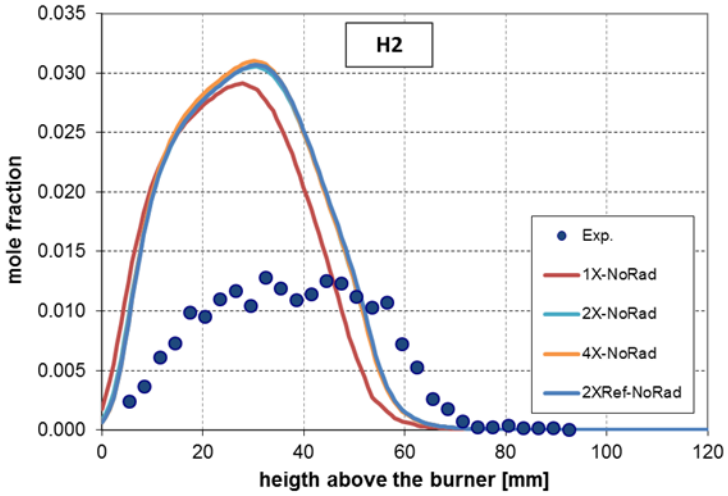

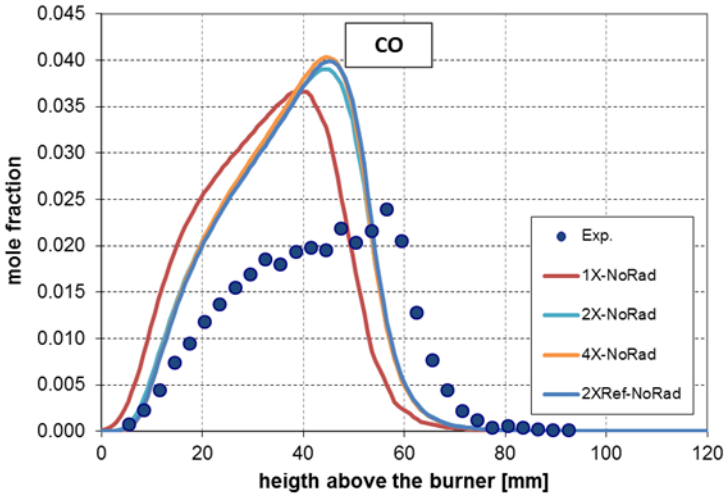

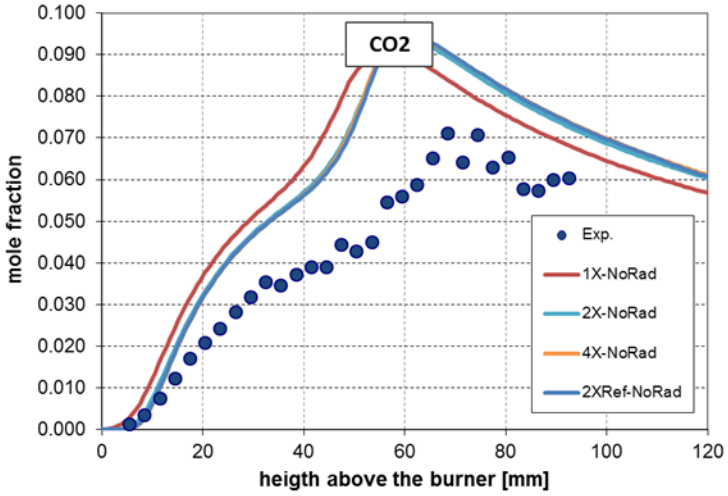

Grid sensitivity (III)

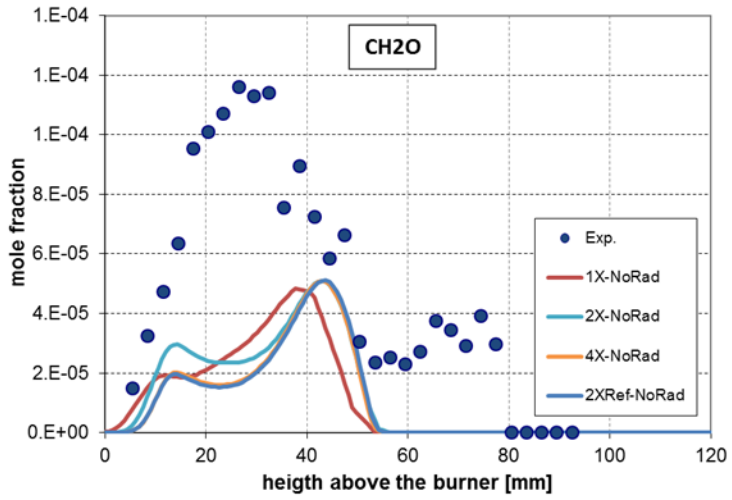

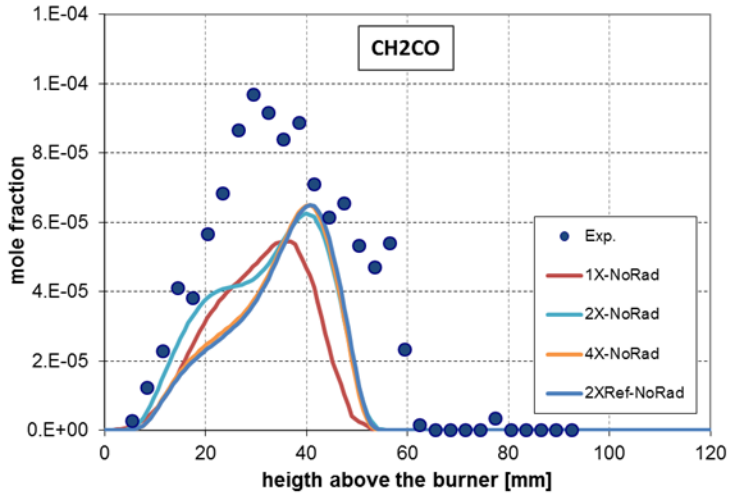

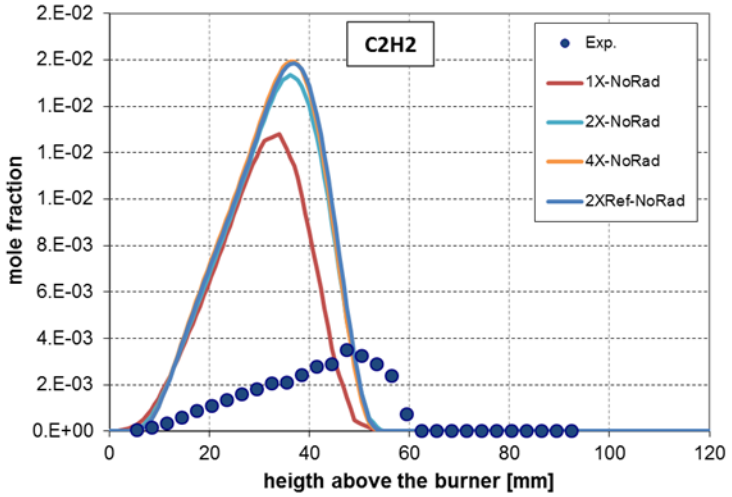

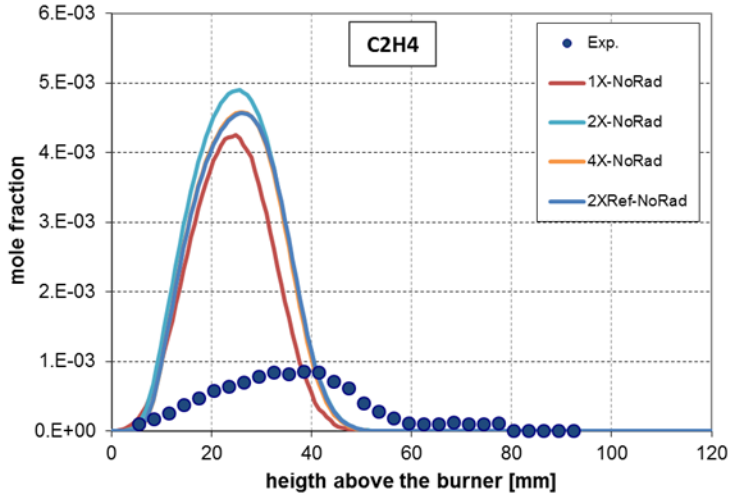

List of detected C5+ species

	Name	Structure
C5H6	1,3-cyclopentadiene	
C6H2	1,3,5-hexatriyne	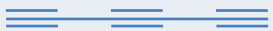
C6H4	hex-3-en-1,5-diyne	
C6H5	phenyl radical	Radical of benzene
C6H6	benzene	
C7H7	benzyl radical	Radical of toluene
C7H8	toluene	
C6H5C2H	phenylacetylene	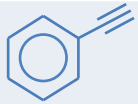
C10H8	naphthalene	
C12H8	acenaphthylene	

C4H2 diacetylene C4H2
C4H4 vinylacetylene C4H4
C4H6 butadienes+butyne C4H6
C5H6 cyclopentadiene CYC5H6
C9H7 indenyl_resonant INDENYL
C9H8 indene INDENE
C4H2 diacetylene C4H2
C6H2 triacetylene C6H2
C8H6 phenylacetylene C6H5C2H
C12H7 acenaphthalene_radicals C12H7
C3H5 allyl CH2CHCH2
C4H6 butadienes+butyne C4H6
C3H6 propylene C3H6
C2H3 vinyl C2H3

Flames studied by McEnally and D'Anna

Fei Qi Flames

Flame	Flow rate(SCCM)				Mole fractions (%)		
	air	N_2	CH_4	Ar	N_2	CH_4	Ar
F1	160,000	314	308	5.87	**50**	49.066	0.934
F2	160,000	345	277	5.87	**55**	44.066	0.934
F3	160,000	377	245	5.87	**60**	39.066	0.934
F4	160,000	408	214	5.87	**65**	34.066	0.934

Flames studied by McEnally and D'Anna

Flame	Flow rate(SCCM)				Mole fractions (%)		
	air	N_2	CH_4	Ar	N_2	CH_4	Ar
F1	44,000	340	340	6.9	**49.5**	49.5	1

CH4 McEnally Flame (CH4)

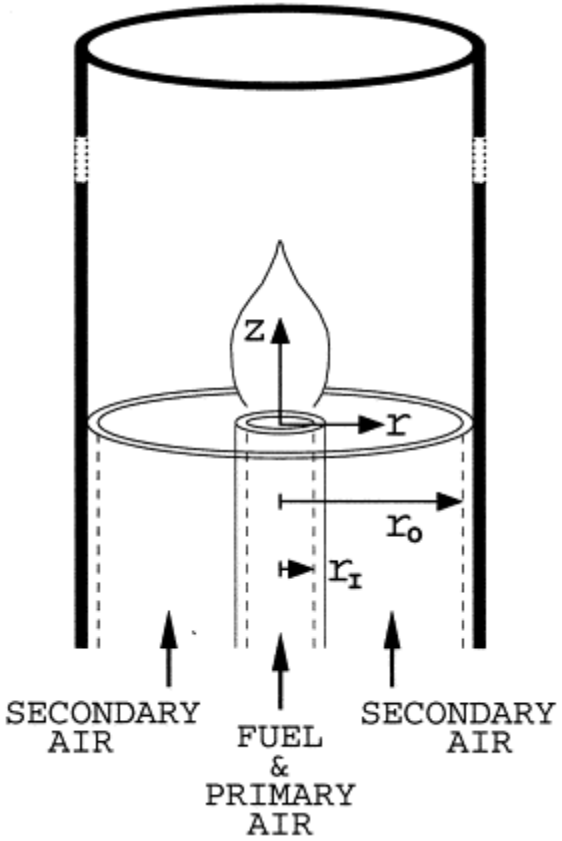

TABLE 1. Flame Parameters for Computations

Φ	Q_{CH_4} (cm^3/min)	Q_{air}(cm^3/min)	v_z (cm/s)	$Y_{CH_4,B}$	$Y_{O_2,B}$	$Y_{N_2,B}$
Inner jet						
∞	330	0	5.67	1.00000	0.00000	0.00000
12.320	330	210	9.28	0.46420	0.15071	0.38509
6.160	330	420	12.89	0.30226	0.19627	0.50147
4.107	330	630	16.50	0.22408	0.21826	0.55766
3.080	330	840	20.11	0.17803	0.23121	0.59076
2.464	330	1050	23.71	0.14769	0.23975	0.61256
Outer jet						
All	0	44000	10.48	0.00000	0.23200	0.76800

Bennett, McEnally, Pfefferle, Smooke, "Computational and experimental study of axisymmetric coflow partially premixed methane/air flames", Combustion and Flame, 123, p. 522-546 (2000)

CH4 McEnally Flame (Φ=inf)

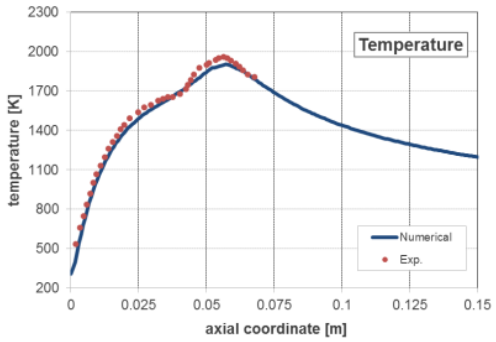

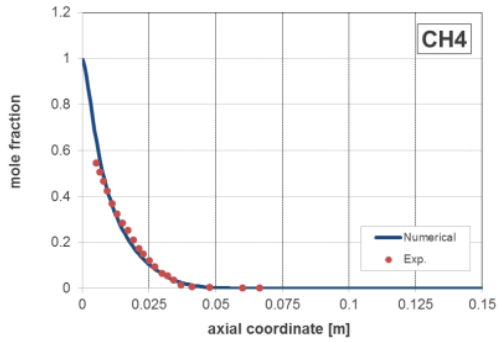

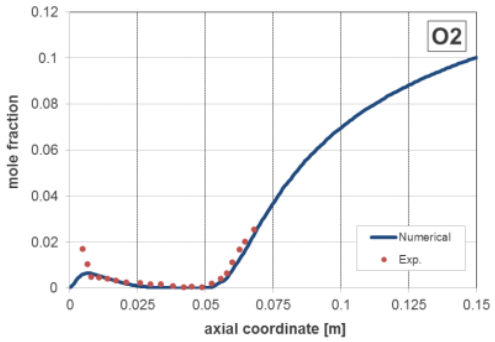

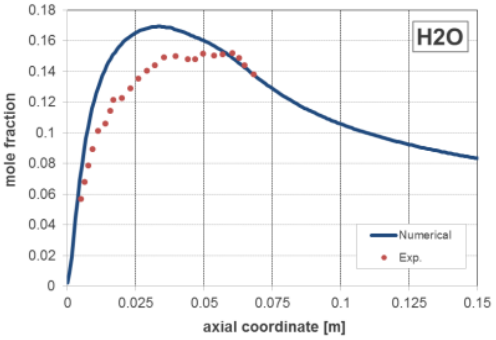

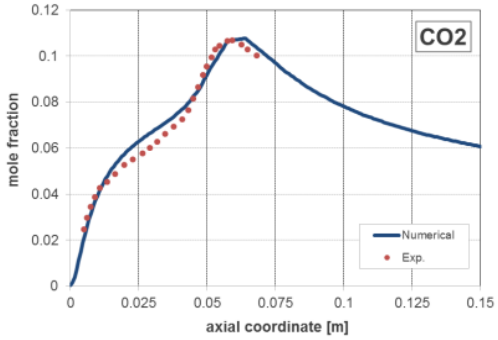

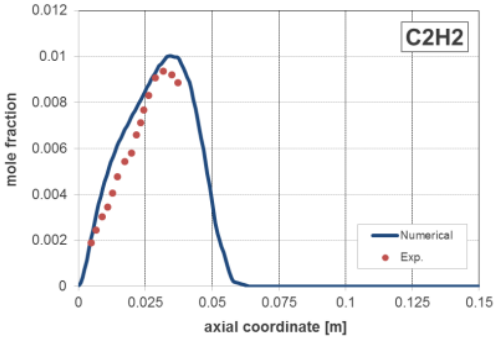

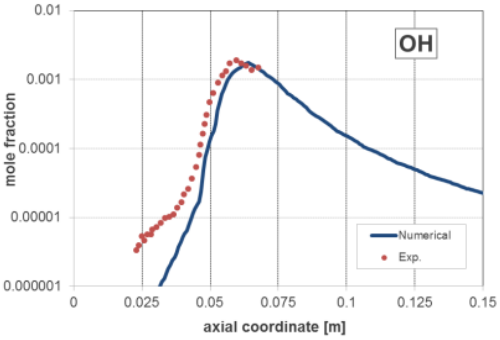

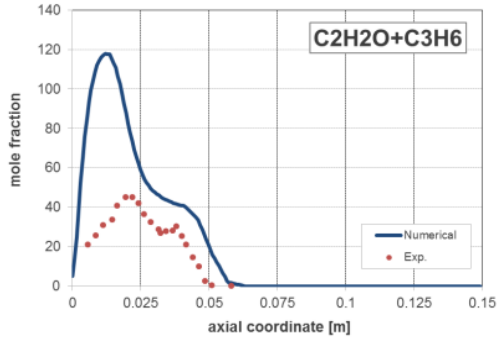

CH4 McEnally Flame (Φ=12.32)

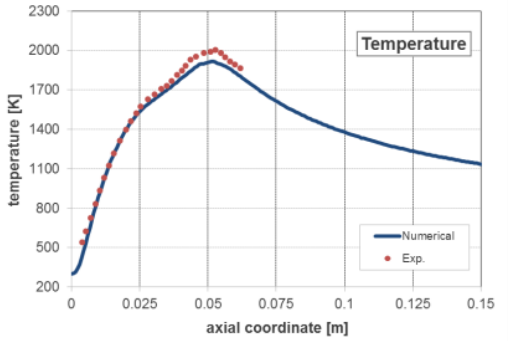

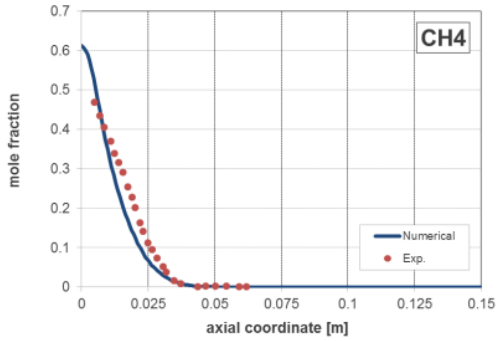

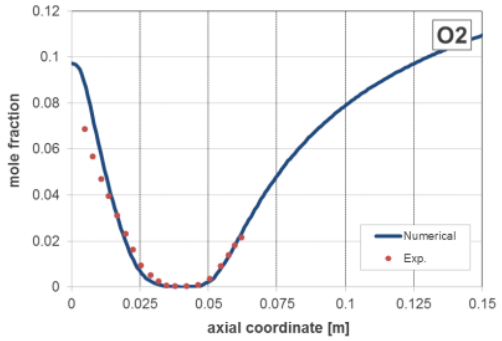

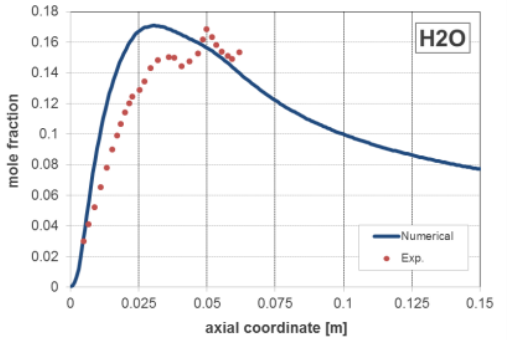

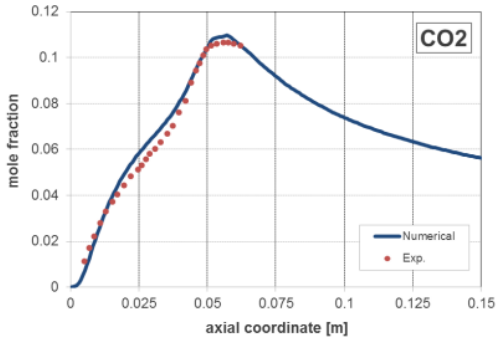

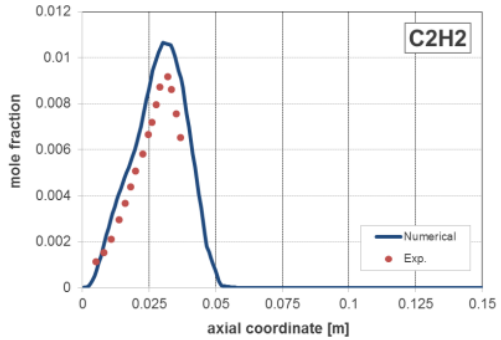

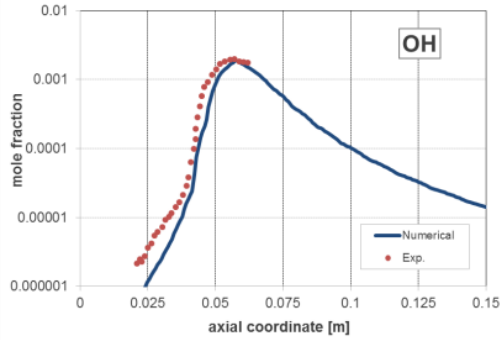

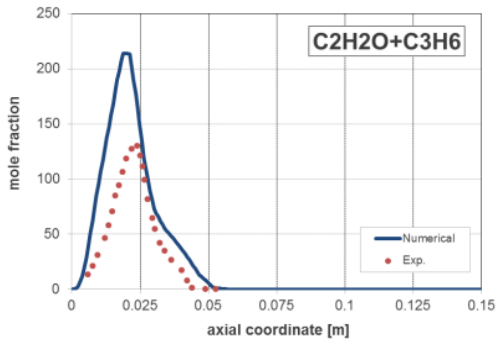

CH4 McEnally Flame (Φ=6.16)

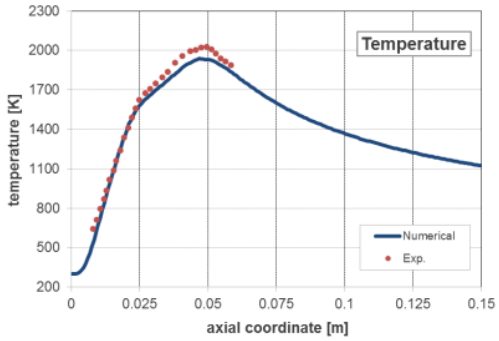

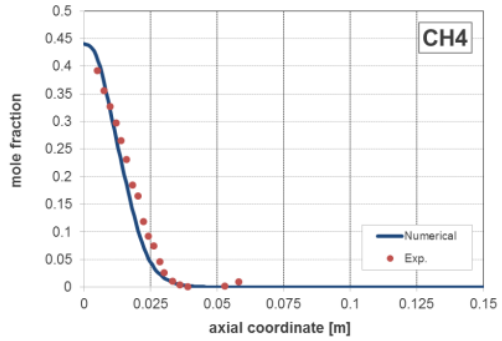

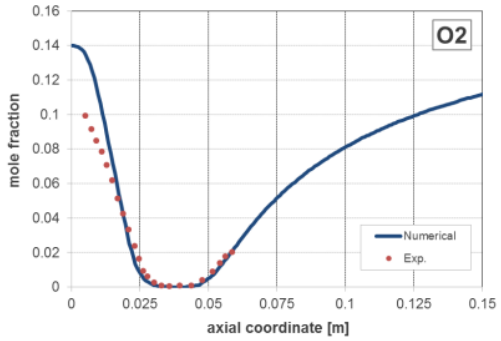

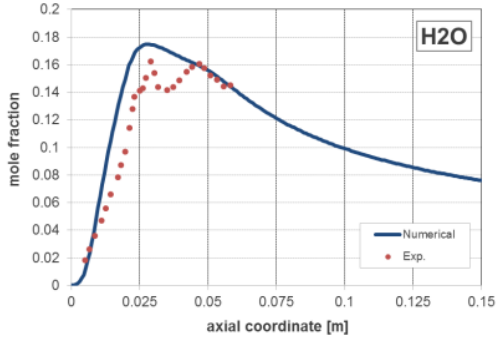

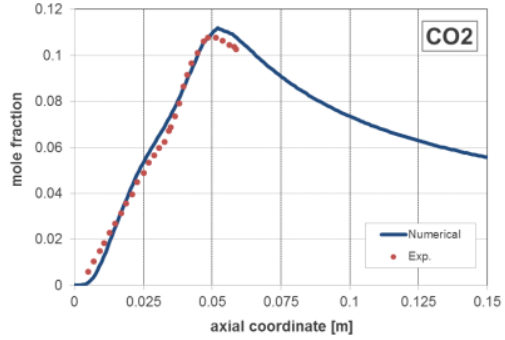

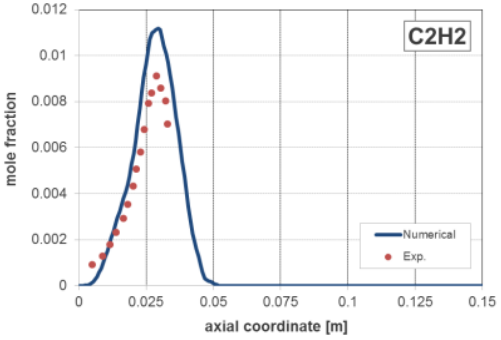

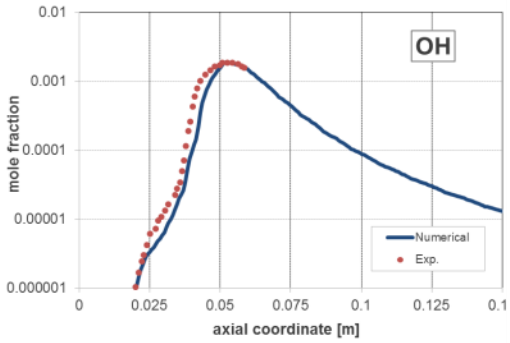

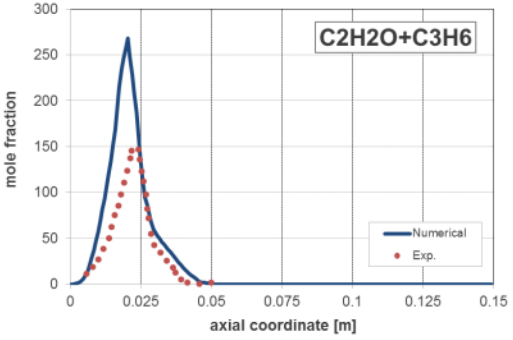

CH4 McEnally Flame (Φ=4.10)

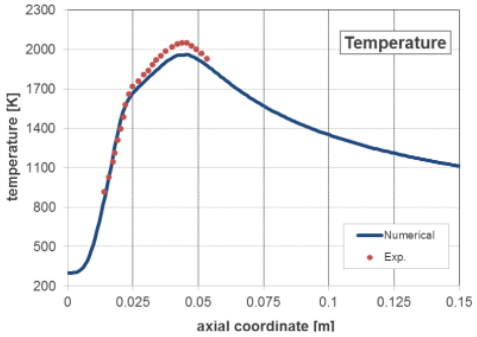

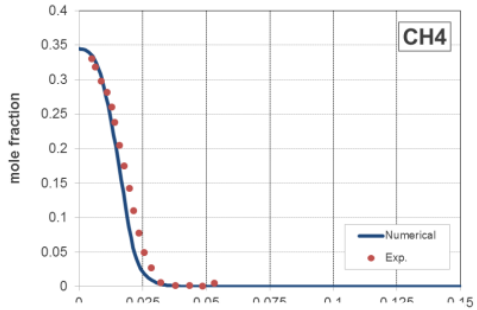

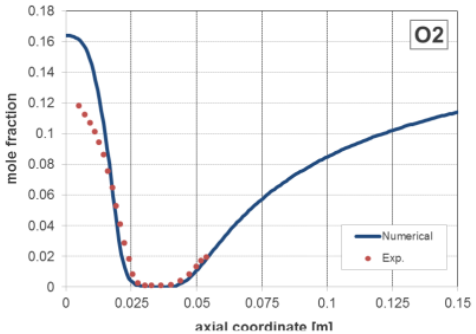

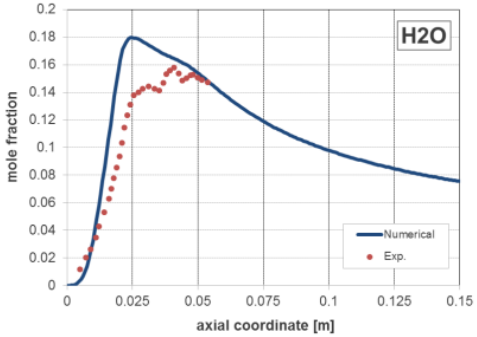

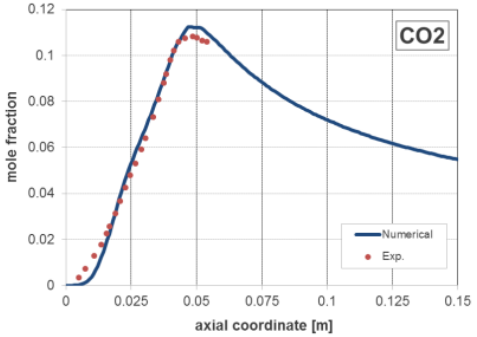

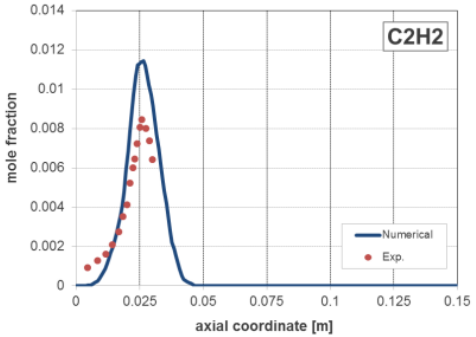

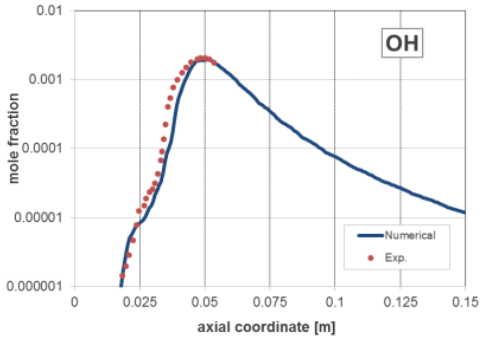

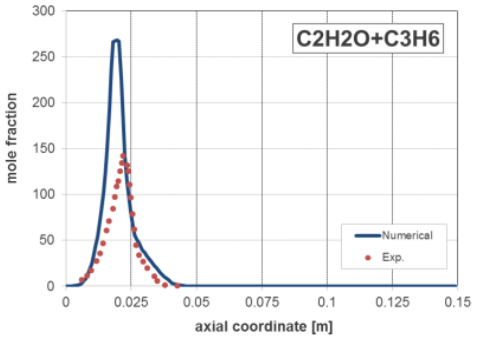

CH4 McEnally Flame (Φ=inf)

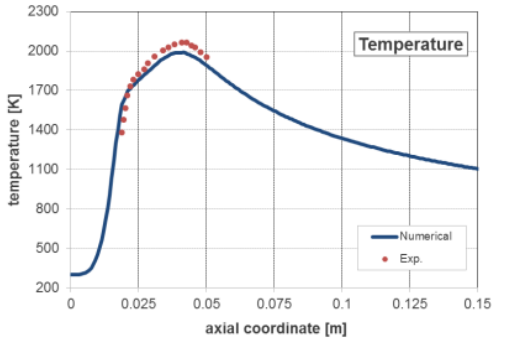

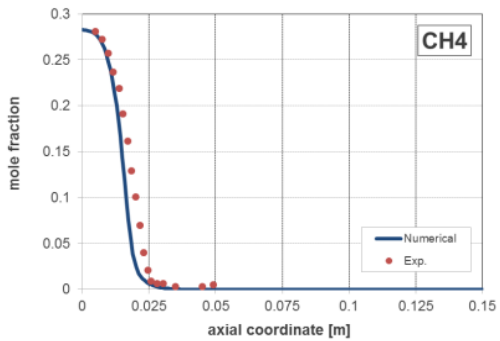

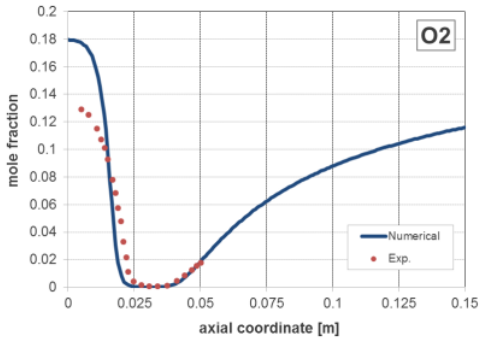

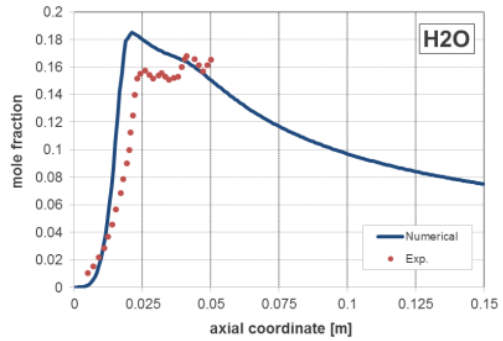

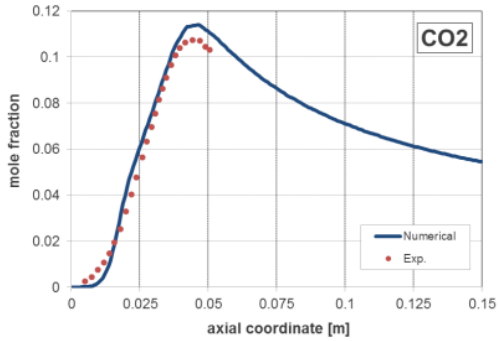

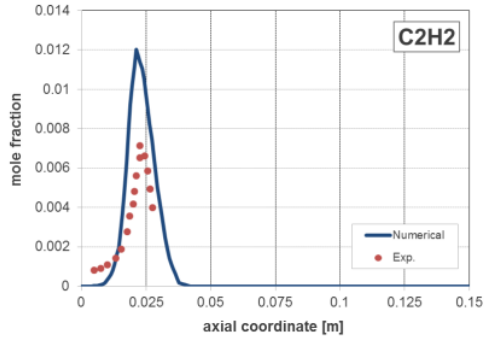

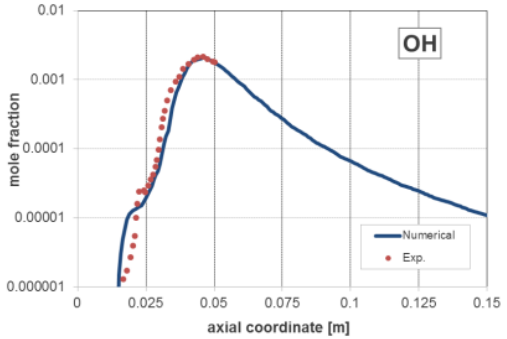

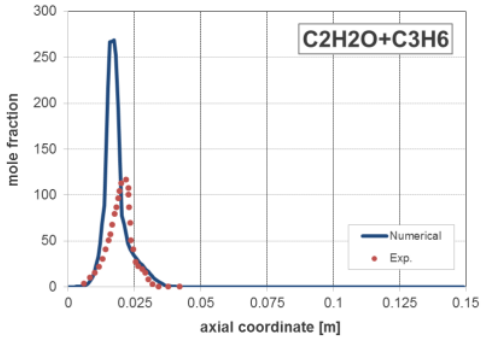

CH4 McEnally Flame (Φ=2.46)

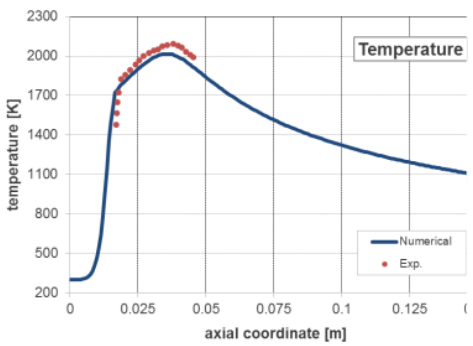

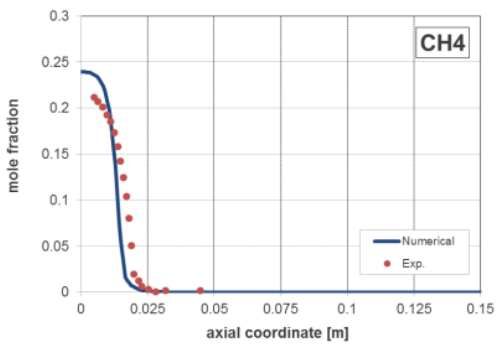

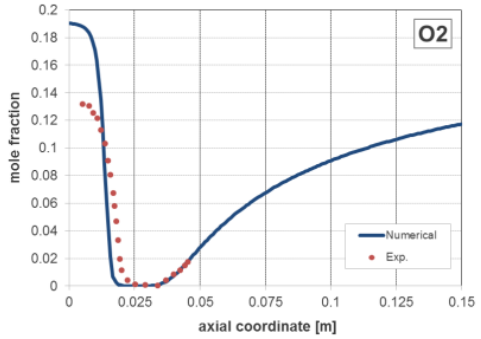

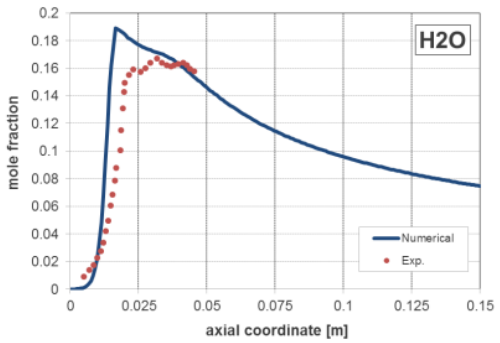

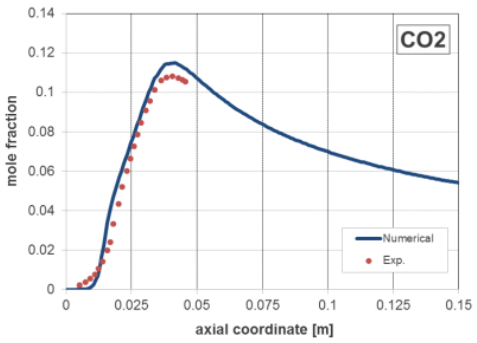

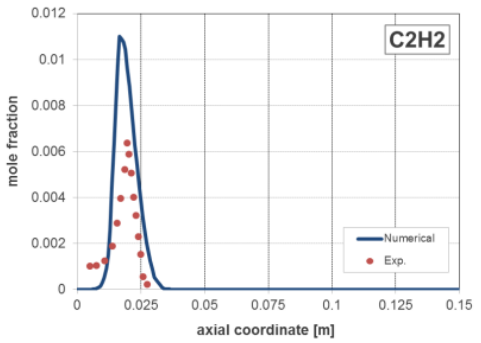

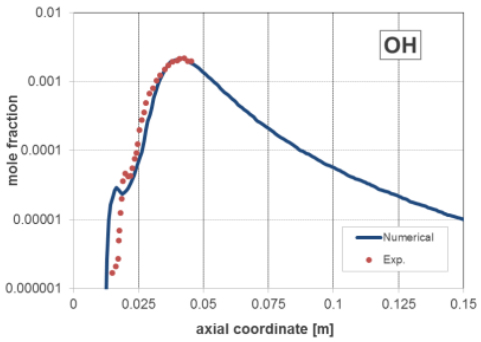

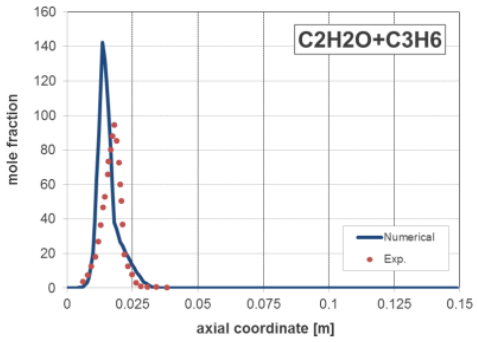

C2H4 McEnally Flame (Φ=inf) (1)

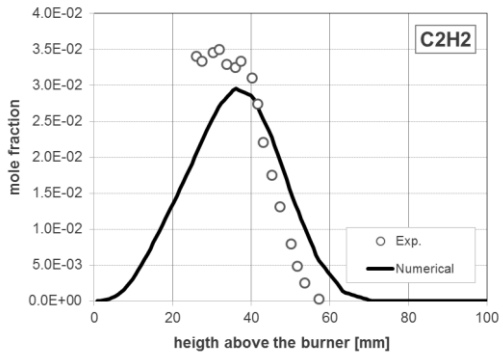

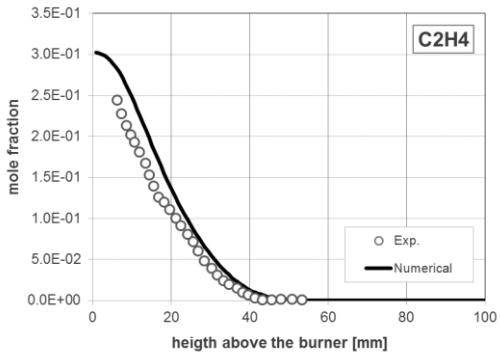

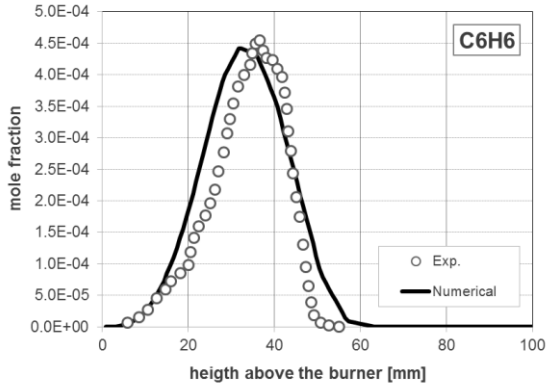

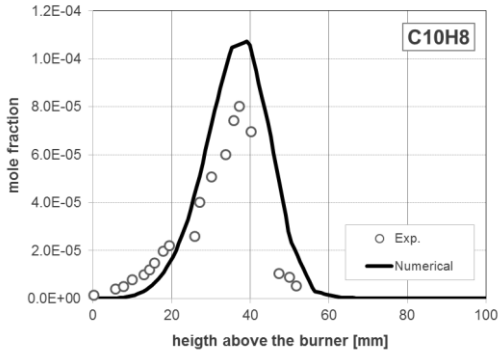

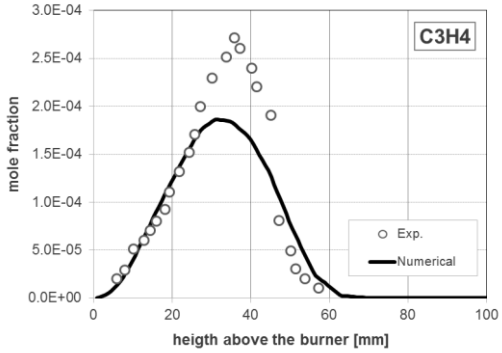

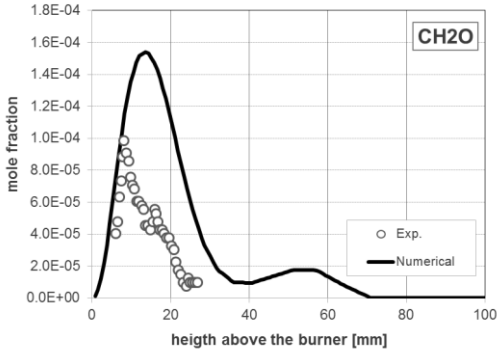

C2H4 McEnally Flame (Φ=inf) (2)

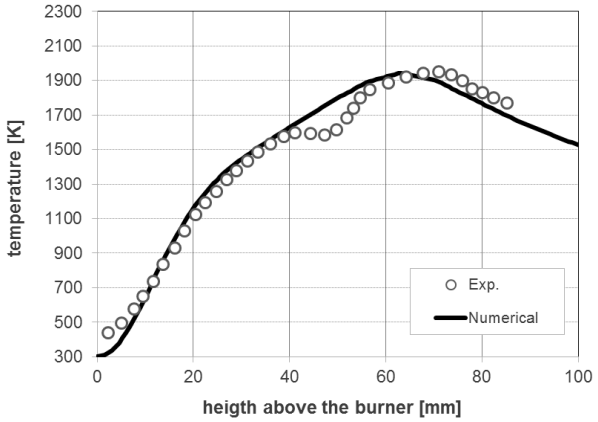

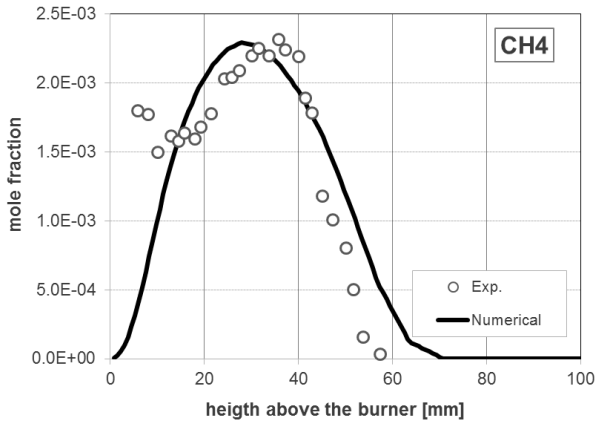

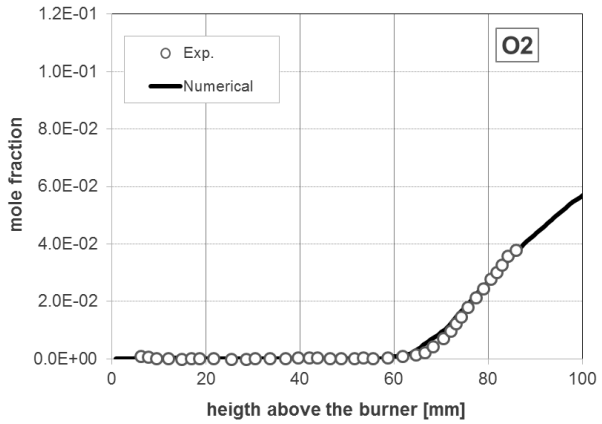

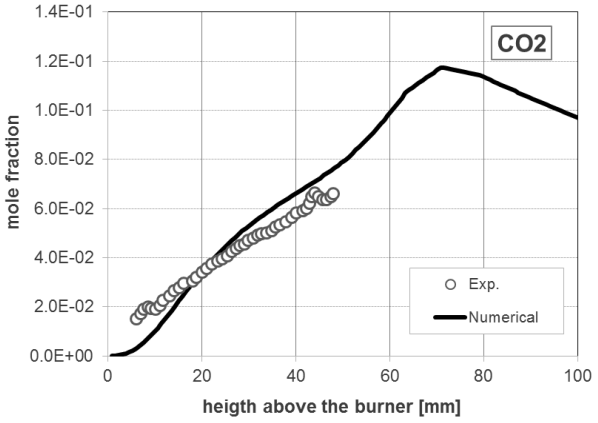

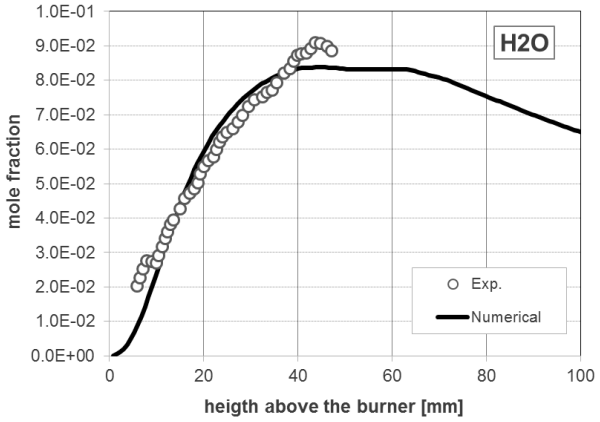

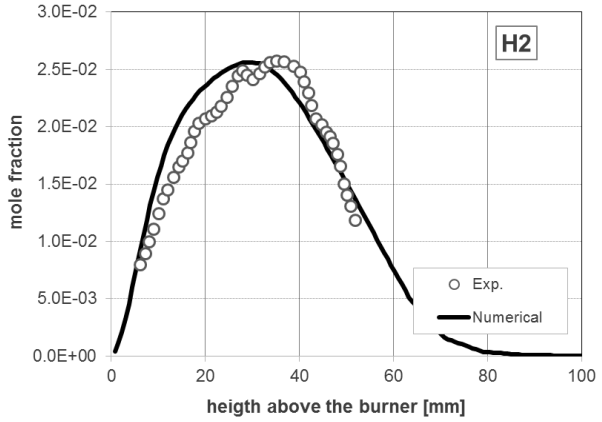

C2H4 McEnally Flame (Φ=inf) (3)

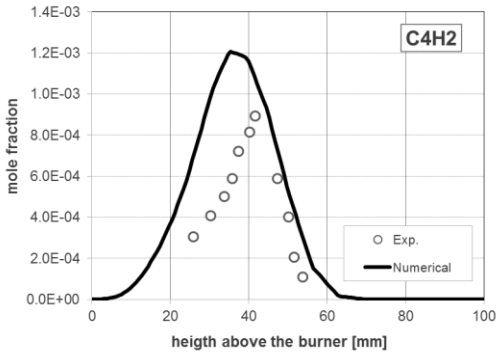

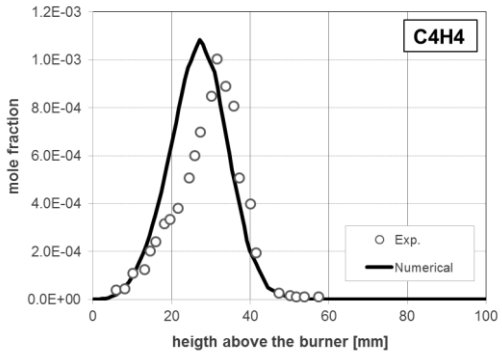

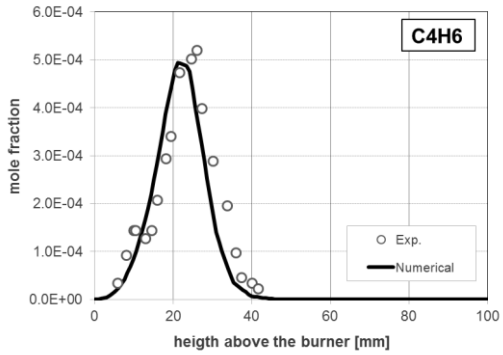

C2H4/CH4 Roesler Flames

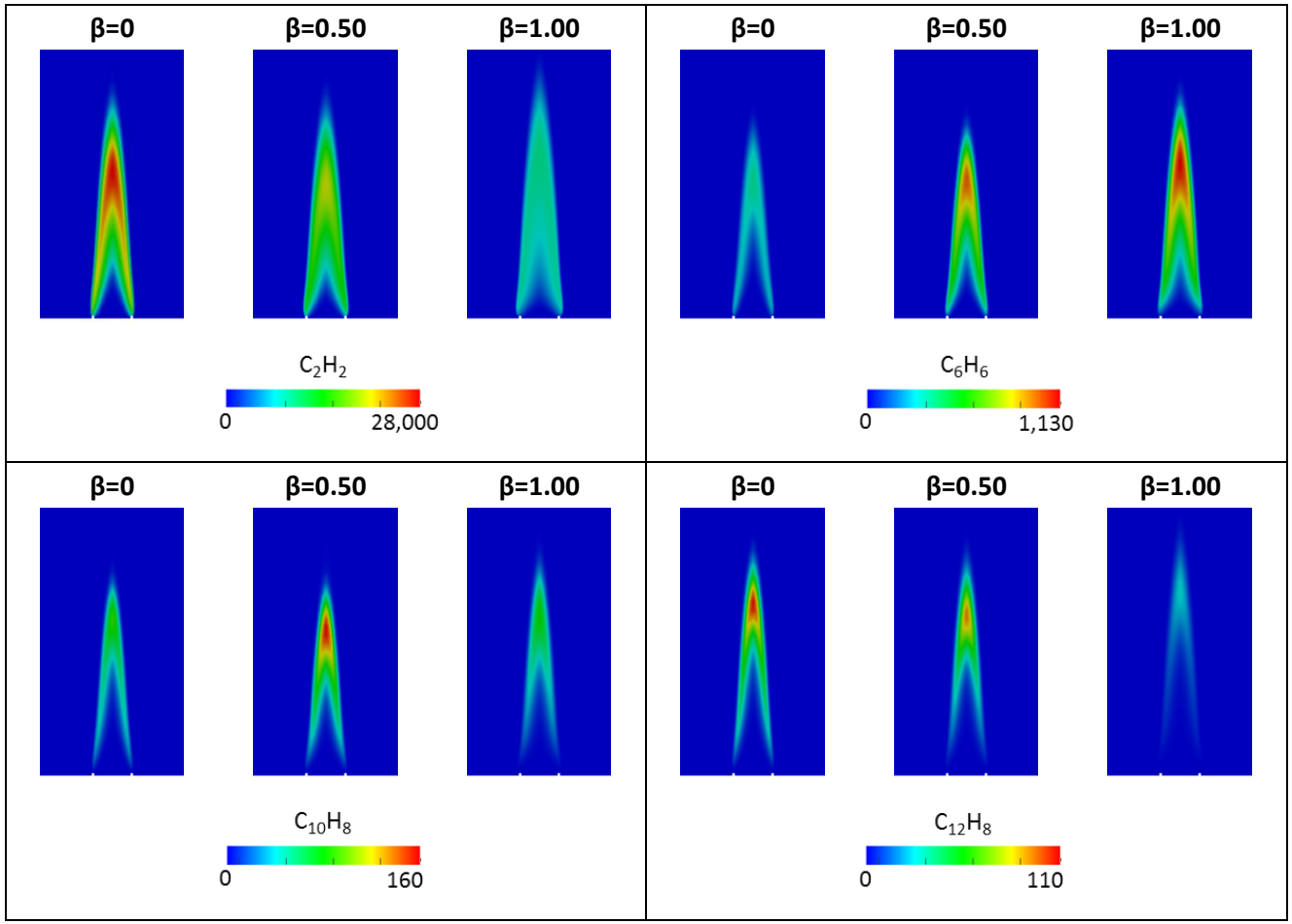

Figure 1. $C_2H_4/CH_4/N_2$ coflow flames: calculated maps of mole fractions (in ppm) of selected species at different values of the mixture parameter β. The maps of species refer to a rectangular region of 4.2 x 8 cm.

C2H4/CH4 Roesler Flames

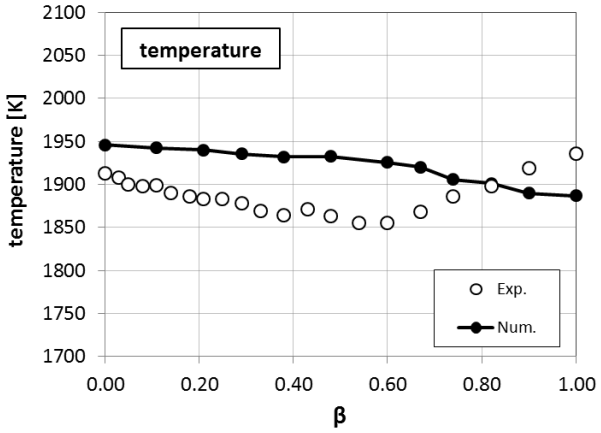

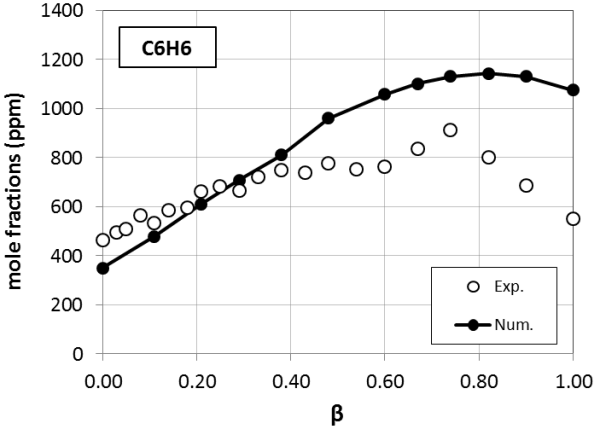

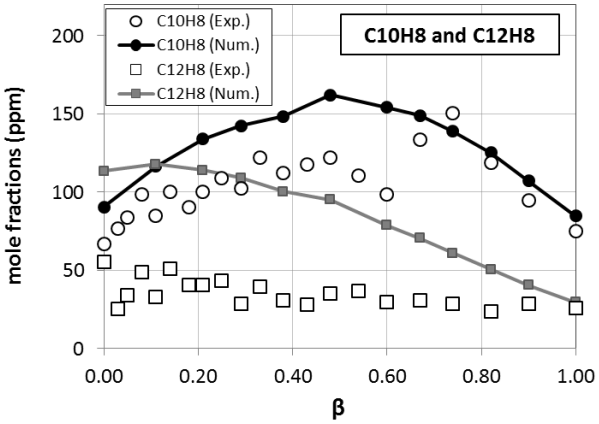

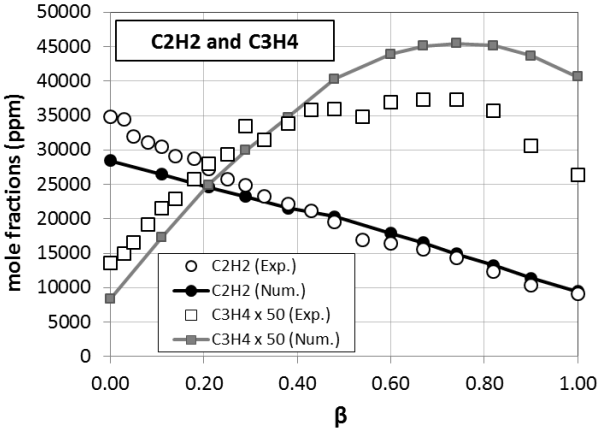

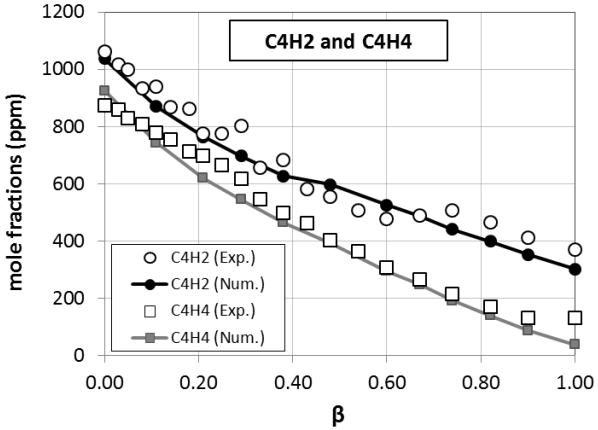

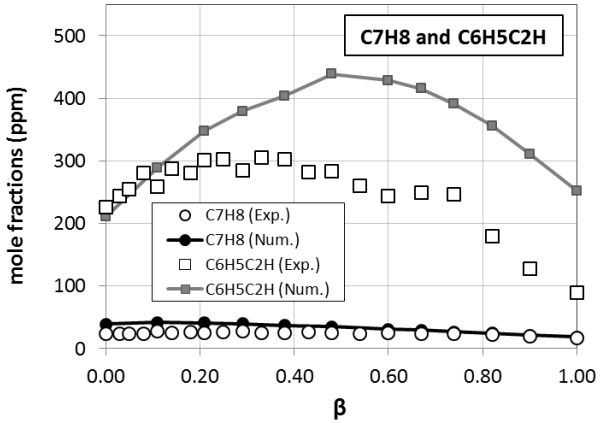

CH4 lifted flame

Flame details
Fuel: CH_4/N_2 (51.5%, 48.5% mass)
Air: O_2/N_2 (23.2%, 76.8% mass)
Temperature: 298 K
Pressure: 1 atm
V_{fuel}: 35 cm/s
V_{air}: 35 cm/s

Geometry
Fuel nozzle diameter: 4 mm
Coflow diameter: 5 mm

Computational details
Domain: 2D axisymmetric (55 x 200 mm)
Computational grid: ~25,000 cells
Discretization: second order centered

Kinetic schemes
GRI30: 53 species, 325 reactions
PolimiC1C16HTNOX: 168 species, 5,400 reactions

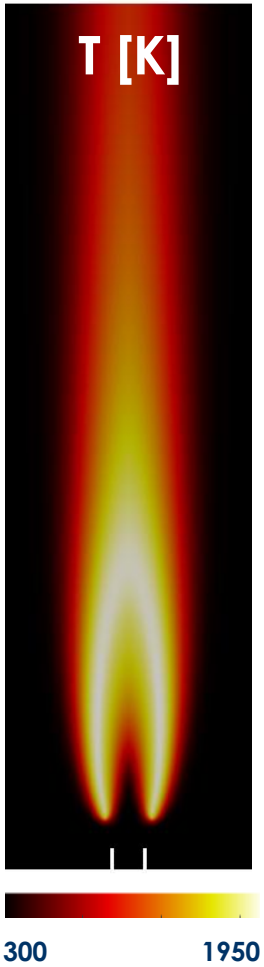

R. H. Mohammed, M. A. Tanoff, M. D. Smooke, A. M. Shaffer, *Proceedings of the Combustion Institute*, 27 (1998) 693-702.

2d maps

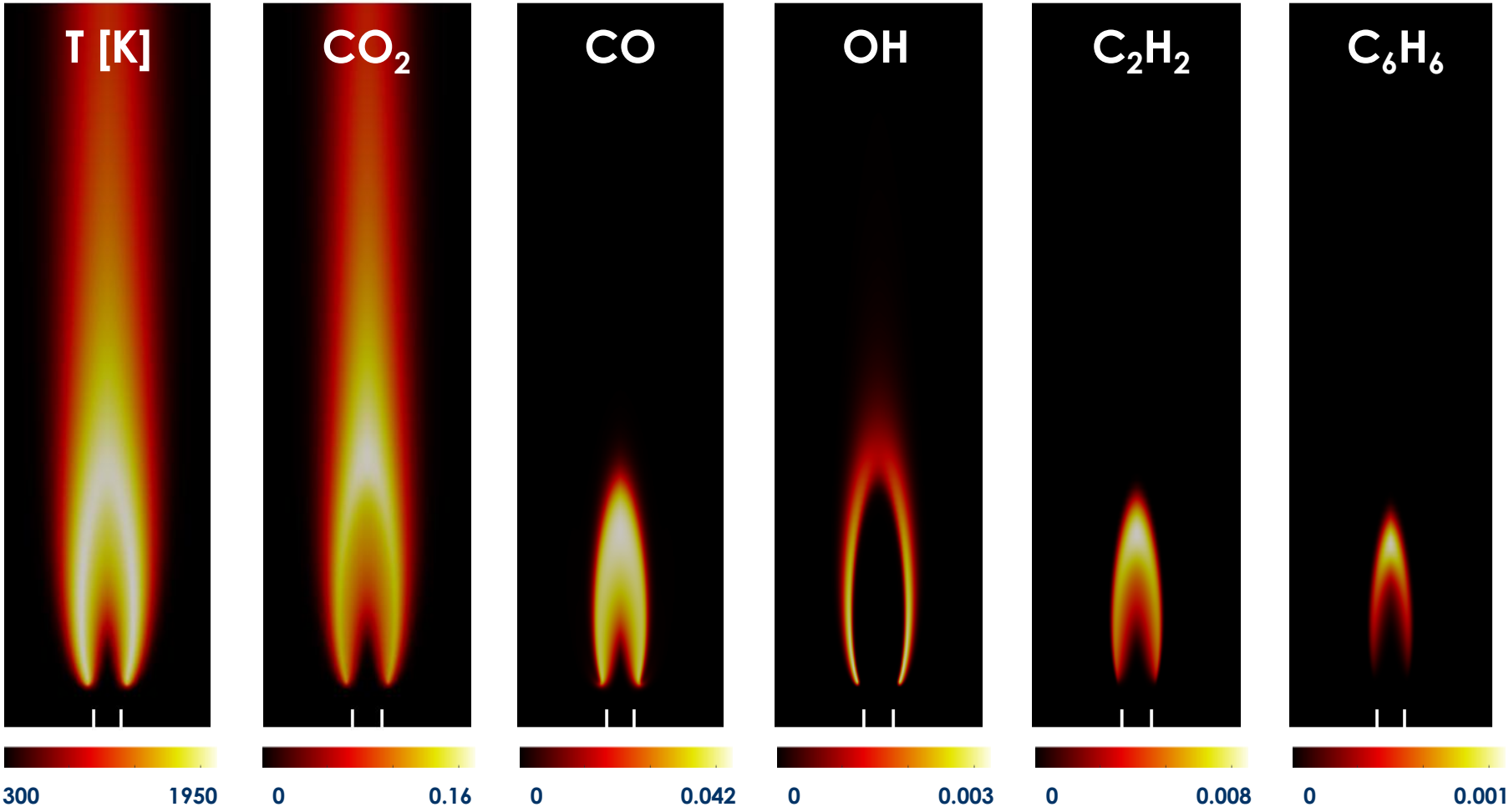

Comparison with the experiments

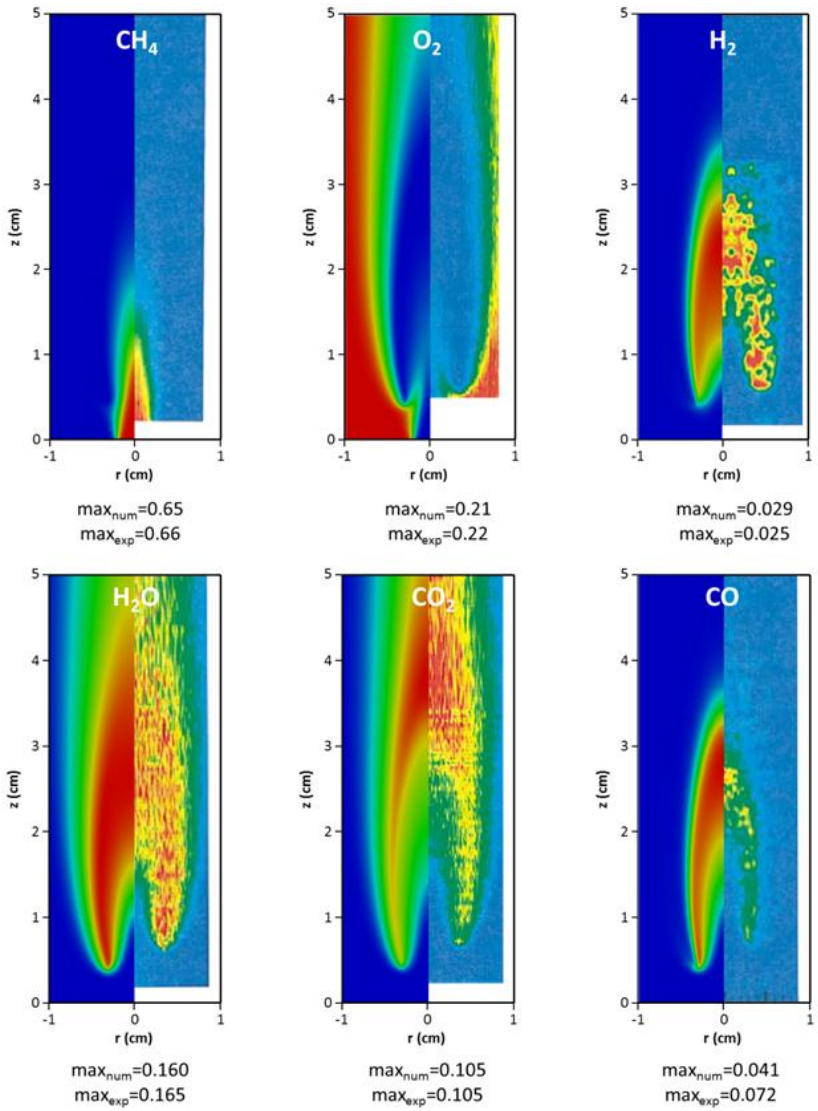

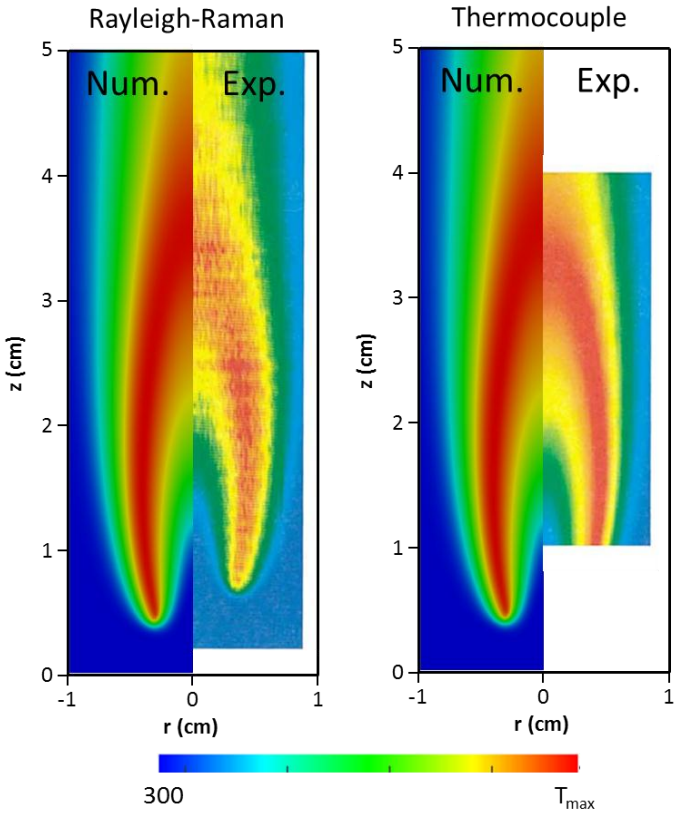

NOx predictions

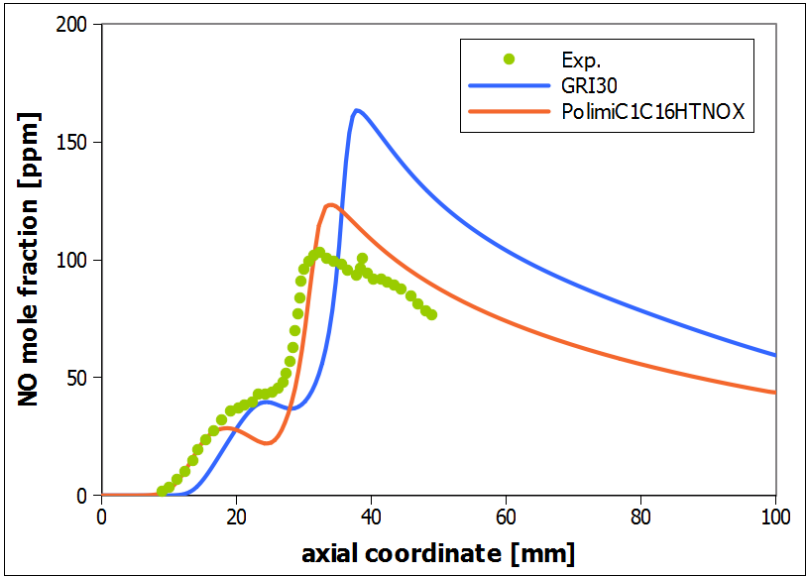

M.D. Smooke, A. Ern, M.A. Tanoff, R.H. Mohammed, D.F. Marran, B. Long *Proceedings of the Combustion Institute*, 26 (1996) 2161-2170.

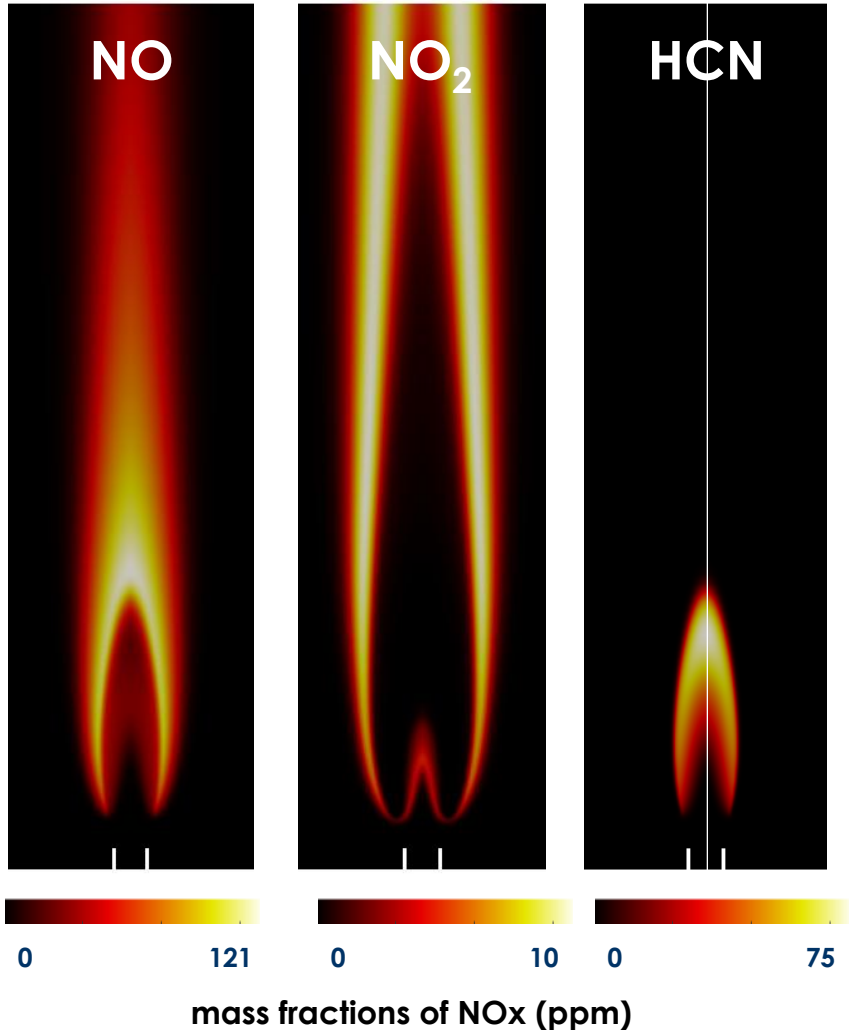

Local refinements of the grid

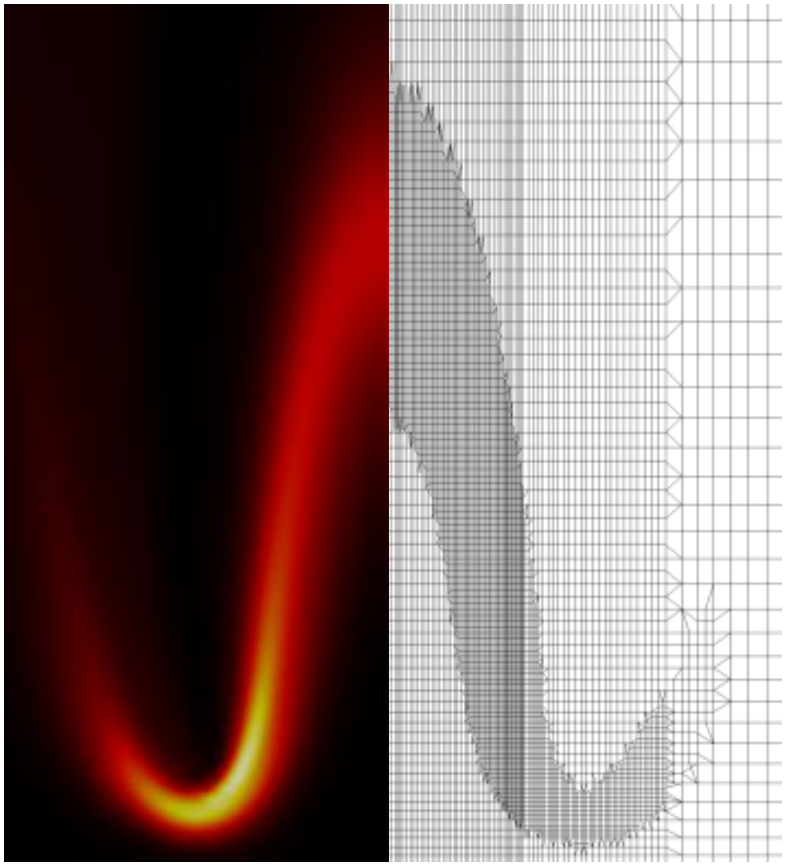

The flame-lift off was obtained by looking at the HO_2 mass fraction maps, reported above. In order to correctly capture the lift-off of the flame several local refinement of the mesh were performed.

Numerical solution

Fully segregated algorithms

☺ easy to implement and computationally efficient
☹ unfeasible when large, stiff kinetic mechanisms are used

Detailed kinetic schemes

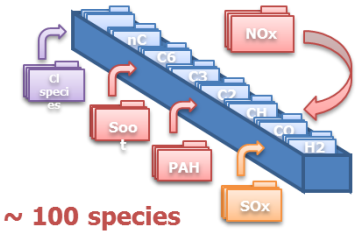

~ 100 species
~ 1000 reactions

Complex geometries

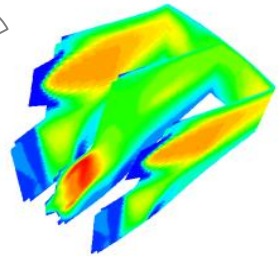

Strong non linearity of reaction terms
High stiffness

Fully coupled algorithms

☺ all the processes and their interactions are considered simultaneously
☺ natural way to treat problems with multiple stiff processes
☹ the resulting system of equations can be extremely large and the computational cost prohibitive

Operator-splitting methods

☺ usually avoid many costly matrix operations
☺ allow the best numerical method to be used for each type of term or process
☹ the resulting algorithms can be very complex and usually differ from term to term

laminarSMOKE

laminarSMOKE structure

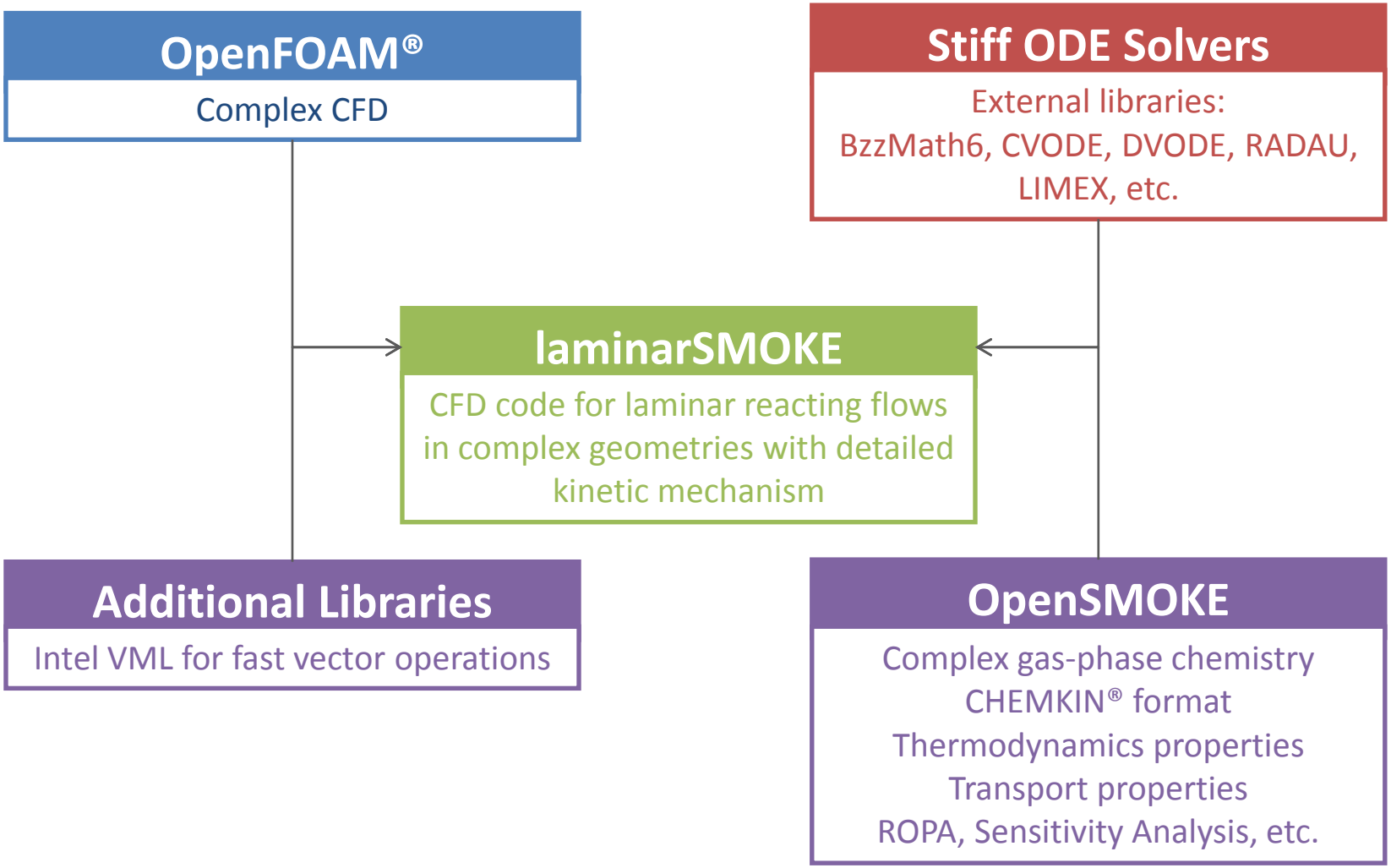

www.opensmoke.polimi.it

Stiff ODE solvers in laminarSMOKE

	Language	Linear system solution	Parallel	Code available	License
BzzMath6	C++	Direct	No	No	Free only for academic use
DVODE	FORTRAN	Direct	No	Yes	Free
CVODE	C	Direct/Iterative	Yes	Yes	Free
DLSODE	FORTRAN	Direct	No	Yes	Free
DLSODA	FORTRAN	Direct	No	Yes	Free
RADAU5	FORTRAN	Direct	No	Yes	Free
LIMEX4	FORTRAN	Direct	No	Yes	Free only for academic use
MEBDF	FORTRAN	Direct	No	Yes	Free

Most of the CPU Time (80-90%) is spent for the numerical integration of the ODE systems corresponding to the reaction step

The best performances are obtained using the following solvers:
BzzMath6, CVODE, DVODE

Performances of stiff ODE solvers: CPU time

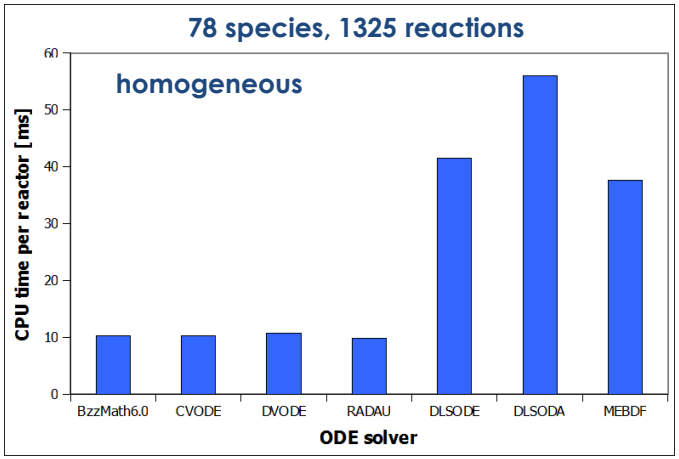

Verification of the code

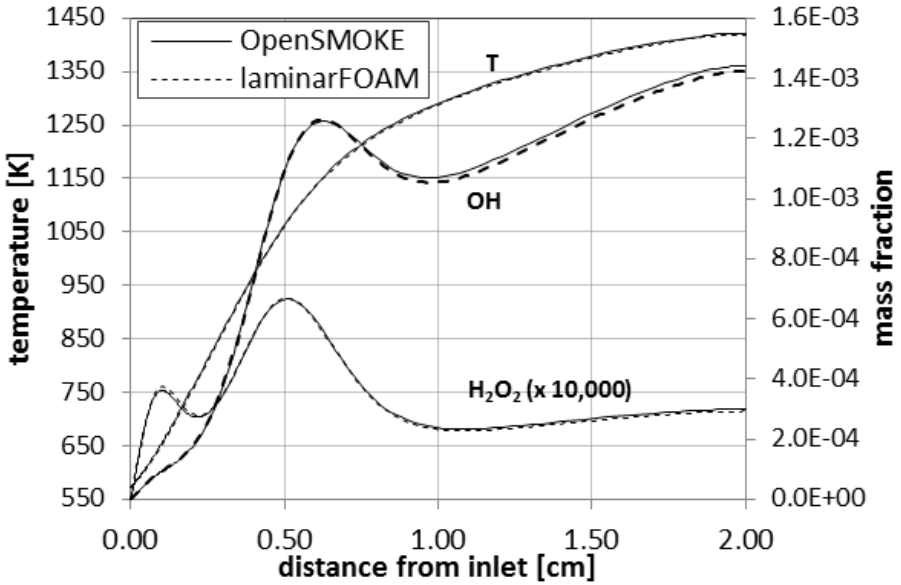

Laminar premixed flame
H_2 (39.7%), Ar (50%) and O_2 (10.3%)

The reactants are fed at T=572 K and p=0.0467 atm at the velocity of 276 cm/s

	Max Values[a]				Mean Values[b]		
	n=1	*n=2*	*n=3*	∞	p	GCI (%)	Rn
T [K]	1415.42	1417.41	1418.03	1418.298	1.71	0.0235	75%
H_2	0.016169	0.016156	0.016152	0.01615	1.72	0.01362	78%
O_2	0.000374	0.000376	0.000377	0.000377	1.62	0.1053	75%
H_2O	0.149387	0.149443	0.149461	0.149469	1.64	0.00706	78%
OH	0.001394	0.001404	0.001407	0.001408	1.58	0.1372	69%
H_2O_2	6.5138E-08	6.6245E-08	6.6596E-08	6.6759E-08	1.65	0.3061	71%
HO_2	1.2465E-05	1.2478E-05	1.2478E-05	1.2484E-05	1.68	0.01812	70%
H	0.00362404	0.0036273	0.0036284	0.0036290	1.55	0.02011	72%
O	0.0016512	0.0016723	0.0016793	0.0016828	1.58	0.2614	69%

[a] For H_2 and O_2 the values at the outlet boundary are reported instead of maximum values
[b] Global values of p and GCI are calculated by means of arithmetic and volumetric and averaging, respectively